

CHAPTER 6

Upper Stratospheric Processes

Lead Authors:

R. Müller
R.J. Salawitch

Coauthors:

P.J. Crutzen
W.A. Lahoz
G.L. Manney
R. Toumi

Contributors:

D.B. Considine
S.J. Evans
J.-U. Grooß
C.H. Jackman
K.W. Jucks
D.E. Kinnison
A.J. Miller
G.A. Morris
G.E. Nedoluha
C.D. Nevison
W.J. Randel
A.R. Ravishankara
J.M. Russell III
K.H. Sage
M.L. Santee
D.E. Siskind
M.E. Summers
J. Trentmann
R.H.J. Wang
J.R. Ziemke

CHAPTER 6

UPPER STRATOSPHERIC PROCESSES

Contents

SCIENTIFIC SUMMARY	6.1
6.1 INTRODUCTION	6.3
6.2 TRANSPORT PROCESSES IN THE UPPER STRATOSPHERE	6.5
6.3 PHOTOCHEMISTRY OF THE UPPER STRATOSPHERE	6.9
6.3.1 Hydrogen Species	6.9
6.3.2 Nitrogen Species	6.14
6.3.3 Chlorine Species	6.18
6.3.4 Atomic Oxygen	6.23
6.3.5 Ozone Production	6.24
6.4 TRENDS AND CYCLES OF UPPER STRATOSPHERIC OZONE	6.25
6.4.1 The Ozone Budget	6.25
6.4.2 Seasonal Cycle of Ozone	6.27
6.4.3 Solar Effects on Ozone	6.28
6.4.4 Ozone Trends	6.29
6.5 THE CURRENT AND HISTORICAL UNDERSTANDING OF THE CONNECTION BETWEEN CFCS AND UPPER STRATOSPHERIC OZONE	6.32
REFERENCES	6.34

SCIENTIFIC SUMMARY

Since the previous Assessment (WMO, 1995), an improved understanding of upper stratospheric processes has been gained through numerous atmospheric observations that have better defined long-term changes in ozone and better constrained our understanding of reactive hydrogen, nitrogen, and chlorine gases. The original hypothesis put forth in 1974 that a release of industrial chlorofluorocarbons (CFCs) to the atmosphere would lead to a significant reduction of upper stratospheric ozone, with the peak percentage decline occurring around 40 km, is now clearly confirmed.

- The global distributions calculated by current two-dimensional “assessment models” of the long-lived source gases (e.g., H₂O, methane (CH₄), nitrous oxide (N₂O), CFCs) of the radicals that catalyze ozone loss compare well with global observations. Consequently, the simplified representations of dynamics used by these models have proved to be useful for studies of the observed changes in upper stratospheric ozone (O₃) during the past several decades.
- Several independent recent studies show increases in upper stratospheric H₂O of about 55 to 150 parts per billion by volume (ppbv) per year from 1992 to 1996/1997, which cannot be explained by a concurrently observed downward trend in upper stratospheric CH₄ (about 15 ppbv/year). Should this rise in H₂O continue to occur, it could have important long-term radiative and photochemical consequences. However, changes in H₂O do not contribute a large fraction to the observed decline in upper stratospheric ozone over the last decades.
- Balloonborne observations of hydroxyl radicals (OH) and hydroperoxyl radicals (HO₂) near 40 km agree with calculated concentrations to within ±20%. Ground-based column observations of OH, which have a substantial contribution from the mesosphere, exhibit larger discrepancies with models. Satellite observations of OH near 50 km are considerably less than calculated using standard photochemical kinetics. These discrepancies are unlikely to have a substantial effect on calculated trends of upper stratospheric ozone.
- Comparisons of recent observations and model calculations show that the overall partitioning of reactive nitrogen and chlorine species is well understood. The previously noted discrepancy for the chlorine monoxide/hydrogen chloride ratio (ClO/HCl) has been resolved, provided allowance is made for production of HCl from a minor channel of the ClO + OH reaction, which is consistent with a recent laboratory study.
- Measurements of the total stratospheric chlorine loading demonstrate that long-lived organic chlorine compounds (mainly CFCs) released by anthropogenic activity are the dominant source of ClO, the chlorine compound that depletes O₃. The observed increases in upper stratospheric hydrogen chloride (HCl) and hydrogen fluoride (HF) are in excellent agreement with the rise of the chlorine and fluorine content of their organic source gases in the troposphere.
- An improved understanding of the relevant kinetic processes has resulted in close balance between the calculated production and loss of O₃ at 40 km (i.e., the long-standing difference between calculated and observed ozone abundance, the so-called “ozone deficit problem,” has been resolved at this altitude). Although there are remaining uncertainties regarding a possible ozone deficit at higher altitudes, the severity of this problem has been substantially reduced throughout the upper stratosphere.
- Several independent long-term datasets show a decline of the concentration of O₃ that peaks around 40 km altitude at a value of $7.4 \pm 1.0\%$ /decade. Photochemical model simulations likewise reveal a long-term decline of ozone throughout the upper stratosphere that is driven by the accumulation of anthropogenic chlorine. There is good quantitative agreement between the observed and simulated meridional and vertical structure of the long-term reductions in upper stratospheric ozone.

6.1 INTRODUCTION

Ozone depletion in the upper stratosphere, predicted more than two decades ago (Molina and Rowland, 1974; Crutzen, 1974), is now clearly observed. In addition to this predicted change, loss of ozone is observed also at lower altitudes (Figure 6-1; see also Chapter 4). The vertical distribution of stratospheric ozone decline has a distinct minimum around 30 km; the focus of this chapter is on the changes in ozone above this altitude. The causes of changes in ozone below 30 km are discussed in Chapter 7.

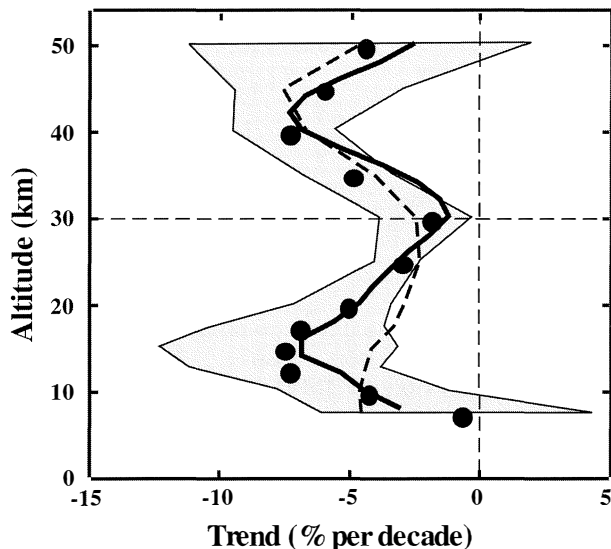


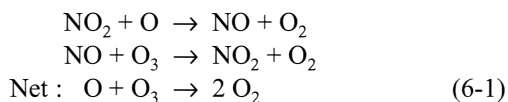
Figure 6-1. Stratospheric ozone decline in % per decade (filled circles) and uncertainties (at the 2σ level; gray area) for northern midlatitudes from the Stratospheric Processes and Their Role in Climate-International Ozone Commission (SPARC-IOC) Assessment of trends (1980-1996) in the vertical distribution of ozone (Stolarski and Randel, 1998). The lines are 2-D model calculations of the ozone trend due to catalytic destruction by halogen radicals: solid line from Solomon *et al.* (1998) and dashed line, a recent calculation using the model of Jackman *et al.* (1996). There is a statistically significant negative trend at all altitudes, except at the lowest and the highest altitudes (see Chapter 4). The minimum ozone depletion occurs around 30 km. The causes of ozone changes above this altitude are discussed in this chapter; those in the region below are discussed in Chapter 7.

Ozone (O_3) in the upper stratosphere, although originally thought to be most vulnerable to catalytic destruction by chlorine radicals (ClO_x) (Molina and Rowland, 1974; Crutzen, 1974), has attracted comparably little scientific attention since the discovery of extreme ozone losses due to perturbed halogen chemistry in the lower stratosphere in Antarctica (WMO, 1995; see also Chapter 7). However, about 15% of the ozone column resides in the upper stratosphere (above about 30 km) and ozone loss in this region affects global stratospheric temperatures and therefore may impact the radiative balance of the stratosphere (see Chapter 10).

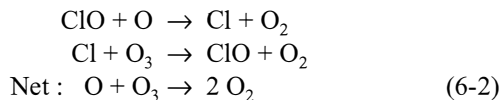
The abundance of stratospheric ozone is governed by photochemical production (mostly the photolysis of O_2), destruction by catalytic cycles involving hydrogen (HO_x), nitrogen (NO_x), and halogen (ClO_x , BrO_x) radicals, as well as transport processes. In the upper stratosphere (between about 30 and 50 km), with the exception of the winter high latitudes (poleward of about $45^\circ N$), photochemical reactions are sufficiently fast that the concentrations of ozone are solely determined by a local balance of photochemical production and loss; i.e., ozone is in photochemical steady state. However, the abundances of gases such as methane (CH_4), H_2O , chlorofluorocarbons (CFCs), and nitrous oxide (N_2O) that act as radical precursors are affected by transport because these gases are longer lived than O_3 . Transport thus has a significant indirect influence on ozone.

Stratospheric ozone is produced by photolysis of molecular oxygen (O_2) at wavelengths below 242 nm, with the subsequent reaction of the photolysis product oxygen atoms (O) with O_2 to form ozone. It is common for the sum $[O_3] + [O]$ to be referred to as odd oxygen, or O_x , because the sum of these compounds varies slowly during the day. The concentrations of O_3 and O adjust rapidly to photochemical steady state via the reactions $O_3 + h\nu \rightarrow O + O_2$ and $O + O_2 + M \rightarrow O_3 + M$. Throughout the altitude range of interest, O_3 constitutes the vast majority of total O_x , and thus a change in the abundance of O_x will for convenience be referred to as change in O_3 . Owing to the large abundance of ground-state atomic oxygen $O(^3P)$ in the upper stratosphere compared with concentrations present at lower altitudes, ozone loss in this region is dominated by cycles whose rate-limiting step involves reaction with $O(^3P)$. In addition to the Chapman reaction, $O + O_3 \rightarrow 2O_2$, the most important loss cycles for ozone in the upper stratosphere are catalytic cycles involving NO_x radicals

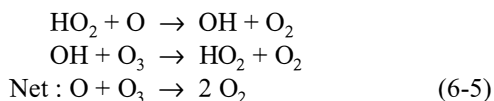
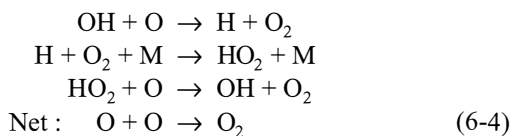
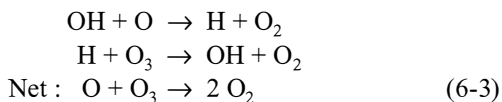
UPPER STRATOSPHERIC PROCESSES



chlorine radicals



and hydrogen radicals



Owing to the strong increase of $\text{O}(^3\text{P})$ with altitude, the rates of these cycles increase substantially between 25 and 40 km (Figure 6-2). Loss of O_3 by the cycle limited by the reaction $\text{BrO} + \text{O}$ occurs at a much slower rate ($\sim 1\%$ of the total loss at 30 km, smaller contributions at higher altitudes) than loss by the cycles given above, and is not considered here. Loss of O_3 through cycles limited by reactions such as $\text{ClO} + \text{ClO}$, $\text{ClO} + \text{BrO}$, $\text{ClO} + \text{HO}_2$, and $\text{BrO} + \text{HO}_2$ is important only for altitudes below ~ 25 km because each of these cycles involves reactions including O_3 , but not $\text{O}(^3\text{P})$. Consequently, these cycles are considered in Chapter 7, but not here.

The relative importance of the various loss cycles varies with altitude (Figure 6-2). Above the 42 to 45 km altitude region, loss of ozone is dominated by catalytic cycles involving hydrogen radicals, whereas for lower altitudes, NO_x -catalyzed loss of ozone is most important. The importance of the chlorine-catalyzed ozone loss cycle peaks at about 40 km where, at present atmospheric chlorine abundances, it is comparable to loss of ozone by the hydrogen and nitrogen catalytic cycles.

Sections 6.2 and 6.3 review our understanding of the dynamical and chemical processes in the upper stratosphere that maintain the distribution of the major

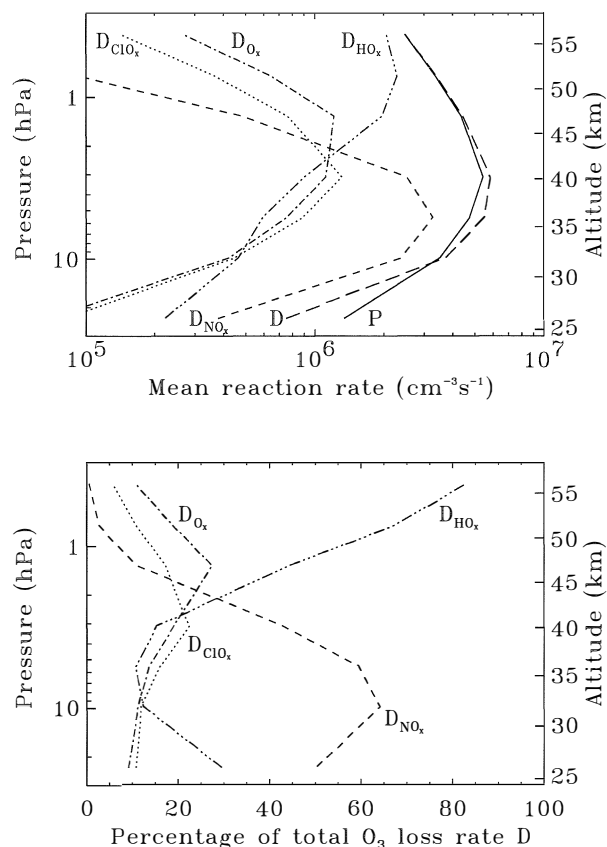


Figure 6-2. The vertical distribution of the total O_x production (P) and destruction rate (D). Also shown are the individual contributions by the HO_x (D_{HO_x}), ClO_x (D_{ClO_x}), and NO_x (D_{NO_x}) cycles as well as the Chapman loss cycle (D_{O_x}). The top panel shows absolute values and the bottom panel shows relative values. Calculations are for conditions of strongest photochemical control on stratospheric chemistry (January 1994, 23°S). Adapted from Crutzen *et al.* (1995); updated to current kinetic parameters (DeMore *et al.*, 1997; Lipson *et al.*, 1997) and using Version 18 HALOE data.

radical precursors, which determine the concentration of the radicals that regulate ozone and that also lead to the observed decline in ozone. Although, owing to the absence of heterogeneous chemical processes, the chemistry in the middle and upper stratosphere appears to be less complicated than in the lower stratosphere, uncertainties still exist in the quantitative understanding of the ozone budget. The fact that models underpredict the observed abundance of ozone in the upper

stratosphere, a long-standing issue commonly referred to as the “ozone deficit” problem (WMO, 1995; see also Section 6.4.1 below), is still not completely resolved. Uncertainties remain in particular for altitudes above 45 km, where the O_x loss cycles are mostly controlled by HO_x chemistry. Here, the rates of several key radical reactions are known only to within relatively large uncertainty limits (see Section 6.3.1 below).

In spite of known deficiencies, calculations using two-dimensional (2-D) models have heretofore been the only means to simulate long-term trends of ozone (WMO, 1995). Both observations of the ozone vertical distribution and model results indicate a downward trend in the ozone concentrations above 30 km (Section 6.4). However, while the signature of both the altitude distribution and the latitudinal variation of the ozone trend were in reasonable agreement between model results and observations, past model calculations tended to overpredict the observed negative trend in ozone (e.g., WMO, 1995; Jackman *et al.*, 1996). This problem has been largely resolved in recent model calculations (Figure 6-1; see in particular Section 6.4.4 below).

Strong evidence has accumulated during the past two decades that the decline of ozone in the upper stratosphere is linked with increased levels of chlorine (e.g., Hilsenrath *et al.*, 1992; WMO, 1995; see also Section 6.5 below). Therefore, as only a slow decline of the stratospheric chlorine loading is predicted over the coming decades (see Chapter 11), the problem of stratospheric ozone loss is expected to persist in the foreseeable future. Nonetheless, because of the direct correspondence between the chlorine burden and loss of ozone in the upper stratosphere (see below), it is conceivable that the “recovery” of ozone due to the declining burden of anthropogenic halogens will first become apparent for the upper stratosphere (Chapter 12).

6.2 TRANSPORT PROCESSES IN THE UPPER STRATOSPHERE

The distributions throughout the stratosphere of long-lived compounds such as H_2O , CH_4 , N_2O , and CFCs are controlled by transport. Because decomposition of these compounds supplies the hydrogen, nitrogen, and chlorine radicals involved in catalytic cycles that remove O_3 , these cycles thus depend indirectly on transport processes in the upper stratosphere. As the chemical reactions are temperature dependent, dynamical processes that affect the temperatures in the upper

stratosphere are also relevant to O_3 changes in this region. Dynamical and transport processes also play a more direct role in the regulation of O_3 between 30 and 40 km in the extratropics, where chemical time scales are longer than at higher altitudes and thus closer to transport time scales.

As discussed in more detail in Chapter 7 (Section 7.3), the Brewer-Dobson circulation (ascent across the tropical tropopause, poleward motion in the stratosphere, descent into the extratropical troposphere in both hemispheres) accounts for the gross features of the annual mean stratospheric meridional circulation. The equinoctial circulation in the upper stratosphere resembles the Brewer-Dobson circulation; the solstice circulation comprises rising motion above 30 km in summer high latitudes, summer pole to winter pole flow in the upper stratosphere and mesosphere, and strong descent in winter middle and high latitudes (e.g., Andrews *et al.*, 1987). This global mass circulation is driven primarily by wave motions in the extratropical stratosphere (e.g., Holton *et al.*, 1995; Chapter 7), with both planetary-scale and gravity waves playing a role. Mesospheric gravity wave drag plays a strong role in determining the temperature structure and circulation of the middle and upper stratosphere (down to below 30 km), with largest effects during southern winter and early northern winter, when planetary wave driving is relatively weak (e.g., Garcia and Boville, 1994). In winter, the polar vortex dominates the extratropical circulation throughout the stratosphere, and planetary-scale waves associated with variability of the polar vortex result in a region of strong quasi-horizontal mixing and weak tracer gradients between regions of strong tracer gradients associated with the polar vortex boundary (e.g., McIntyre and Palmer, 1984) and the sub-tropical transport barrier (e.g., Plumb, 1996; Chapter 7). Trajectory modeling studies (Sutton *et al.*, 1994; Schoeberl and Newman, 1995; Manney *et al.*, 1998) have shown that generation of filaments in the midlatitude region of strong mixing is common in the middle and upper stratosphere as well as in the lower stratosphere (Chapter 7); Schoeberl and Newman (1995) applied their filamentation calculations to quantification of this mixing in Northern Hemisphere winter, showing most rapid mixing to be associated with large planetary-scale wave amplitudes. Recent tracer data from satellites (e.g., the Upper Atmosphere Research Satellite (UARS)) with hemispheric or global and year-round coverage, and other observations (e.g., Atmospheric Trace Molecule Spectroscopy (ATMOS))

UPPER STRATOSPHERIC PROCESSES

with vertical profile information through the upper stratosphere, confirm that the above picture gives a reasonably good description of the largest scale features of observed distributions of N_2O (Figure 6-3), CH_4 (Figure 6-4), H_2O , hydrogen fluoride (HF), and CFCs (e.g., Randel *et al.*, 1993, 1994, 1998a; Ruth *et al.*, 1994; Luo *et al.*, 1995; Nightingale *et al.*, 1996; Michelsen *et al.*, 1998). A useful, although not directly observable, measure of transport in the meridional plane is the age of stratospheric air (e.g., Hall and Plumb, 1994; Chapter 7); the mean age of air typically shows a pattern similar to that of a long-lived tracer, with the oldest air (possibly as old as 10-12 years) residing in the polar upper stratosphere (see Figure 7-8). The air in the midlatitude stratosphere has a mean age of about 5-6 years (e.g., Harnisch *et al.*, 1996; Waugh *et al.*, 1997; Bacmeister *et al.*, 1998; see also Chapter 7). Models (including general circulation models, chemical transport models, and 2-D models) can reproduce the main ingredients of the meridional distribution of long-lived tracers and the age-of-air spectrum (e.g., Randel *et al.*, 1994; Waugh *et al.*, 1997; Bacmeister *et al.*, 1998), although details such as quantitative determinations of age vary widely between

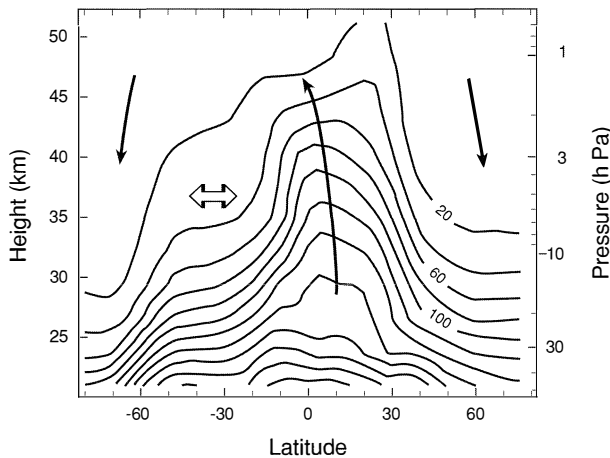


Figure 6-3. Longitudinally averaged structure of N_2O mixing ratios (in ppbv) during 1-20 September 1992 measured by the Cryogenic Limb Array Etalon Spectrometer (CLAES) instrument on the Upper Atmosphere Research Satellite (UARS). Heavy solid lines denote the mean stratospheric circulation in the latitude-height plane, and the horizontal arrows denote the location of quasi-horizontal mixing by planetary waves. Adapted from Randel *et al.* (1993).

models (e.g., Hall and Waugh, 1997; Waugh *et al.*, 1997; Bacmeister *et al.*, 1998).

Seasonal variations in the tropics are dominated by a semi-annual oscillation (SAO) above about 35 km and a quasi-biennial oscillation (QBO) below about 35 km. Theories regarding the QBO and its influence on the lower stratosphere and total O_3 are discussed in Chapter 7; it is recognized to be driven by wave momentum

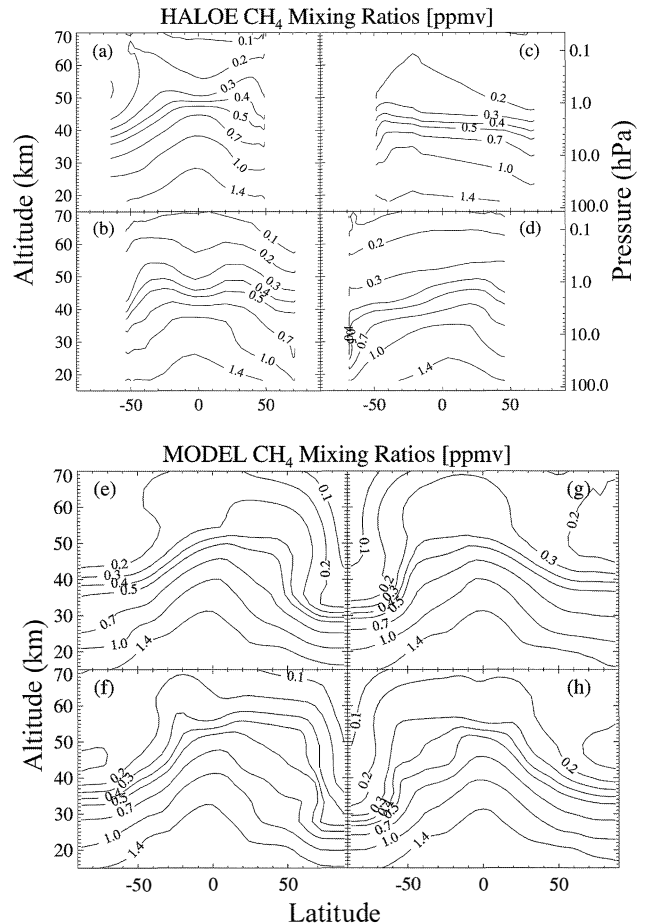


Figure 6-4. Comparison of zonal mean CH_4 mixing ratios as observed by the Halogen Occultation Experiment (HALOE) (panels a-d) and calculated using a two-dimensional model that includes interactive temperatures and transport circulation, but uses climatological ozone for the radiation calculations (panels e-h). Fields are shown for (a) and (e) NH winter solstice, (b) and (f) NH vernal equinox, (c) and (g) NH summer solstice, and (d) and (h) NH autumnal equinox. Adapted from Summers *et al.* (1997b).

transport, which involves planetary-scale equatorial waves, intermediate inertia-gravity waves, and mesoscale gravity waves (Dunkerton, 1997). Several momentum sources are thought to contribute to generation of the SAO (e.g., Sassi and Garcia, 1997, and references therein), including forcing of westerly accelerations via momentum deposition by Kelvin and gravity waves propagating into the upper stratosphere and forcing of easterly accelerations by planetary waves. Both QBO and SAO drive meridional transport circulations that affect the distribution of long-lived tracers (Gray and Pyle, 1986), as discussed below. Filtering of upward-propagating waves by the QBO modulates the SAO, so that transport in the upper stratosphere is influenced by both the QBO and the SAO. Dunkerton and Delisi (1997) also show evidence that descending westerly phases of the SAO are strongly influenced by the underlying QBO.

That the QBO strongly influences long-lived tracer distributions in the equatorial upper stratosphere (Gray and Pyle, 1986) has been verified in several recent studies (e.g., Ruth *et al.*, 1997; Kennaugh *et al.*, 1997; Luo *et al.*, 1997b; Randel *et al.*, 1998a; Jones *et al.*, 1998); a QBO signal has also been seen in HCl, HF, nitrogen dioxide (NO₂), and O₃ in the middle stratosphere (Zawodny and McCormick, 1991; Luo *et al.*, 1997b). Evidence of the SAO appears in satellite observations of temperature and O₃ (Ray *et al.*, 1994), as well as long-lived tracer distributions (Carr *et al.*, 1995; Ruth *et al.*, 1997; Randel *et al.*, 1998a). Modulation of the position and intensity of subtropical tracer gradients (sharpening gradients during QBO easterlies) in the middle stratosphere is associated with the QBO (Hitchman *et al.*, 1994; Randel *et al.*, 1998a; Jones *et al.*, 1998). The QBO modulation of NO₂ is caused by transport-induced variations in NO_y, and indirectly causes the QBO in O₃ above 30 km through chemical effects (Chipperfield *et al.*, 1994; Jones *et al.*, 1998). A double peak in long-lived tracer distributions seen below the equatorial stratopause near equinox (e.g., Ruth *et al.*, 1994, 1997; Luo *et al.*, 1995; Eluszkiewicz *et al.*, 1996; Randel *et al.*, 1998a) is associated with the SAO. During westerly SAO acceleration, there is induced descent near the equator and ascent in the subtropics below the level of maximum forcing, and ascent near the equator and descent in the subtropics above this level; for an easterly acceleration, the induced circulation has the opposite sense (Gray and Pyle, 1986; Kennaugh *et al.*, 1997). However, recent evidence (Randel *et al.*, 1998a) suggests

that this induced circulation may not be the determining factor in producing the double peak. Recent model studies show a double peak when QBO winds are westerly, but a single peak in the summer hemisphere when QBO winds are easterly (Kennaugh *et al.*, 1997), in agreement with satellite observations of CH₄ (Ruth *et al.*, 1997; Randel *et al.*, 1998a).

The dominant feature of the extratropical stratospheric circulation in winter is a cold westerly polar vortex extending throughout the depth of the stratosphere. The wave-driven mass circulation and associated radiative cooling result in strong descent in and around the polar vortex, with mesospheric air descending through the middle stratosphere (Fisher *et al.*, 1993; Abrams *et al.*, 1996a,b; Aellig *et al.*, 1996a). Inter-hemispheric differences in the intensity, variability, and persistence of the polar vortex in the middle and upper stratosphere and the impact of these differences on long-lived tracer distributions are elucidated in recent studies (e.g., Lahoz *et al.*, 1994, 1996; Manney *et al.*, 1994a, 1995b; Considine *et al.*, 1998) (see Chapter 7 for related studies of the lower stratosphere). Northern winter is characterized by strong planetary-scale variability, with a strong persistent anticyclone typically occurring near the dateline (e.g., Harvey and Hitchman, 1996), large interannual variability, and frequent occurrence of stratospheric sudden warmings. The largest effects of sudden warmings are in the middle and upper stratosphere, where “major” warmings (e.g., Andrews *et al.*, 1987) result in a temporary transition to zonal mean easterlies at and above 10 hPa (about 30 km), zonal mean temperatures that increase toward the pole, and may result in a temporary or permanent breakdown of the upper stratospheric vortex. The flow in the southern winter upper stratosphere is characterized by an intense polar vortex with weak planetary-scale variability represented by one or more eastward-traveling anticyclones, with a transition in late winter/early spring to a circulation with a weakened upper stratospheric vortex and a quasi-stationary anticyclone (e.g., Lahoz *et al.*, 1996). This Southern Hemisphere spring flow regime shares many of the characteristics of the Northern Hemisphere winter flow regime (Lahoz *et al.*, 1994, 1996). The northern vortex typically breaks down in the upper stratosphere at about the time of the spring equinox; the southern upper stratospheric vortex persists for 1 to 2 months longer (e.g., Manney *et al.*, 1994a). Although many studies have focused on the lower stratosphere (Chapter 7), several recent studies based on

UPPER STRATOSPHERIC PROCESSES

trajectory modeling (Fisher *et al.*, 1993; Manney *et al.*, 1994a; Eluszkiewicz *et al.*, 1995) and observations of long-lived tracers (Manney *et al.*, 1994b, 1995b; Lahoz *et al.*, 1994, 1996; Abrams *et al.*, 1996a,b; Aellig *et al.*, 1996a; Michelsen *et al.*, 1998) have refined our understanding of transport, interhemispheric differences in transport, and the impact of these processes on the distribution of long-lived tracers in the upper stratosphere. The interhemispheric differences in large-scale variability described above are associated with hemispheric asymmetries in the global mass circulation; such asymmetries are predicted in calculations based on observed fields (e.g., Rosenlof, 1995; Appenzeller *et al.*, 1996; Eluszkiewicz *et al.*, 1996; Coy and Swinbank, 1997) and confirmed by observations of hemispheric asymmetries in long-lived tracer distributions (e.g., Rosenlof *et al.*, 1997; Morrey and Harwood, 1998; Considine *et al.*, 1998).

The region between approximately 25 and 35 km represents a transition region between dynamical (in the absence of heterogeneous chemistry in the polar vortex; see Chapter 7) control of O₃ in the lower stratosphere and photochemical control in the upper stratosphere (e.g., Hartmann and Garcia, 1979). Recent studies using UARS Microwave Limb Sounder (MLS) ozone data (Allen *et al.*, 1997) confirm that the response of O₃ to planetary-scale waves in winter is consistent with Hartmann and Garcia's model wherein the O₃ distribution below about 30 km is determined primarily by transport by time-varying wave motions and above about 50 km is determined by temperature variations associated with wave motions through temperature-dependent photochemistry, with both processes playing a role in the region between. Luo *et al.* (1997a) showed that transport of O₃ and other gases by summertime planetary waves at 30-40 km could take place on time scales comparable to or shorter than their chemical relaxation times. Manney *et al.* (1998) showed that many small vertical-scale O₃ variations seen in lidar observations at altitudes up to about 40 km can be explained by advection of filaments of air with varying O₃ concentrations, verifying the importance of transport in determining the details of the O₃ distribution in the middle stratosphere. The common phenomenon of low ozone pockets forming in the anticyclone between 30 and 45 km (Manney *et al.*, 1995a) is another example of the interplay between transport and chemistry in the transition region. Long-lived tracer observations show that air from low latitudes is drawn into the anticyclone and confined there for days

to weeks; O₃ mixing ratios in this air decrease rapidly as it becomes confined in the anticyclone (Manney *et al.*, 1995a). Nair *et al.* (1998) and Morris *et al.* (1998) confirmed that the isolation of this air results in relaxation (via known chemical processes) to O₃ concentrations much lower than those prevailing in midlatitudes outside the anticyclone where air experiences strong mixing. In contrast to the above examples, Douglass *et al.* (1997) showed a chemical transport model simulation where, near 40 km, tropical to midlatitude distributions of long-lived tracers were not well simulated but, because O₃ lifetimes are very short in the tropics and sub-tropics at this altitude, reasonably good agreement was obtained between model and observed O₃. The above examples illustrate that the degree to which transport at altitudes in the transition region influences ozone chemistry varies widely depending on location, season, and dynamical conditions.

To date, the vast majority of assessment studies relevant to the upper stratosphere have been done using two-dimensional models (see Chapter 12) in which many of the processes discussed above cannot be explicitly represented. Realistic zonal mean temperature distributions and transport in such models are highly dependent on parameterizations of gravity waves and planetary-scale waves. Bacmeister *et al.* (1995) and Summers *et al.* (1997b), for example, discuss the adjustment of these parameters to obtain realistic distributions of long-lived tracers and zonal mean temperatures. Such tuning of 2-D models is greatly assisted by improved understanding of processes being parameterized, as detailed above, as well as by the availability of global observations of long-lived tracers for all seasons from satellite instruments such as those on UARS. As shown in Figure 6-4, good agreement can be obtained between satellite-observed long-lived tracer fields and those obtained from 2-D models, including representation of strong tracer gradients in the subtropics and along the polar night jet, a region of very weak tracer gradients in midlatitudes, a signature of strong descent in the polar vortex, and separation of relationships between long-lived tracers in tropics and extratropics (e.g., Bacmeister *et al.*, 1995; Luo *et al.*, 1995; Jackman *et al.*, 1996; Nightingale *et al.*, 1996; Summers *et al.*, 1997b; Rosenfield *et al.*, 1997). Considine *et al.* (1998) simulated interhemispheric differences in high latitude CH₄ and N₂O, and Summers *et al.* (1997b) were able to simulate interhemispheric differences in both stratospheric and mesospheric H₂O. These asymmetries may

impact the distribution of chlorine and hydrogen radicals, and thus both the upper stratospheric O_3 concentrations and decadal trends (Section 6.4.4). Two-dimensional models typically fail to capture, or else underestimate, the double-peaked structure in long-lived tracers in the equatorial upper stratosphere (see Figure 6-4), a problem related to deficiencies in their ability to model the SAO and QBO (e.g., Summers *et al.*, 1997b).

Although most 2-D models capture the general features of the upper stratospheric circulation mentioned above, a number of different approaches to parameterizing planetary-scale and gravity waves are used in various models, and there is considerable model-to-model variability in details of temperature structure, tracer-tracer relationships, age spectra, and the shapes of tracer isopleths (Park *et al.*, 1998). In addition, many 2-D models used for assessment are further simplified by using transport circulations based on a specified climatology of zonal mean temperatures, so that the circulation and chemistry are not interactive (Jackman *et al.*, 1996; Chapter 12); significant differences can result in otherwise similar models that are run with interactive versus non-interactive chemistry, radiation, and dynamics (Considine *et al.*, 1998; Chapter 12). For multi-year simulations, a single annual cycle of the circulation and temperature is typically repeated for the duration of the simulation, making it impossible to represent interannual variability, trends in long-lived gases or temperatures, or multi-year oscillations such as the QBO. Thus, although 2-D models can be adjusted to give adequate representations of contemporary temperature and tracer fields, possible effects on simulations of ozone change due to interannual variability, long-term temperature and source gas trends, and QBO cycles have not as yet been thoroughly evaluated. Despite these obvious deficiencies in the representation of transport processes in current assessment models, these models can give reasonable representations of many of the large-scale features of the distribution of long-lived source gases; such simplified assessment models have been quite successful in reproducing observed trends in ozone in the upper stratosphere (Section 6.4).

6.3 PHOTOCHEMISTRY OF THE UPPER STRATOSPHERE

6.3.1 Hydrogen Species

The role of hydrogen radicals in regulating the abundance of stratospheric O_3 was first described by

Bates and Nicolet (1950). In the upper stratosphere, hydrogen radicals (HO_x) are produced by the reactions of excited-state atomic oxygen ($O(^1D)$) with H_2O and with CH_4 . Loss of HO_x occurs primarily by the reaction $HO_2 + OH$, with important contributions from the $OH + HNO_3$ reaction below ~ 35 km. Hydrogen radicals catalyze loss of ozone in the upper stratosphere by the catalytic cycles (6-3), (6-4), and (6-5) (see Section 6.1).

HYDROGEN SOURCE GASES

Global distributions of H_2O (Harries *et al.*, 1996) and CH_4 (Park *et al.*, 1996) measured by the Halogen Occultation Experiment (HALOE) instrument aboard UARS have been reproduced fairly well by a three-dimensional (3-D) general circulation model (GCM) (Mote, 1995). The observed shapes of tracer isopleths, bowing in the tropics and flattening at midlatitudes, are consistent with calculated isopleths. Similarly, 2-D models provide an adequate representation of observed CH_4 and H_2O fields (see Section 6.2). Abbas *et al.* (1996a) have shown that vertical profiles of H_2O and CH_4 measured by the ATMOS instrument are consistent with production of H_2O from oxidation of CH_4 as well as the general features of the profile for molecular hydrogen (H_2) calculated by 2-D models. These studies suggest good overall understanding of the distributions of H_2O and CH_4 in the upper stratosphere.

Current issues of importance regarding the budget of upper stratospheric hydrogen are long-term trends of H_2O and CH_4 . Evans *et al.* (1998), Nedoluha *et al.* (1998a), and Randel *et al.* (1998b) reported an upward trend of 55 to 150 ppbv/year in the volume mixing ratio of upper stratospheric H_2O based on analyses of HALOE data obtained between altitudes of 30 to 60 km during the years 1992 to 1996/1997 (Figure 6-5). The time series for upper stratospheric H_2O exhibits nonlinear variations due to numerous forcings, such as quasi-biennial and seasonal variations in stratospheric winds (e.g., Evans *et al.*, 1998). The H_2O mixing ratio increase between 1992 and 1996 measured by HALOE is not monotonic with time and appears to have leveled off during 1997 (Randel *et al.*, 1998b). Consequently, the computed H_2O trend is sensitive to the statistical technique used to extract the linear component from the nonlinear signal, to the time period of the data record, and also to the range of latitudes and altitudes under consideration (Evans *et al.*, 1998; Nedoluha *et al.*, 1998a; Randel *et al.*, 1998b). Evans *et al.* (1998) (data obtained between 1992 and 1996, inclusive) and Nedoluha *et al.* (1998a) (data

UPPER STRATOSPHERIC PROCESSES

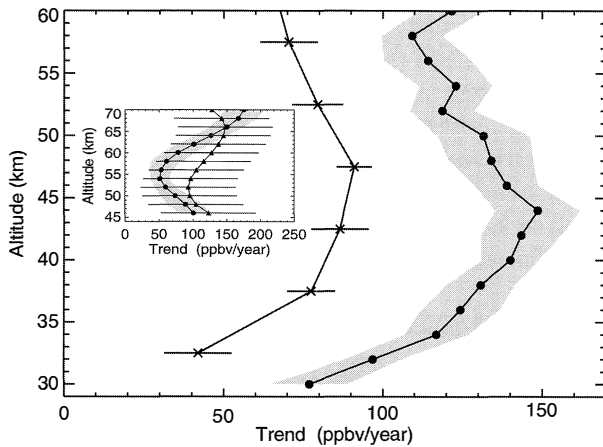


Figure 6-5. Global average linear trends in upper stratospheric water vapor derived from HALOE Version 18 observations by Evans *et al.* (1998) for 1992 to 1996 inclusive (crosses) and by Nedoluha *et al.* (1998a) for September 1991 to February 1997 (circles). The error bars for the Evans *et al.* (1998) points represent 95% confidence intervals of the trend based on a least squares linear fit to the de-seasonalized data. The shaded region for the Nedoluha *et al.* (1998a) curve represents 1-sigma estimates of the accuracy of the trend based on the quality of the fit of the linear and sinusoidal terms used to model the data. The insert shows a comparison of the trend for H₂O between May 1993 and October 1997 measured by a ground-based Water Vapor Millimeter-wave Spectrometer (WVMS) at Table Mountain, California (34.4°N, 242.3°E) (triangles; error bars represent the 1-sigma uncertainty of the trend), to the HALOE trend for coincident measurements obtained within ±5° latitude and ±30° longitude of Table Mountain (circles; shaded area denotes 1-sigma uncertainty of the trend). Data in insert from Nedoluha *et al.* (1998a).

obtained between September 1991 and February 1997) report values of 73.1 ± 16.3 ppbv/year and 123.1 ± 18.3 ppbv/year, respectively, for the globally averaged increase of H₂O between altitudes of 30 and 60 km. The primary difference between the two estimates is due to the statistical technique used to estimate the linear component of the nonlinear H₂O time series: the method of Nedoluha *et al.* (1998a) yields a trend of 126.6 ± 19.9 ppbv/year if the time range of the observations is restricted to 1992 to 1996 inclusive.

The recent rise of upper stratospheric H₂O has been confirmed by independent ground-based measurements that also show an appreciable increase in H₂O over the same time period as the HALOE observations (insert of Figure 6-5; Nedoluha *et al.*, 1998a). The difference in the ground-based trend for H₂O at 34.4°N and the coincident HALOE trend for H₂O shown in Figure 6-5 is caused in part by differences in the frequency of the sampling of air by the ground-based instrument (nearly continuous measurements) and by HALOE at 34.4°N (periodic observations), which is important because the magnitude of the linear H₂O trend is small relative to changes in H₂O on short timescales. The ground-based trends at 34.4°N and at 45.0°S are in better agreement with the globally averaged HALOE trend than with the coincident HALOE trend (Nedoluha *et al.*, 1998a). Furthermore, Oltmans and Hofmann (1995) earlier found an increase in the mixing ratio of H₂O between 1981 and 1994 in the lower stratosphere ranging from ~15 ppbv/year to ~32 ppbv/year, and Abbas *et al.* (1996a) noted a substantial increase with time in the H₂O content of air entering the stratosphere for observations obtained at Northern Hemisphere midlatitudes by ATMOS in 1985, 1992, 1993, and 1994.

The increases in H₂O reported by the three studies that have examined HALOE data are larger than can be accounted for by the rise in tropospheric CH₄. Stratospheric [2×CH₄ + H₂O] also shows a significant increase over the time period 1992 to 1996, suggesting the total hydrogen content of stratospheric air has risen (Evans *et al.*, 1998; Nedoluha *et al.*, 1998a; Randel *et al.*, 1998b). The observations could be explained by a rise of a few tenths of a degree in the temperature of the air entering the tropical stratosphere, a change that would be difficult to detect directly (Nedoluha *et al.*, 1998a).

Appreciable long-term trends in H₂O could have important implications for upper stratospheric O₃ due to both the radiative effects of H₂O and photochemical effects of HO_x (e.g., Evans *et al.*, 1998; Siskind *et al.*, 1998; see also Section 6.4.4). To date there have been no attempts to quantify the impact on contemporary upper stratospheric O₃ of the increase in H₂O observed by HALOE using a model that allows for both radiative and photochemical effects. The calculations of Evans *et al.* (1998) (which extrapolated the observed increase of H₂O to time periods comparable to that for the doubling of atmospheric CO₂) suggest that the rise of H₂O observed by HALOE had a smaller effect on upper stratospheric

O₃ than the change due to the build-up of stratospheric chlorine over the same time period. The analysis of Siskind *et al.* (1998), which considered only photochemical effects, concluded changes in H₂O between 1992 and 1995 should have had a larger effect on O₃ than did the build-up of chlorine over this time period. However, Siskind *et al.* (1998) note that a predicted decrease in mesospheric O₃ over the same time period was not observed by HALOE, suggesting atmospheric O₃ may be less sensitive to the build-up of H₂O than indicated by current photochemical theory. It is important to note that Oltmans and Hofmann (1995) report an increase for H₂O of only 0.34 ± 0.34 ppmv for altitudes of 24 to 26 km (the highest altitude bin reported in their study) over the time period 1981 to 1995. According to the model calculations of both Siskind *et al.* (1998) and Evans *et al.* (1998), an increase in upper stratospheric H₂O of 0.34 ppmv between 1981 and 1995 would have a much smaller effect on O₃ than the decrease driven by the build-up of ClO.

Recent HALOE observations (Version 18) reveal a significant decline (10 to 20 ppbv/year) in the mixing ratio of upper stratospheric CH₄ between 1991 and 1996/1997 (Evans *et al.*, 1998; Nedoluha *et al.*, 1998a,b; Randel *et al.*, 1998b). Nedoluha *et al.* (1998a) have hypothesized that this change is due to decreased upwelling following the eruption of Mt. Pinatubo. A change in upper stratospheric CH₄ has important implications for the partitioning of Cl_y gases and for O₃ trends, because the $\text{Cl} + \text{CH}_4 \rightarrow \text{HCl} + \text{CH}_3$ reaction is the primary mechanism for conversion of reactive Cl species to the unreactive HCl reservoir. Siskind *et al.* (1998) find that the CH₄-driven increase in ClO causes a larger decrease in upper stratospheric O₃ between 1992 and 1995 than changes expected based on the increase in atmospheric chlorine loading or the decline in solar ultraviolet (UV) radiation during solar cycle 22. There have been no reports of trends of upper stratospheric CH₄ over longer time periods, but ATMOS observations obtained at Northern Hemisphere midlatitudes in 1985 and 1994 reveal approximately similar levels of upper stratospheric CH₄ (e.g., Figure 5 of Gunson *et al.*, 1990; Figure 2 of Abbas *et al.*, 1996a). The HALOE observations of significant recent trends for upper stratospheric CH₄ warrant further study owing to the important role played by CH₄ in the partitioning of Cl_y species. Better definition of the long-term trend of both H₂O and CH₄ would be aided not only by continued

observation but also by understanding the cause of the $\pm 20\%$ discrepancy for the H₂O content of the stratosphere measured by various in situ and satellite instruments (e.g., Dessler *et al.*, 1994; Abbas *et al.*, 1996b; Engel *et al.*, 1996; Harries *et al.*, 1996; Mote *et al.*, 1996; Rosenlof *et al.*, 1997) so that data from different instruments could be combined in a meaningful fashion.

There has recently been renewed debate concerning the importance of extraterrestrial sources of H₂O (e.g., Siskind and Summers, 1998, and references therein). Frank and Sigwarth (1997) have presented new observations of intense showers of comet-like objects entering the Earth's atmosphere. However, the conclusion that these images are actually due to extraterrestrial bodies has been called into question based on a dissenting interpretation of the Ultraviolet Imager data (Parks *et al.*, 1997) and an analysis that concludes objects as large as those originally proposed by Frank and Sigwarth (1993) should be readily and frequently visible from the ground, especially during dawn and dusk (Rizk and Dessler, 1997). Recent observations of enhanced layers of mesospheric H₂O (Peter, 1998; Siskind and Summers, 1998) and enhancements of the mixing ratio profile of H_{TOT} (2×CH₄ + H₂O) in the same altitude region (Hannegan *et al.*, 1998; Siskind and Summers, 1998) have been used to derive upper limits for the rate of influx of H₂O due to extraterrestrial sources. Hannegan *et al.* (1998) reported an upper limit of 2 Tg/year, at least a factor of 100 less than the influx rate suggested by Frank and Sigwarth (1997). Siskind and Summers (1998) reached similar conclusions and noted that the sharply peaked (in altitude) structure of the maximum of mesospheric H_{TOT} as well as observations of dry middle atmospheric air in the winter (i.e., descending) hemisphere both argue against an extraterrestrial source. The nearly conserved nature of H_{TOT} throughout all regions of the upper stratosphere and the overall dryness of the stratosphere demonstrate extraterrestrial sources of H₂O do not affect the budget of stratospheric hydrogen (Hannegan *et al.*, 1998; Siskind and Summers, 1998).

REACTIVE HYDROGEN SPECIES

Observations of OH and HO₂ as well as the precursors O₃, H₂O, and CH₄ provide a rigorous test of our understanding of the processes that regulate the abundance of hydrogen radicals. Our understanding of

UPPER STRATOSPHERIC PROCESSES

upper stratospheric HO_x has been guided by the numerous atmospheric observations described below, as well as the recognition that a larger quantum yield of $\text{O}(^1\text{D})$ from photolysis of O_3 (Michelsen *et al.*, 1994; DeMore *et al.*, 1997; Ravishankara *et al.*, 1998, and references therein) leads to an increase in calculated concentrations of $\text{O}(^1\text{D})$ and OH of $\sim 12\%$ and $\sim 6\%$, respectively, at 30 km (Michelsen *et al.*, 1994), with larger effects at lower altitudes.

An analysis of balloonborne observations of radicals and precursors obtained with a far-infrared Fourier transform spectrometer (FIRS-2) that detects atmospheric thermal emission in a limb-viewing geometry revealed generally good agreement (differences less than 10%) between theory and observation of OH between 25 and 36 km (Chance *et al.*, 1996). The largest discrepancy occurred near 38 km, where measured OH exceeded model estimates by $\sim 20\%$. Osterman *et al.* (1997) and Pickett and Peterson (1996) reached similar conclusions based on analyses of near-simultaneous profiles of OH obtained by the Far Infrared Limb Observing Spectrometer (FILOS) and HO_2 measured by the Submillimeter Limb Sounder (SLS), O_3 measured by an in situ UV photometer, and H_2O , CH_4 , and NO_y detected by the MkIV Fourier transform spectrometer. The measured profile for OH extended to 40 km altitude and was shown to agree with model values to better than 5%. Theory and observation of HO_2 agreed to better than 10% below 40 km. However, observed values of HO_2 exceeded model values by 20 to 30% between 40 and 50 km, although the discrepancy was within the uncertainty of measurement. A similar conclusion of $\sim 20\%$ excess HO_2 relative to standard models for altitudes near 38 km was reached by Chance *et al.* (1996) based on earlier FIRS-2 observations. Osterman *et al.* (1997) and Jucks *et al.* (1996) have shown that rates for removal of O_3 by the HO_x catalytic cycles inferred from simultaneous measurements of profiles of OH and HO_2 obtained by the FILOS, SLS, and FIRS-2 instruments between 30 and 50 km agree with theoretical removal rates to within the uncertainties of the atmospheric observations and laboratory measurements of the relevant kinetic rate constants.

Summers *et al.* (1997a), in contrast to the above studies, have concluded that a serious deficiency exists in our understanding of the processes that regulate HO_x in the upper stratosphere based on their analysis of observations of OH and O_3 obtained by the Middle Atmosphere High Resolution Spectrograph Investigation

(MAHRSI) (Conway *et al.*, 1996) and the Cryogenic Infrared Spectrometers and Telescopes for the Atmosphere (CRISTA) shuttle-borne instruments, and near-simultaneous profiles of H_2O and CH_4 obtained by HALOE. Concentrations of OH observed by MAHRSI were found to be 30 to 40% lower than calculated values near 50 km (Figure 6-6). Summers *et al.* (1997a) outlined two scenarios that would lead to good agreement between theory and observation of OH : either a 50% reduction in the rate of $\text{O} + \text{HO}_2 \rightarrow \text{OH} + \text{O}_2$ (based on an earlier suggestion by Clancy *et al.* (1994) from a study of ground-based microwave observations of HO_2 and O_3), or a 20% reduction in the rate of $\text{O} + \text{HO}_2 \rightarrow \text{OH} + \text{O}_2$ and a 30% increase in the rate of $\text{OH} + \text{HO}_2 \rightarrow \text{H}_2\text{O} + \text{O}_2$. Both scenarios predict lower concentrations of HO_2 in the upper stratosphere relative to standard model values, an important consequence that cannot yet be tested by shuttle and spaceborne instruments. Additionally, both

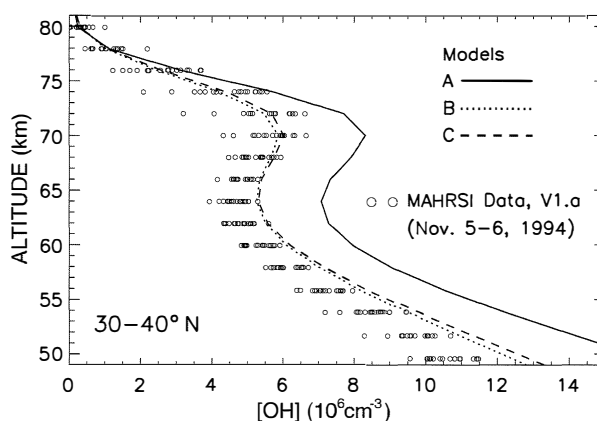


Figure 6-6. Concentration profiles of OH (open circles) retrieved by the Middle Atmosphere High Resolution Spectrograph Investigation (MAHRSI) instrument from 18 orbits of observations during 5 and 6 November 1994 between 30° and 40°N . The photochemical model results (lines, as indicated) at the appropriate local solar times were convolved with the MAHRSI weighting functions. Results are shown for three models. Model A used rate constants and cross sections from DeMore *et al.* (1994); model B used a 50% reduction for the rate constant of $\text{O} + \text{HO}_2 \rightarrow \text{OH} + \text{O}_2$; and model C used a 20% reduction for the rate constant of $\text{O} + \text{HO}_2 \rightarrow \text{OH} + \text{O}_2$ and a 30% increase for the rate constant of $\text{OH} + \text{HO}_2 \rightarrow \text{H}_2\text{O} + \text{O}_2$. Adapted from Summers *et al.* (1997a).

scenarios lead to a decrease in the removal rate of O_3 by catalytic cycles involving HO_x in the upper stratosphere because of the reduction in the rate of $O + HO_2$ (the rate-limiting step of the most important HO_x cycle) and the decrease in the concentration of HO_2 . The shuttle-borne measurements of OH (Summers *et al.*, 1997a) reach only to altitudes as low as 50 km and the balloonborne profiles (Pickett and Peterson, 1996; Chance *et al.*, 1996) typically extend upward to 40 km, limiting direct comparison of observations obtained by the two techniques. However, the MAHRSI retrievals are currently being extended downward to 45 km altitude and the balloonborne observations have been extended upward to 50 km (Jucks *et al.*, 1998), allowing for direct comparisons in the future.

Jucks *et al.* (1998) have recently presented FIRS-2 balloonborne measurements of OH and HO_2 to 50 km altitude (Figure 6-7). The profiles of OH reported by Jucks *et al.* (1998) were within 5% of model values between 30 and 50 km. However, observed concentrations of HO_2 exceeded calculated values by 20% between altitudes of 40 and 50 km. Observations of the $[OH]/[HO_2]$ ratio place constraints on the rates of $O + HO_2$ and $O + OH$, the reactions that control the partitioning of HO_x in the upper stratosphere. Jucks *et al.* (1998) concluded their observations of OH and HO_2 were best described by a model using rate constants for $O + HO_2$ and $OH + HO_2$ that are 25% slower than recommended values, adjustments consistent with the uncertainties for both reactions (DeMore *et al.*, 1997). The implications for catalytic removal of O_3 by HO_x were determined to be minor, however, because the decrease for the rate of $O + HO_2$ was offset by higher-than-expected concentrations of HO_2 . The observations of Jucks *et al.* (1998) and Summers *et al.* (1997a) appear to point to a significant difference in the concentration of upper stratospheric OH measured by the two spectrometers.

Observations of the abundance of HO_2 in the uppermost stratosphere and mesosphere obtained at Kitt Peak, Arizona, United States ($31^\circ N$), using microwave line-emission spectrometry exceeded model estimates by 25 to 45% (Clancy *et al.*, 1994; Sandor and Clancy, 1998). Agreement between theory and observation of HO_2 was obtained allowing for a 40% reduction in the rate of $O + HO_2$ (Sandor and Clancy, 1998). Because Clancy *et al.* (1994) and Sandor and Clancy (1998) do not obtain data below 50 km, the implications of these observations for the upper stratosphere are unclear.

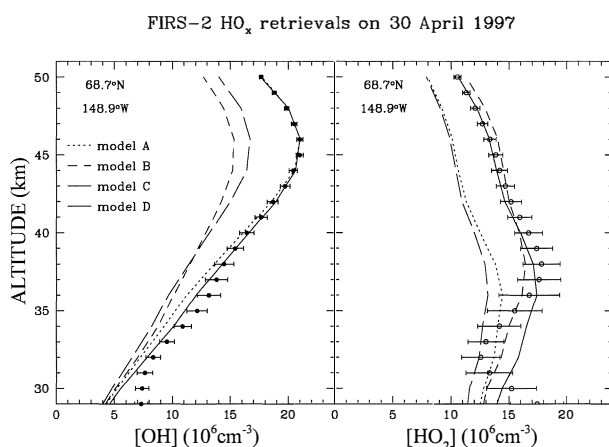


Figure 6-7. Concentration profiles of OH and HO_2 measured during mid-morning by FIRS-2 on 30 April 1997 near Fairbanks, Alaska ($65^\circ N$). Photochemical model results (lines, as indicated) are for the appropriate local solar time, constrained by FIRS-2 measurements of O_3 , H_2O , and CH_4 . Overhead O_3 was constrained by a near-coincident profile measured by the ILAS instrument on ADEOS. Results are shown for four models. Models A, B, and C are the same as described by Summers *et al.* (1997a) (see caption for Figure 6-6), except that standard kinetic parameters originated from DeMore *et al.* (1997). Model D, which provides a good simulation of measured OH and HO_2 , is the same as model A except that the rates of both $O + HO_2 \rightarrow OH + O_2$ and $OH + HO_2 \rightarrow H_2O + O_2$ were reduced by 25%. Adapted from Jucks *et al.* (1998).

However, mesospheric observations provide a strong test of the link between HO_x chemistry and O_3 , because nitrogen and chlorine radicals do not contribute significantly to loss of mesospheric O_3 . The reductions for the rate constant of $O + HO_2$ (which exceed the reported uncertainties of the laboratory measurements) proposed by Summers *et al.* (1997a) and Sandor and Clancy (1998) would, in the absence of any other kinetic changes, resolve the long-standing ozone deficit problem in the lower mesosphere and also have important implications for the balance between production and loss of upper stratospheric O_3 . However, this kinetic change alone leads to a poorer simulation of the observed diurnal variation of ozone in the upper stratosphere and mesosphere (Connor *et al.*, 1994) than found using standard kinetic parameters (Siskind *et al.*, 1995).

Long-term observations of the column abundance of OH have been obtained using polyetalon pressure scanned interferometric optical spectrometers at Fritz Peak Observatory, Colorado, United States (40°N) (Burnett and Burnett, 1996), and more recently at Lauder, New Zealand (45°S) (Wood *et al.*, 1994). The observations of column OH tended to exceed theory by about 30% and exhibited a steeper increase near noon than calculated by models. Other features of these observations have also not been adequately explained, such as the tendency of column OH in the Southern Hemisphere to exceed values in the Northern Hemisphere by ~20% (Wood *et al.*, 1994) and the sudden drop in column OH over Fritz Peak observed during late summer and fall of 1991 to 1995, relative to comparable seasonal averages observed during 1980 to 1990 (Burnett and Burnett, 1996). It is also unclear why the column abundance of OH reported by Burnett and Burnett (1996) peaks at considerably higher levels, $(8 \text{ to } 10) \times 10^{13} \text{ cm}^{-2}$, than peak values of $(5 \text{ to } 6) \times 10^{13} \text{ cm}^{-2}$ measured by Iwagami *et al.* (1995) over Tokyo, Japan (35.7°N) during 1992. Recently published observations of a 3-year record of column OH over Tokyo are 20 to 30% less than values calculated using a one-dimensional model (Iwagami *et al.*, 1998). The implications of these observations to our understanding of upper stratospheric photochemistry are difficult to assess owing to the large contribution from the mesosphere to the column abundance of OH, unexplained features of the observations, and the considerable differences between measurements obtained by different groups.

The observations of OH and HO₂ by different techniques and instruments summarized above lead to conflicting conclusions about how well we understand the abundance of HO_x radicals in the upper stratosphere. One consistent theme that has emerged from numerous investigations of upper stratospheric HO_x is that observations are better explained by a reduction in the currently recommended rate constant of the reaction $\text{O} + \text{HO}_2 \rightarrow \text{OH} + \text{O}_2$ (Clancy *et al.*, 1994; Summers *et al.*, 1997a; Jucks *et al.*, 1998; Sandor and Clancy, 1998). Further atmospheric and laboratory observations are required to resolve the discrepancy between measurements of OH and HO₂ by the various instruments and techniques. Simultaneous measurements of both OH and HO₂ are particularly useful owing to the important constraint provided by the [OH]/[HO₂] ratio and the role of both gases in the catalytic removal of upper stratospheric O₃.

6.3.2 Nitrogen Species

The importance of catalytic removal of ozone by oxides of nitrogen was first established by Crutzen (1970). Loss of ozone by nitrogen radicals occurs mainly by a single cycle limited by the reaction $\text{NO}_2 + \text{O} \rightarrow \text{NO} + \text{O}_2$. Reactive nitrogen (NO_y) is produced in the stratosphere by a channel of the reaction of O(¹D) with N₂O. Other processes such as lightning and exhaust from aircraft might possibly affect the abundance of NO_y in the lower stratosphere but are not thought to be important for altitudes above 30 km. Loss of stratospheric NO_y occurs at high altitudes by the reaction $\text{N} + \text{NO} \rightarrow \text{N}_2 + \text{O}$ and at low altitudes by denitrification in the polar regions or by transport to the troposphere, where nitric acid (HNO₃) is removed by precipitation.

THE NITROGEN BUDGET

Nitrous oxide, the dominant source of upper stratospheric NO_y, is produced by microbial processes in soils and oceans and is photochemically stable in the troposphere. Its tropospheric concentration is currently rising at a rate of ~0.25%/year. Changes in NO_y in the upper stratosphere associated with the long-term rise in N₂O have a small effect on O₃ over decadal time scales (Jackman *et al.*, 1996) but could play an important role in regulating ozone and the radiative state of the stratosphere on centennial time scales (Nevison and Holland, 1997).

The global budget of N₂O has long been the subject of controversy, hindering efforts to identify the cause of the observed atmospheric increase (Watson *et al.*, 1990). Recent estimates of the sources and sinks of N₂O have led to a more or less balanced budget, due mainly to upward revisions in the strength of the agricultural and natural oceanic sources (e.g., Prather *et al.*, 1995; Nevison and Holland, 1997; Mosier *et al.*, 1998). It is believed that the long-term rise in N₂O is due to anthropogenic nitrogen fixation associated with the production of fertilizer (e.g., Nevison and Holland, 1997). However, there are still large uncertainties concerning the budget of N₂O, particularly the strength of its source.

Isotopic analyses first reported by Kim and Craig (1993) and later confirmed by Rahn and Whalen (1997) revealed that stratospheric N₂O is enriched in both ¹⁵N and ¹⁸O relative to tropospheric, soil, and oceanic N₂O. A laboratory study of photodissociation of N₂O at 185 nm, the peak of the N₂O absorption continuum, showed much smaller fractionation than required to explain the

enrichment of stratospheric N_2O (Johnston *et al.*, 1995). These studies and the possibility of an imbalance for the source and sink of N_2O have led to numerous proposals of the possible existence of upper stratospheric sources of N_2O (e.g., Prasad, 1994, 1997; McElroy and Jones, 1996). If N_2O were shown to have a significant upper stratospheric source, there could be important consequences for NO_y and O_3 .

The dilemma posed by the isotopic analyses of N_2O appears to have been resolved. Yung and Miller (1997) have shown, based on an analysis of laboratory data for the zero point vibrational energies of heavy isotopomers of N_2O , that the photolytic destruction of N_2O has an isotopic signature that maximizes near 205 nm. They pointed out that the 185-nm region, the portion of the absorption spectrum probed by the laboratory experiment of Johnston *et al.* (1995), is not expected to exhibit strong fractionation. Their model was able to explain the observed enrichments of both ^{15}N and ^{18}O without invoking stratospheric sources. Furthermore, they predicted that different degrees of fractionation will occur depending on the position of the ^{15}N substitution in N_2O , a hypothesis testable by infrared measurements capable of distinguishing different isotopomers with the same atomic weight. Yung and Miller (1997) also stressed the importance of future laboratory studies of photodissociative fractionation of N_2O near 205 nm.

Simultaneous measurements of N_2O and NO_y provide a powerful test of our understanding of the budget of nitrogen oxides in the upper stratosphere. Many studies have focused on observations obtained in the lower stratosphere, where deviations from the expected compact, near-linear anticorrelations of NO_y versus N_2O (Plumb and Ko, 1992) have been used to quantify permanent removal of HNO_3 by polar stratospheric clouds. Two recent studies, however, have focused on data for NO_y and N_2O obtained in the upper stratosphere.

Kondo *et al.* (1996) showed that correlations of NO_y versus N_2O calculated using the Atmospheric and Environmental Research, Inc. (AER) 2-D model agreed well with observations obtained by both in situ balloonborne instruments and by ATMOS (Figure 6-8). Their comparisons focused on the altitude region below the peak level of NO_y (~17 ppbv near 35 km). Nevison *et al.* (1997) have examined more closely the distribution of NO_y at altitudes above the peak mixing ratio. They concluded that abundances of NO_y found using the Garcia and Solomon 2-D model are up to 50% larger than concentrations observed between 40 and 55 km by

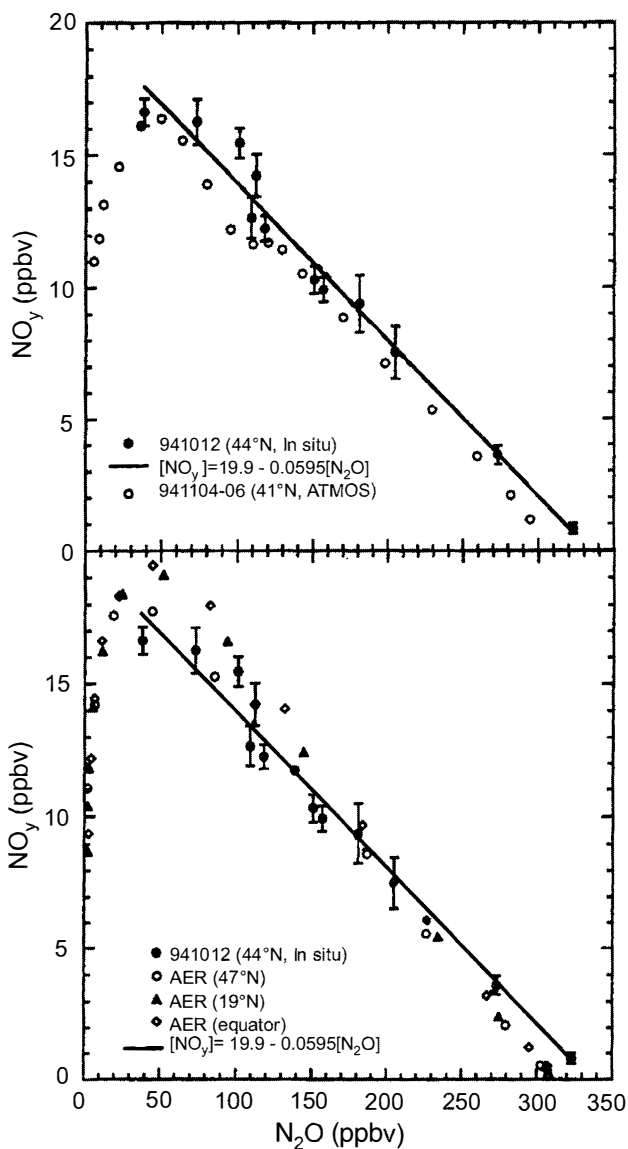


Figure 6-8. Volume mixing ratios of NO_y versus N_2O observed by balloonborne in situ instruments at 44°N during October 1994 (closed circles, both panels) and by ATMOS at 41°N during November 1994 (open circles, top panel). The solid line shows a linear fit to the balloonborne data (both panels). Bottom panel shows model results from the AER 2-D model for 47°N (open circles), 19°N (solid triangles), and 0° (open diamonds). Adapted from Kondo *et al.* (1996).

UPPER STRATOSPHERIC PROCESSES

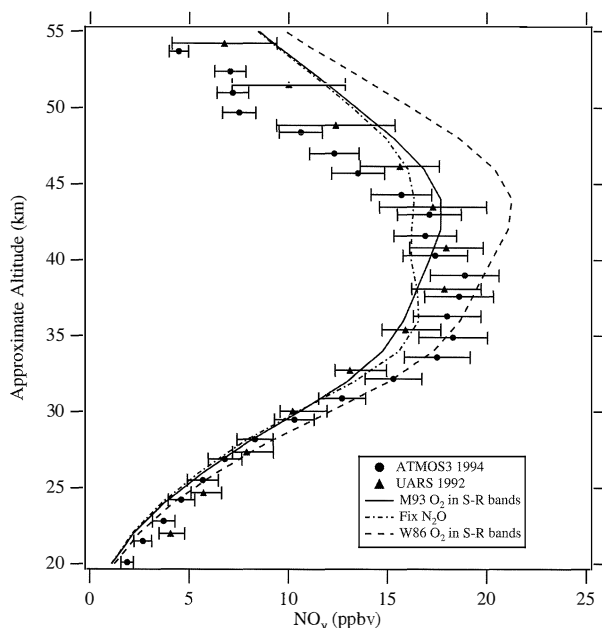


Figure 6-9. Volume mixing ratio profiles of NO_y measured in November at 24°N by ATMOS (circles) and UARS (triangles) compared to profiles calculated by the Garcia and Solomon 2-D model (Nevison *et al.*, 1997, and references therein) using the Minschwaner *et al.* (1993) formulation for O_2 photolysis in the Schumann-Runge bands (solid line), a fixed N_2O profile specified from CLAES observations (long dashed line), and the WMO (1986) formulation for O_2 photolysis in the Schumann-Runge bands (short dashed line). All calculations used the Minschwaner and Siskind (1993) formulation for the photolysis rate of nitric oxide (NO) and other kinetic parameters from DeMore *et al.* (1994). Adapted from Nevison *et al.* (1997).

instruments aboard UARS as well as ATMOS (Figure 6-9). Nevison *et al.* (1997) stated that this result was relatively insensitive to assumptions concerning transport because of the short photochemical lifetime of NO_y in the upper stratosphere. They suggested an increase in the photochemical sink for NO_y was necessary to resolve the discrepancy and noted this could be accommodated by an increase in either the photolysis rate of NO or the $\text{N} + \text{NO}$ rate constant, or a decrease in the $\text{N} + \text{O}_2$ rate constant. Each of these rates is subject to considerable uncertainty.

Descent during polar winter of NO_y produced by auroral processes in the thermosphere has been thought

to be an additional source of upper stratospheric NO_y . Recent HALOE and ATMOS observations have confirmed that such a source most likely does exist (Callis *et al.*, 1996; Rinsland *et al.*, 1996; Siskind and Russell, 1996). However, an analysis of HALOE observations of NO_x has suggested models may overestimate the magnitude of this source (Siskind *et al.*, 1997). An analysis of Improved Stratospheric and Mesospheric Sounder (ISAMS) data indicates mesospheric NO_y formed during particular precipitating electron events affects upper stratospheric NO_2 to latitudes as low as 30° to 40° in both hemispheres (Callis and Lambeth, 1998). It is unclear whether this process has an appreciable effect on the overall budget of stratospheric NO_y (Callis and Lambeth, 1998).

Theory and observation of NO_y appear to be in reasonably good agreement between 25 and 40 km (Nevison *et al.*, 1997; Kondo *et al.*, 1996), the altitude range where photochemical loss of O_3 is dominated by the nitrogen oxide cycle (e.g., Jucks *et al.*, 1996; Osterman *et al.*, 1997; see also Figure 6-2). The discrepancy at higher altitudes noted by Nevison *et al.* (1997) is unlikely to have a profound effect on calculated values of O_3 because of the relatively minor role of the NO_x cycle above 40 km.

NITROGEN PARTITIONING

Recent satellite and balloonborne observations have allowed for stringent tests of our understanding of the partitioning of the NO_y family of gases. Accurate knowledge and use of observed profiles of O_3 , and aerosol surface area at lower altitudes, are essential for proper interpretation of these observations (e.g., Morris *et al.*, 1997). Sen *et al.* (1998) examined concentration profiles of NO, NO_2 , HNO_3 , HNO_4 , N_2O_5 , and ClONO_2 obtained at sunset between 20 and 39 km by the MkIV Fourier transform interferometer using solar occultation. They showed good agreement between measured profiles of the NO_y gases and calculated concentrations, with the only serious disagreement being the tendency of the observed $[\text{NO}_2]/[\text{NO}]$ and $[\text{NO}_2]/[\text{HNO}_3]$ ratios to exceed calculated values for altitudes below 30 km (Figure 6-10). They stated that these discrepancies could largely be explained by the use of recent laboratory measurements of the pressure broadened half-widths of NO_2 lines near 2900 cm^{-1} as well as a 15% increase in the rate constant of $\text{NO} + \text{O}_3 \rightarrow \text{NO}_2 + \text{O}_2$ at temperatures near 220 K that would be consistent with existing laboratory measurements at low temperature.

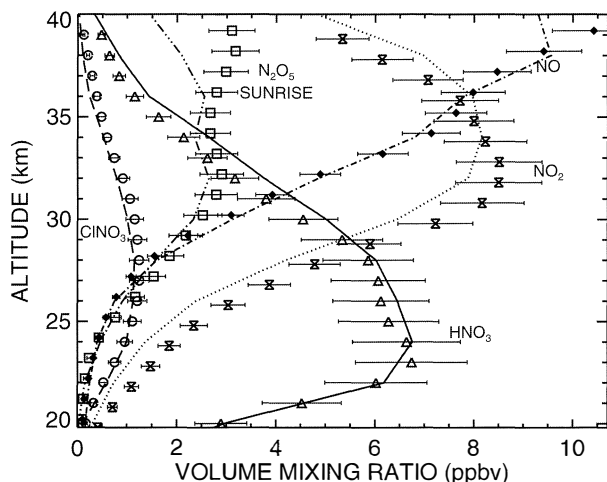


Figure 6-10. Volume mixing ratio profiles of NO, NO₂, HNO₃, and ClONO₂ measured at sunset and of N₂O₅ measured at sunrise by the MkIV balloonborne FTIR instrument at 35°N on 25 September 1993 (symbols, as indicated) compared to calculated profiles assuming photochemical steady state over a 24-hour period (lines, as indicated). Model profiles were constrained by values for NO_y, Cl_y, O₃, H₂O, CH₄, etc., from MkIV, and aerosol surface area from SAGE II, and are shown for the appropriate solar times. Calculations used kinetic parameters from DeMore *et al.* (1994) except for the Michelsen *et al.* (1994) formulation for the quantum yield of O(¹D). Adapted from Sen *et al.* (1998).

Modeling studies of NO_x partitioning have been affected by recent revisions to the rate constant of the OH + NO₂ + M → HNO₃ + M reaction. Donahue *et al.* (1997) reported that, at room temperature, the rate constant for the reaction OH + NO₂ + M is about 20% lower than the previously recommended rate constant (DeMore *et al.*, 1994). In contrast, for temperatures and pressures typical of the upper stratosphere, the DeMore *et al.* (1997) recommendation for the rate constant of OH + NO₂ + M is larger than the rate constant given by DeMore *et al.* (1994). Use of the DeMore *et al.* (1997) rate constant leads to lower values of the [NO_x]/[NO_y] ratio near 30 km compared to models based on the DeMore *et al.* (1994) value, resulting in poorer agreement with the observed NO_x/NO_y ratio (Sen *et al.*, 1998).

Morris *et al.* (1997) examined the ratio of NO_x/NO_y between 20 and 35 km based on observations by the HALOE and Cryogenic Limb Array Etalon Spectro-

meter (CLAES) instruments aboard UARS and calculations using the Goddard photochemical model constrained by observed O₃ and aerosol surface area. They concluded the measured [NO_x]/[NO_y] ratio was systematically higher than the model at all altitudes between ~22 to ~35 km, with the largest disparity between ~26 and 31 km. The disparity was found to decrease with altitude above ~31 km (Figure 6-11). Similar conclusions regarding the tendency of the [NO_x]/[NO_y] ratio to exceed theory between 20 and 30 km were reached by Rinsland *et al.* (1996), Kondo *et al.* (1997), Lary *et al.* (1997), and Sen *et al.* (1998). For altitudes above 30 km, theory and observation of the [NO_x]/[NO_y] ratio have been shown to be in good agreement by many studies (Rinsland *et al.*, 1996; Kondo *et al.*, 1997; Lary *et al.*, 1997; Morris *et al.*, 1997; Sen *et al.*, 1998). The observed upper stratospheric ratio of [NO₂]/[NO] is also simulated reasonably well (Sen *et al.*, 1998). Consequently, these measurements indicate that the catalytic removal of O₃ by the NO_x cycle in the upper stratosphere proceeds at a rate consistent with theory (Jucks *et al.*, 1996; Osterman *et al.*, 1997).

Further evidence of a strong fundamental understanding of the processes that partition NO_y gases was shown by two studies that examined the relation between NO_x and N₂O₅. Nevison *et al.* (1996) showed that sunset/sunrise ratios for NO_x measured by HALOE are consistent with the calculated diurnal variation of N₂O₅. Sen *et al.* (1998) similarly concluded that the measured variation of concentrations of N₂O₅ and NO_x between sunrise and sunset agreed well with model simulations and exhibited the expected ~2:1 stoichiometry at all altitudes between 22 and 35 km. These studies have important implications also for the lower stratosphere, because the hydrolysis of N₂O₅ on sulfate aerosols is an important sink for NO_x below 30 km.

The most notable exception to the numerous studies showing relatively good understanding of the partitioning of NO_y gases in the upper stratosphere is the study of Kawa *et al.* (1995) that focused on CLAES and ISAMS measurements of N₂O₅ and HNO₃ at high altitude. An analysis of these observations using the Goddard 3-D model indicated the occurrence of an unknown process that converts N₂O₅ to HNO₃ above ~35 km in polar regions during winter. Kawa *et al.* (1995) suggested heterogeneous conversion on hydrated ion clusters as a possible explanation for the observations. Bekki *et al.* (1997) suggested that the observed partitioning may be caused in part by enhanced

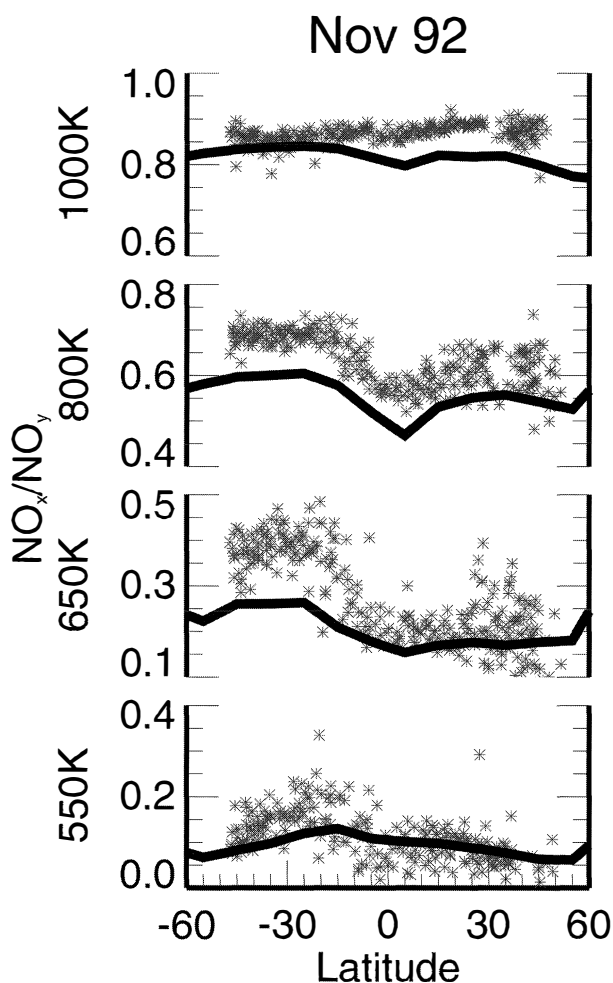


Figure 6-11. The NO_x/NO_y ratio at four potential temperature levels (550, 650, 800, and 1000 K that correspond to approximately 22, 26, 31, and 35 km, respectively) for November 1992 based on a trajectory mapped analysis of UARS data (asterisks) compared to calculated values from the Goddard 2-D model (solid line), constrained by distributions of temperature, O_3 , H_2O , N_2O , and CH_4 from UARS instruments and aerosol surface area from SAGE II. Kinetic parameters from DeMore *et al.* (1994). Adapted from Morris *et al.* (1997).

concentrations of small sulfate aerosol particles. Although this problem bears further investigation, it is important to note that the anomalous ratios of $[\text{N}_2\text{O}_5]/[\text{HNO}_3]$ are confined to high latitudes. Ratios observed for the midlatitude upper stratosphere agree well with theory (Kawa *et al.*, 1995).

Catalytic removal of O_3 by the NO_x cycle in the upper stratosphere has been shown to proceed at a rate consistent with theory *provided the distribution of NO_y is known accurately* (e.g., Jucks *et al.*, 1996; Osterman *et al.*, 1997). However, few studies have focused on quantitative comparisons of calculated and observed NO_y in the upper stratosphere. The substantial variability in the concentration of NO_y between 30 and 50 km exhibited by 2-D model simulations underscores the need for further investigations (Park *et al.*, 1998). A wealth of existing balloon (Kondo *et al.*, 1996; Oelhaf *et al.*, 1996; Sen *et al.*, 1998), ATMOS (Rinsland *et al.*, 1996), and UARS (Gordley *et al.*, 1996) observations of NO_y in the upper stratosphere are available to better quantify our understanding of the seasonal and altitude distribution of NO_y . Instruments on each of these platforms also measure the concentration of N_2O ; correlation diagrams of NO_y (sink) versus N_2O (source) provide a stringent test of our understanding of processes that regulate NO_y . Nevison *et al.* (1997) have pointed out possible deficiencies in our understanding of upper stratospheric NO_y that should be addressed by future studies.

6.3.3 Chlorine Species

Catalytic removal of ozone by chlorinated compounds derived from industrial chlorofluorocarbons (CFCs) was first suggested by Molina and Rowland (1974). Chlorine monoxide (ClO) participates in numerous catalytic cycles that lead to removal of ozone in the lower stratosphere. In the upper stratosphere, however, the cycle limited by the reaction $\text{ClO} + \text{O} \rightarrow \text{Cl} + \text{O}_2$ is the only significant halogen-related loss process. Organic chlorine gases such as CFCs and CCl_4 are extraordinarily inert in the troposphere, demonstrated by observations of nearly uniform volume mixing ratios for these compounds in the lower atmosphere (Montzka *et al.*, 1996). These gases decompose in the stratosphere due to increased levels of ultraviolet radiation as well as much higher concentrations of OH and $\text{O}(^1\text{D})$. Inorganic chlorine species (Cl_y) are produced in the stratosphere following photolysis and reaction of the organic source species. Because HCl and sodium chloride (NaCl) are highly water soluble, they are effectively scavenged in the troposphere, and air entering the stratosphere does not normally contain significant concentrations of either compound. Removal of Cl_y from the stratosphere occurs by transport to the troposphere, where HCl is removed by precipitation.

THE CHLORINE BUDGET

The global distribution of CCl_2F_2 (CFC-12) was observed for six seasons (January 1992 to May 1993) by the CLAES instrument aboard UARS (Nightingale *et al.*, 1996). The observations indicate features such as upward bowing of isopleths in the tropics and minimum values in the polar regions consistent with progressively faster removal of CFC-12 at higher altitudes. The overall patterns and morphology of the CLAES observations of CFC-12 are simulated well by the Lawrence Livermore National Laboratory (LLNL) 2-D model and are also consistent with profiles of CFC-12 measured by ATMOS, MkIV, and a whole-air sampler (Nightingale *et al.*, 1996; see also Section 6.2).

Our understanding of the budget of chlorinated compounds can be tested in a simpler and more precise manner than for the hydrogen and nitrogen families of gases owing to the long lifetime of Cl_y at all levels in the stratosphere and the fact that the entire chlorine content of the organic source molecules is converted directly to Cl_y gases. In contrast, only a fraction of N_2O is converted to NO_y , and this fraction varies with altitude, latitude, and season. The sum of the total organic and inorganic chlorine content should be nearly uniform throughout the stratosphere, with slight variations due to the ensemble age of air parcels that reflects the changing tropospheric burden of organic chlorine. Zander *et al.* (1996) constructed profiles of the total organic chlorine content (CCl_y) of the midlatitude stratosphere during November 1994 from ATMOS and balloon measurements of the eight most important chlorinated source gases. The profile of CCl_y was compared to measurements of HCl and ClONO_2 obtained by ATMOS, ClO from the shuttle-borne Millimeter-wave Atmospheric Sounder (MAS), and HOCl from the MkIV interferometer (Figure 6-12). The total chlorine burden of the stratosphere, defined as $\text{Cl}_{\text{TOT}} = [\text{CCl}_y] + [\text{HCl}] + [\text{ClONO}_2] + [\text{ClO}] + [\text{HOCl}] + [\text{COCIF}]$, was shown to be nearly constant with altitude at a value of ~ 3.5 ppbv.

The stratospheric chlorine loading derived by Zander *et al.* (1996) for 1994 is similar to the tropospheric organic chlorine content that prevailed in 1989-1990 (Kaye *et al.*, 1994). Observations of CO_2 , SF_6 , and HF have demonstrated that upper stratospheric air at midlatitudes is about 5-6 years old (Hamisch *et al.*, 1996; Russell *et al.*, 1996; Sen *et al.*, 1996; see also Chapter 7 and Section 6.2), accounting for the ~ 6 -year lag in the chlorine loading of the upper stratosphere relative to the

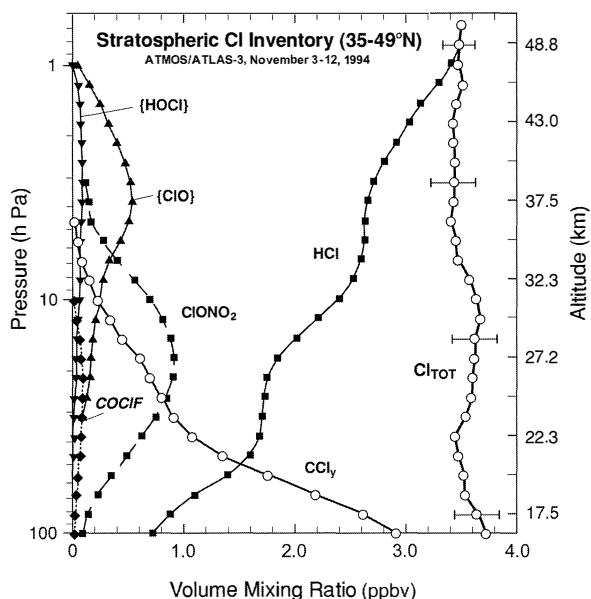


Figure 6-12. Profiles of CCl_y (total chlorine content of organic source gases) for the Northern Hemisphere midlatitude region based on ATMOS measurements during November 1994 (the Atmospheric Laboratory for Applications and Science-3 (ATLAS-3) mission) of CCl_3F , CCl_2F_2 , CHClF_2 , and CH_3Cl as well as in situ measurements of CH_3CCl_3 and $\text{C}_2\text{Cl}_3\text{F}_3$ obtained by the Research Center Jülich cryogenic whole-air sampler during a balloon flight in October 1994. Profiles of HCl and ClONO_2 were obtained by ATMOS during the same mission. The braces denote gases whose mixing ratio profile was measured by an instrument other than ATMOS. The profile for ClO was measured by the MAS experiment on the same ATLAS-3 Space Shuttle payload (Aellig *et al.*, 1996b) and the profile for HOCl was measured by the MkIV FTIR during September 1993 at 32°N . The profile for chlorofluorocarbonyl (COCIF) originates from a model calculation (Zander *et al.*, 1996). Cl_{TOT} represents a summation of concentrations of CCl_y , HCl, ClONO_2 , ClO, HOCl, and COCIF. Adapted from Zander *et al.* (1996).

surface. The only organic source gas with a significant natural source is CH_3Cl , which contributes about 0.55 ppbv to the organic chlorine content of the troposphere (Kaye *et al.*, 1994; Chapter 2). The observations of Zander *et al.* (1996) provide strong scientific evidence that the bulk of stratospheric inorganic chlorine is derived

UPPER STRATOSPHERIC PROCESSES

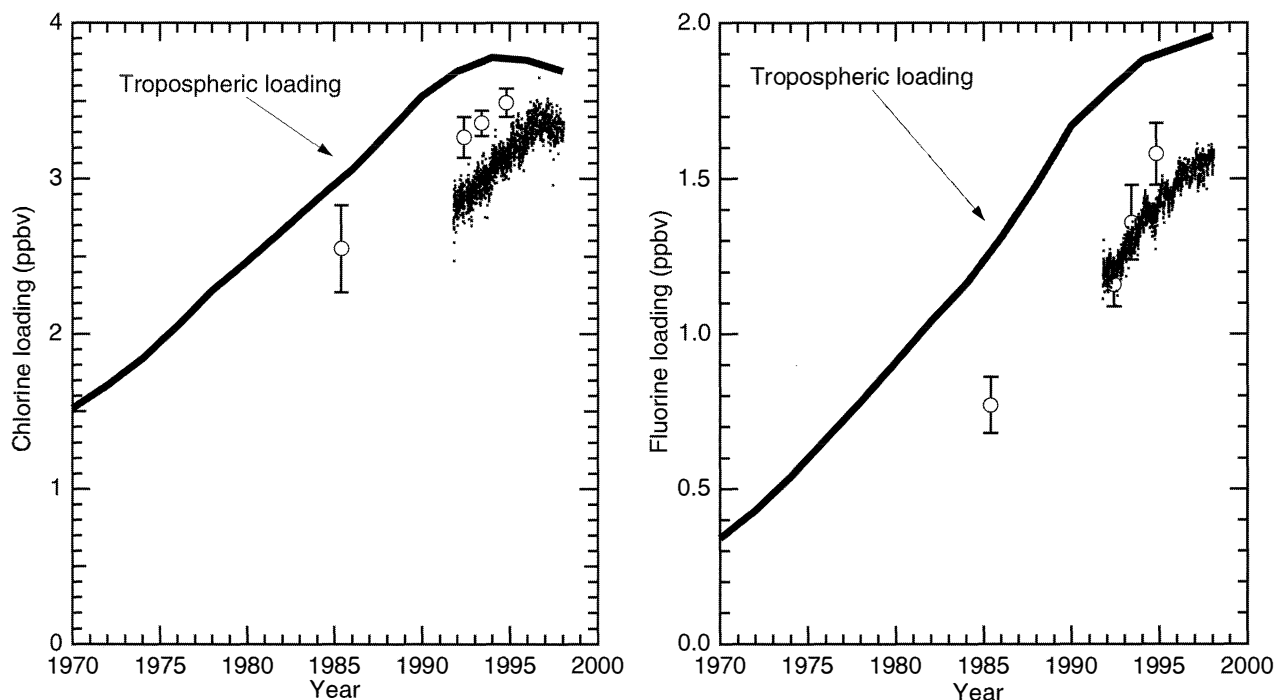


Figure 6-13. The concentration of HCl (left panel) and HF (right panel) in the upper stratosphere (near 55 km altitude) measured by ATMOS during Space Shuttle flights in 1985, 1992, 1993, and 1994 (circles with error bars) and measured by HALOE (dots) since October 1991. The HALOE points represent daily global average values of observations in the 54-56 km altitude range. The observations are compared to estimates of the total chlorine and fluorine content of the troposphere calculated assuming emissions and lifetimes from Kaye *et al.* (1994) and recent measurements of the tropospheric halogen burden (Montzka *et al.*, 1996). The offset between the atmospheric observations of HCl and the tropospheric chlorine loading curve represents the approximately 5 to 6-year age of stratospheric air (Harnisch *et al.*, 1996; Waugh *et al.*, 1997; see also Chapter 7 and Section 6.2). The temporal offset between upper stratospheric HF and tropospheric fluorine loading appears longer than the offset for HCl because HF constitutes only ~80% of the total fluorine abundance at 55 km (Russell *et al.*, 1996). Adapted from Gunson *et al.* (1994, 1996) and Russell *et al.* (1996) (adapted to present time and updated for Version 18 HALOE retrievals).

from the decomposition of organic chlorine compounds produced industrially, released at the ground, and transported to the stratosphere.

Further evidence of the connection between inorganic chlorine loading in the upper stratosphere and the release of industrial chlorine compounds at the ground is provided by measurements of the long-term trend in upper stratospheric HCl. Theoretical models indicate that the vast majority of inorganic chlorine should reside in the form of HCl for altitudes greater than 55 km (e.g., Minschwaner *et al.*, 1993). Gunson *et al.* (1994, 1996) reported measurements of HCl near 55 km by ATMOS in 1985, 1992, 1993, and 1994 (Figure 6-13) that showed an increase in the chlorine loading of the upper

stratosphere that followed the increasing tropospheric burden of chlorine, with about a 6-year lag due to the ensemble age of stratospheric air. Observations of upper stratospheric HCl by HALOE (Russell *et al.*, 1996) between October 1991 and the present show a similar increase in the chlorine burden of the upper stratosphere (Figure 6-13). The small offset between the HALOE and ATMOS measurements bears further investigation, but both datasets reveal a similar rate of increase for upper stratospheric HCl. The record provided by ATMOS extending back to 1985 and the thousands of observations by HALOE during the past 7 years provide confidence that the build-up of upper stratospheric HCl closely mirrors the increasing burden of tropospheric chlorine.

Finally, the long-term records of column HCl above the International Scientific Station of the Jungfrauoch (ISSJ) and above the Kitt Peak National Solar Observatory, discussed in Chapter 1, are consistent with the expected build-up of Cl_y during the past several decades.

Volcanic activity has the potential to alter the HCl content of the stratosphere. Coffey (1996) has recently reviewed observations of the impact of recent volcanic activity on stratospheric chlorine. Following the eruption of El Chichón in 1982, a 40% enhancement of the column abundance of HCl was observed near 35°N , the northern limit of the immediate deposition of volcanic debris to the stratosphere. If this increase were assumed to apply to the entire area covered by the volcanic cloud, the global increase of stratospheric HCl would be about 9% (Coffey, 1996). Observations following the eruption of Mt. Pinatubo in 1991, which perturbed the stratospheric aerosol layer by a considerably larger degree than El Chichón, showed a much smaller increase in column HCl (Coffey, 1996). Tabazadeh and Turco (1993) have provided a theoretical framework for the scavenging of HCl during the early phases of a volcanic eruption. Injection of HCl to the stratosphere following the eruption of El Chichón has been attributed to the high content of halite (NaCl) particles in the volcanic plume (Woods *et al.*, 1985; Coffey, 1996). Thus, while there is evidence volcanoes can deposit HCl directly to the

stratosphere, the perturbation to Cl_y between 1980 and present from volcanoes has been small compared to the build-up of Cl_y from industrial chlorinated source gases (Gunson *et al.*, 1994; Coffey, 1996; Russell *et al.*, 1996).

The final evidence that CFCs are indeed transported to the stratosphere, where they subsequently decompose to supply the majority of stratospheric Cl_y , is provided by observations of HF. There are no known natural sources of HF in the middle atmosphere, except the sporadic injection of HF into the stratosphere by volcanoes. Profiles of HF measured by MkIV and globally by HALOE show near-zero values at the tropopause, consistent with no significant transport of HF into the stratosphere (e.g., Sen *et al.*, 1996). The total fluorine budget of the stratosphere, defined in a similar manner to the total chlorine budget, was shown to be nearly constant with altitude and to agree well with values calculated by the Goddard 2-D model, demonstrating that stratospheric HF is supplied by the decomposition of CFCs (Sen *et al.*, 1996) (Figure 6-14). Observations by ATMOS (Gunson *et al.*, 1996) and HALOE (Russell *et al.*, 1996) revealed rates of increase for upper stratospheric HF similar to the rising tropospheric burden of fluorine, which is attributed entirely to CFCs (Figure 6-13). Observations of the increase in column HF above the ISSJ at the Jungfrauoch lead to similar conclusions (Chapter 1, Figure 1-9).

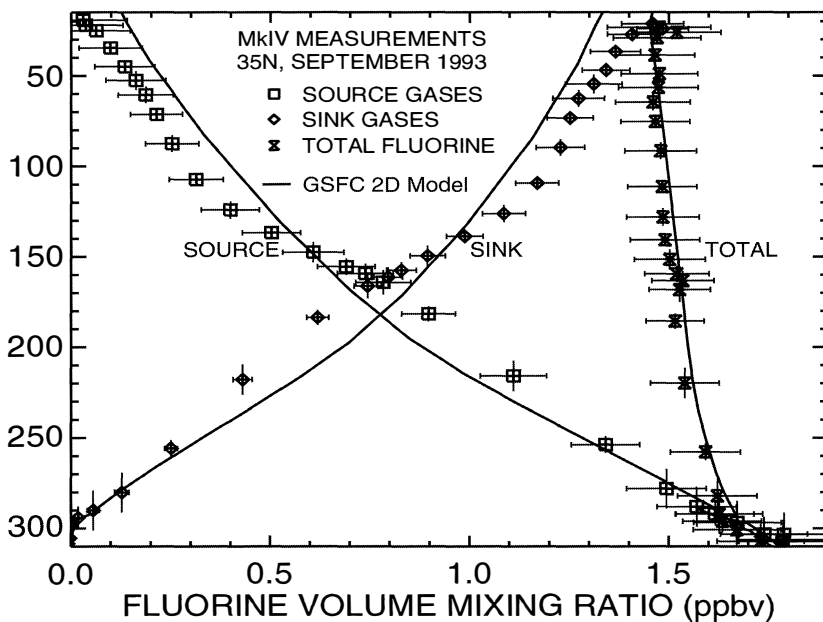


Figure 6-14. Profiles of the total organic fluorine content of source gases CCl_3F , CCl_2F_2 , CHClF_2 , and $\text{C}_2\text{Cl}_3\text{F}_3$ and total inorganic fluorine content of sink gases HF and carbonyl fluoride (COF_2) measured by the MkIV FTIR at 35°N during September 1993 (symbols, as indicated). The concentration profile for COClF , a minor source gas not measured by MkIV, has been calculated by the Goddard Space Flight Center (GSFC) 2-D model and added to the measured sink gas profile. Total fluorine (symbols, as indicated) represents the sum of organic and inorganic fluorine. Calculated profiles for organic, inorganic, and total fluorine from the GSFC 2-D model are also shown. Adapted from Sen *et al.* (1996).

UPPER STRATOSPHERIC PROCESSES

Recent observations of HF at 55 km altitude by HALOE reveal a reduction in the growth rate of HF (Consideine *et al.*, 1997) consistent with the decline in growth rates of tropospheric CFC-11 and CFC-12 in the early 1990s (Montzka *et al.*, 1996) (Figure 6-13). The measurement of Cl_{TOT} at 55 km by HALOE agrees to within 2% compared to Cl_{TOT} obtained by shifting the tropospheric organic source gas observations forward by a lag time determined from the HALOE measurements of HF and tropospheric fluorine measurements (Russell *et al.* (1996), adjusted to include additional data and updated using Version 18 retrievals). There is consensus among the scientific community, and no observational evidence to the contrary, that the vast majority of inorganic chlorine in the upper stratosphere is derived from industrial chlorine compounds released at the ground.

INORGANIC CHLORINE PARTITIONING

Recent atmospheric and laboratory observations have led to an accurate and apparently complete understanding of the partitioning of species within the Cl_y family. Prior to the previous Assessment (WMO, 1995), it had been established that models allowing for production of HCl only via reactions of Cl with hydrocarbons and $Cl + HO_2 \rightarrow HCl + O_2$ tended to underestimate concentrations of HCl and overpredict concentrations of $ClONO_2$, ClO, and HOCl for altitudes above ~24 km (e.g., McElroy and Salawitch, 1989; Allen and Delitsky, 1991; Natarajan and Callis, 1991; Stachnik *et al.*, 1992; Toumi and Bekki, 1993). Suggestions for resolving the disagreement involved increasing the production rate of HCl either by enhancing the rate of $Cl + HO_2 \rightarrow HCl + O_2$ (Allen and Delitsky, 1991) or by including a channel for formation of HCl from the reaction of $ClO + OH$ (McElroy and Salawitch, 1989; Natarajan and Callis, 1991; Stachnik *et al.*, 1992; Toumi and Bekki, 1993).

Numerous recent studies involving simultaneous observation of a more complete set of Cl_y and related gases have substantiated these earlier findings. Chance *et al.* (1996) concluded, based on an analysis of the first simultaneous observations of O_3 , ClO, HCl, and OH from FIRS-2 and the Balloon Microwave Limb Sounder, that models using recommended rates overpredicted the observed $[ClO]/[HCl]$ and $[HOCl]/[HCl]$ ratios throughout the stratosphere. Because measured [OH] was shown to agree well with model values, it was clear the sink for HCl was being calculated correctly, assuming

the validity of the rate constant for $OH + HCl$. Chance *et al.* (1996) firmly established that an imbalance existed between production and loss of HCl in the upper stratosphere and stated that the imbalance could be resolved if 5 to 10% of the $ClO + OH$ reaction produced $HCl + O_2$. Michelsen *et al.* (1996) examined nearly simultaneous observations of O_3 , ClO, HCl, $ClONO_2$, and CH_4 from the shuttle-borne ATMOS and MAS instruments. They concluded that the best fit between theory and observation of this suite of Cl_y gases was obtained for a 7% yield of HCl from $OH + ClO$ (Figure 6-15). Michelsen *et al.* (1996) ruled out uncertainties in the rates of $Cl + CH_4$ and $OH + HCl$ as being the cause of the discrepancy. Most importantly, they showed that profiles of ClO, $ClONO_2$, and HCl (the dominant components of the Cl_y family) in the tropics, midlatitudes, and high latitudes could each be described by a single adjustment to standard models.

Observations from UARS have led to similar conclusions. Eckman *et al.* (1995) showed that MLS observations of ClO and HALOE measurements of HCl in the upper stratosphere were better simulated allowing for a 6% yield of HCl from $ClO + OH$. Finally, Dessler *et al.* (1995) examined HALOE and CLAES observations of HCl and $ClONO_2$ and reported the $[ClONO_2]/[Cl_y]$ ratio for the 800 K potential temperature surface was overpredicted by models that did not allow for production of HCl from $ClO + OH$.

This long-standing problem has apparently been resolved by the recent laboratory study of Lipson *et al.* (1997). The primary products of the reaction of $ClO + OH$ are Cl and HO_2 . Production of HCl is exothermic, but involves a four-center reaction with the breaking and reformation of multiple chemical bonds. At the time of the previous Assessment, the existing kinetics literature could not rule out HCl yields as high as 14% or as low as 0%. Lipson *et al.* (1997) used a chemical ionization mass spectrometer to detect reactants and products of the $ClO + OH$ reaction and measured an Arrhenius expression for the rate constant of both reaction pathways. An isotopically labeled source was used to observe directly the production of DCl from $OD + ClO$. Lipson *et al.* (1997) inferred a ~6% yield for production of HCl from the $ClO + OH$ reaction, close to the yield implied by numerous analyses of atmospheric observations.

The many field measurements and modeling studies described above together with the laboratory study of Lipson *et al.* (1997) provide confidence that the

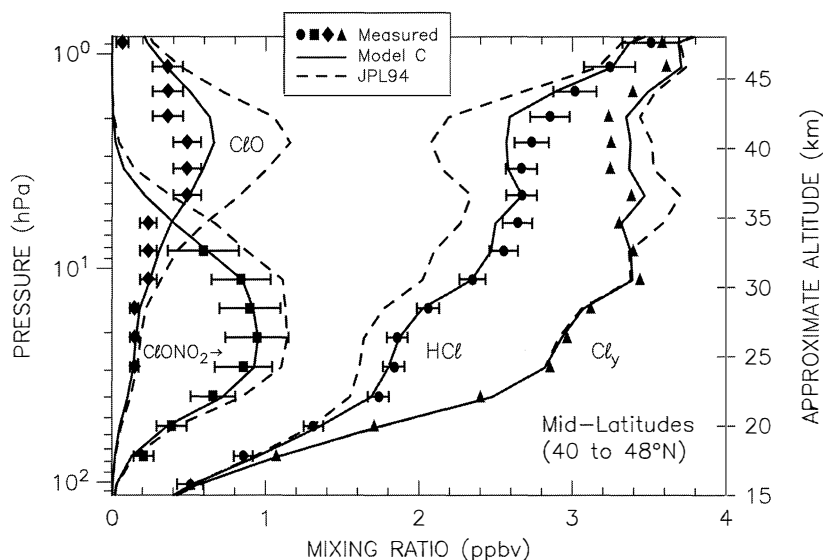


Figure 6-15. Profiles of ClO measured at mid-day by the shuttle-borne Millimeter-wave Atmospheric Sounder (MAS) experiment and ClONO₂ and HCl observed at sunset by the Atmospheric Trace Molecule Spectroscopy (ATMOS) experiment during November 1994 at midlatitudes of the Northern Hemisphere compared with calculated profiles assuming photochemical steady state over a 24-hour period (lines, as indicated). The sum of HCl + ClONO₂ + ClO is shown by the closed triangles (calculated values for ClONO₂ using “Model C” have been used to compute this sum for altitudes

partitioning and budget of chlorine compounds in the upper stratosphere is now very well understood. Catalytic removal of upper stratospheric O₃ by ClO has been shown to proceed at a rate consistent with photochemical models, provided allowance is made for production of HCl from the ClO + OH reaction (Jucks *et al.*, 1996; Osterman *et al.*, 1997). The concentration of Cl_y in the upper stratosphere found by 2-D models exhibits much less scatter and agrees more closely with observations than does the concentration of NO_y, owing to the lack of a high-altitude sink for Cl_y (Park *et al.*, 1998). There are currently no major outstanding scientific uncertainties concerning the budget and partitioning of upper stratospheric chlorine. Future observations will most likely be directed toward confirming the expected decrease in upper stratospheric inorganic chlorine loading due to declines in the organic chlorine content of the troposphere.

6.3.4 Atomic Oxygen

Removal of O₃ by reaction with atomic O contributes between 10 and 20% of the total loss for altitudes above 30 km (e.g., Jucks *et al.*, 1996; Osterman *et al.*, 1997). Knowledge of the concentration of O is crucial to our understanding of upper stratospheric O₃ not only because O + O₃ is an important sink, but also because the rate-limiting step of all other catalytic cycles important for altitudes higher than 40 km (e.g., cycles (6-1) to (6-5)) involves reaction with atomic O. The concentration of O in the upper stratosphere is maintained by a balance between production from photolysis of O₃

above 32 km, where measurements are unavailable). Model profiles were constrained by values for Cl_y (lines, as indicated), NO_y, O₃, H₂O, CH₄, etc., from ATMOS and MAS, and aerosol surface area from Stratospheric Aerosol and Gas Experiment II (SAGE II), and are shown for the appropriate solar times. The “JPL94” model used kinetic parameters from DeMore *et al.* (1994). “Model C” used the Michelsen *et al.* (1994) formulation for the quantum yield of O(¹D), revised rates for Cl + CH₄ and OH + HCl based on a reanalysis of laboratory data (Michelsen *et al.*, 1996), and allows for a 7% yield of HCl from the reaction of ClO + OH. Adapted from Michelsen *et al.* (1996).

and loss by the reaction $O + O_2 + M \rightarrow O_3 + M$. There have been no recent measurements of the concentration of atomic oxygen in the upper stratosphere.

Eluszkiewicz and Allen (1993) have suggested that a 20% increase in the rate of $O + O_2 + M$ would lead to better agreement between production and loss of O₃ in the upper stratosphere. This change, consistent with the DeMore *et al.* (1997) uncertainty, lowers the concentration of O and consequently the rate of each catalytic cycle making a significant contribution to loss of O₃ above 40 km. Good agreement between theory and observation of the [NO₂]/[NO] ratio in the upper stratosphere (Sen *et al.*, 1998) suggests that concentrations of O are calculated correctly, but this conclusion is contingent on the validity of the various kinetic parameters that describe this ratio. The suggestion

UPPER STRATOSPHERIC PROCESSES

of Eluszkiewicz and Allen (1993) underscores the need for future observations of the concentration of atomic O in the upper stratosphere as well as laboratory studies to better define the uncertainty of the rate constant of the $O + O_2 + M$ reaction.

6.3.5 Ozone Production

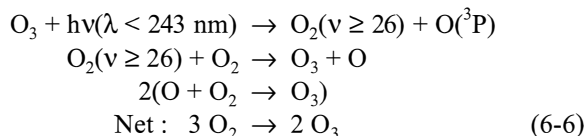
PRODUCTION BY PHOTOLYSIS OF OXYGEN

Ozone production by photolysis of O_2 at wavelengths below 242 nm is included in all models of stratospheric chemistry. High-quality spectroscopic measurements are available for the O_2 absorption both within the Herzberg continuum (185-242 nm) and in the Schumann-Runge bands (175-205 nm); however, uncertainties remain. Recently, Amoruso *et al.* (1996) have measured cross sections in the Herzberg continuum that are 15% lower than the currently accepted values (DeMore *et al.*, 1997).

Even larger uncertainties remain regarding the broadband parameterizations of the highly structured O_2 absorption cross sections in the Schumann-Runge bands (DeMore *et al.*, 1997). Indeed, a comparison of computations with a model (PhotoGT) that resolves the Schumann-Runge cross sections at 0.5 cm^{-1} (Blindauer *et al.*, 1996) using cross sections of Minschwaner *et al.* (1992) against values computed employing broadband parameterizations reveals differences in $J(O_2)$ of up to 10% (Figure 6-16). Analogous results (differences of up to 6%) were reported by Siskind *et al.* (1994) and Koppers and Murtagh (1996). Additionally, Koppers and Murtagh (1996) suggested a new parameterization that agrees more favorably with line-by-line calculations.

THE ROLE OF VIBRATIONALLY EXCITED OXYGEN

Because of the long-standing ozone deficit problem (see Section 6.4.1 below), the possibility of new, additional ozone formation mechanisms has been explored. In particular, the following mechanism has been proposed by Rogaski *et al.* (1993):



This autocatalytic ozone production mechanism has several steps, which are understood to varying degrees. Ozone photolysis yielding atomic oxygen in

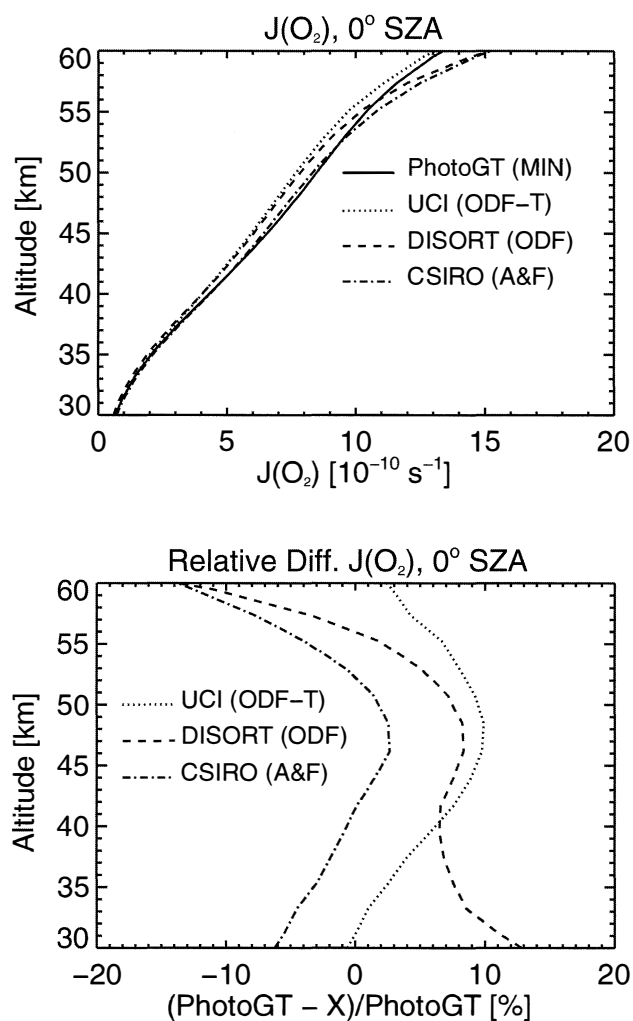


Figure 6-16. Comparison of four models with different parameterizations for the O_2 absorption cross sections in the Schumann-Runge bands: the high-resolution University of Bremen model referred to as PhotoGT (Blindauer *et al.*, 1996); the Commonwealth Scientific and Industrial Research Organization (CSIRO) model (Randeniya *et al.*, 1997) using the Allen and Frederick (1982) parameterization (A&F); and two models (University of California, Irvine (UCI), Prather and Remsberg, 1993; the DIScrete Ordinate Radiative Transfer (DISORT) model, Dahlback and Stamnes, 1991) employing “opacity distribution functions” (ODF) (Minschwaner *et al.*, 1993). Photolysis frequencies, $J(O_2)$, of the three models (top panel) and relative differences to PhotoGT (bottom panel) at 0° solar zenith angle (SZA). Results for the UCI, DISORT, and CSIRO models were taken from the NASA Photolysis Rate Intercomparison (Stolarski, 1995).

the electronic ground state leaves sufficient energy for high vibrational excitation of molecular oxygen. The production of highly vibrationally excited oxygen within the Hartley band is now well established (e.g., Miller *et al.*, 1994). For the reaction $O_2 + O_2 \rightarrow O_3 + O$ to proceed, energetics require that one O_2 molecule must be in vibrational quantum level 26 or higher. The fraction of oxygen in $v \geq 26$ is dependent on the photolysis wavelength. Sensitivity studies of the production mechanism (Toumi *et al.*, 1996) have shown that at 40 km, the 210 to 225 nm region is most important. At this wavelength region the $O_2(v \geq 26)$ yield has been measured to be about 1% (Miller *et al.*, 1994). The occurrence of $O_2(v \geq 26) + O_2 \rightarrow O_3 + O$ is the most uncertain and critical aspect of the mechanism. Laboratory experiments show that the removal rate constant increases sharply for $O_2(v \geq 26)$. This is in disagreement with quenching theories (Hernandez *et al.*, 1995). Furthermore, monitoring of vibrational levels shows that $O_2(v \geq 26)$ is not relaxed to lower vibrational levels and the temperature dependence of the relaxation rate constant is theoretically consistent with the formation of ozone from the reaction of $O_2(v \geq 26) + O_2$ (Rogaski *et al.*, 1995). Thus far, no direct formation of O_3 through this mechanism has been observed in the laboratory and there are serious experimental difficulties to achieve this. Isotopic labeling may provide a solution. Toumi *et al.* (1996) have shown that assuming a wavelength-dependent $O_2(v \geq 26)$ yield and that all $O_2(v \geq 26)$ reacts to form O_3 , then upper stratospheric O_3 calculated using a 2-D model increases by 5-10%. The maximum increases are found near 40 km in the tropics. Laboratory confirmation of the direct formation of ozone by vibrationally excited O_2 is required before further progress can be made.

6.4 TRENDS AND CYCLES OF UPPER STRATOSPHERIC OZONE

6.4.1 The Ozone Budget

The photochemical lifetime of ozone is shorter than the time for replacement by transport for altitudes above ~35 km (with the exception of the winter high latitudes). Consequently, production and loss of O_3 integrated over a 24-hour period are expected to balance. Equivalently, the concentration of O_3 calculated using photochemical models and reasonable constraints for H_2O , CH_4 , NO_y , and Cl_y is expected to match observed concentrations.

Historically, concentrations of ozone calculated using photochemical models have been ~20 to 40% lower than observed values at 40 km altitude, with the discrepancy increasing with altitude (e.g., Crutzen and Schmailzl, 1983; Froidevaux *et al.*, 1985; Jackman *et al.*, 1986; McElroy and Salawitch, 1989; Eluszkiewicz and Allen, 1993). This discrepancy, in which models exhibit a deficit relative to observations, has been termed the “ozone deficit” problem and has prompted the search for O_3 formation mechanisms in addition to the photolysis of O_2 (see Section 6.3.5).

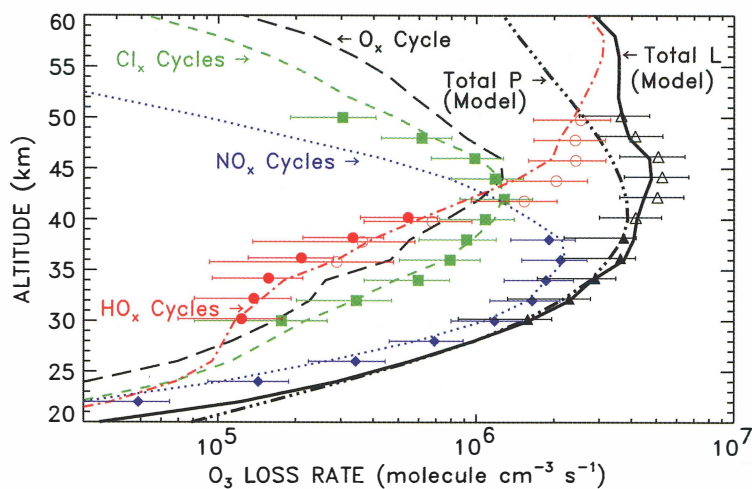
It has been instructive to approach this problem by examining the balance of production and loss of O_3 found using photochemical models constrained by observed concentrations of O_3 , to ensure a proper treatment of the radiative field. The radiative field affects the production of O_3 from photolysis of O_2 , as well as the concentration of hydrogen, nitrogen, and chlorine radicals that control the loss of O_3 in the upper stratosphere.

There have been numerous recent investigations of the ozone deficit problem. Each of these studies, described below, concludes that production and loss of ozone are in balance near 40 km. This result has important implications for understanding trends of O_3 : to within the uncertainty of the atmospheric measurements and relevant kinetic parameters, there is no evidence for “missing chemistry” at 40 km, the altitude in the upper stratosphere where the decadal decline of O_3 peaks.

Minschwaner *et al.* (1993) examined this problem using constraints for NO , NO_2 , $ClONO_2$, HCl , and O_3 from ATMOS. They concluded that the production and loss of O_3 were in balance at 40 km and attributed the earlier tendency of models to underestimate O_3 at 40 km to two factors: (1) use of a treatment for transmission of radiation in the Schumann-Runge bands and Herzberg continuum of O_2 (WMO, 1986) by these models that allowed for less transmission than found by line-by-line calculations employing the latest spectroscopic parameters (e.g., previous models had underestimated the production of O_3); and (2) the tendency of these models to overestimate the observed concentration of ClO at 40 km by 20 to 40% due to the neglect of production of HCl from $ClO + OH$. Minschwaner *et al.* (1993) also concluded that a sizable ozone deficit was present for altitudes above 50 km.

Connor *et al.* (1994) and Crutzen *et al.* (1995) drew attention to the likelihood that measurements of daytime

UPPER STRATOSPHERIC PROCESSES



O_3 from LIMS (Limb Infrared Monitor of the Stratosphere), which were of ten employed in earlier studies of the ozone deficit problem (e.g., Eluszkiewicz and Allen, 1993, and references therein), appear to be systematically high for pressures less than 1.0 hPa as a result of chemical excitation effects. The use of observations of O_3 that are biased high in photochemical model studies could result in an artificially produced ozone deficit. Connor *et al.* (1994) suggest that measurements of nighttime O_3 from LIMS, which compare well with ground-based microwave measurements of O_3 , should be used instead of daytime O_3 in studies of the ozone deficit based on LIMS data.

Dessler *et al.* (1996) examined UARS observations of O_3 , ClO, and NO_2 and concluded that production and loss of O_3 were in balance between 40 and 46 km to within the uncertainty of the atmospheric measurements and relevant kinetic parameters. They emphasized that uncertainties between HALOE (Version 17) and MLS observations of O_3 prevented a definitive statement concerning the existence of an ozone deficit. Crutzen (1997) and Groß *et al.* (1998) have recently revised earlier results of Crutzen *et al.* (1995) (where an “ozone surplus” was found), stating that production and loss of O_3 are in balance at 40 km and higher altitudes. This new result was due to the use of HALOE Version 18 profiles for O_3 and the allowance for production of HCl from ClO + OH.

Our understanding of the balance between the production and loss of O_3 has recently been strengthened by studies that have examined constraints posed by simultaneous measurements of hydrogen, nitrogen, and

Figure 6-17. Ozone loss rates for the hydrogen (HO_x), nitrogen (NO_x), and chlorine (Cl_x) families of gases and the $O + O_3$ cycle (O_x), as well as total production and loss, for 35°N, September 1993. Curves represent 24-hour averaged rates found using a photochemical model constrained by MkIV measurements of radical precursors, SAGE II, MkIV, and in situ UV photometer measurements of O_3 , and SAGE II measurements of aerosol surface area. Points with error bars represent loss rates inferred from balloonborne measurements of the concentrations of OH, HO_2 , NO, NO_2 , ClO, and O_3 . The contribution to

loss of ozone from cycles involving $BrO + HO_2$ and $BrO + O$ (not shown, but included in the total model loss curve) is ~20% at 20 km and declines rapidly with increasing altitude. Adapted from Osterman *et al.* (1997).

chlorine radicals. Jucks *et al.* (1996) examined FIRS-2 measurements of OH, HO_2 , and NO_2 and observations of ClO from a balloonborne microwave limb sounder between the altitudes of 30 and 38 km and concluded that production and loss of O_3 were in balance and that loss of O_3 by each of the major catalytic families occurred at a rate close to theoretical expectation. They noted that the total O_3 loss rate at 38 km found using the measured profile of ClO was 17% lower than the total loss rate calculated assuming no production of HCl from ClO + OH. Osterman *et al.* (1997) examined simultaneous balloonborne observations of OH, HO_2 , NO, NO_2 , ClO, and O_3 between 24 and 50 km. They concluded that production and loss of O_3 are in balance at 40 km and that loss exceeds production (e.g., an ozone deficit) by as much as ~35% between 45 and 60 km. Furthermore, they showed that the hydrogen, nitrogen, and chlorine families make nearly equal contributions to loss of O_3 at 40 km for contemporary levels of chlorine loading (Figure 6-17). Khosravi *et al.* (1998) have analyzed the ozone budget in the upper stratosphere in a time-dependent 3-D model of the middle atmosphere in conjunction with observations of ClO from MLS and of NO_x , H_2O , and CH_4 from HALOE (Version 18). Allowing for production of HCl from ClO + OH and constraining the model by observed CH_4 results in model

profiles for ClO that are in good agreement with the observations. Under these circumstances, the calculated abundances of ozone at 40 km are within the uncertainties of the measurements. Siskind *et al.* (1998) have also noted that irradiance near 200 nm of the solar spectrum measured by UARS (Lean *et al.*, 1997) is 9 to 12% higher than the WMO (1986) spectrum and that use of the UARS spectrum leads to an increase in calculated O₃ due to more photodissociation of O₂.

The numerous recent studies (e.g., Dessler *et al.*, 1996; Jucks *et al.*, 1996; Crutzen, 1997; Osterman *et al.*, 1997; Groß *et al.*, 1998; Khosravi *et al.*, 1998) that conclude the production and loss of O₃ are in balance at 40 km differ from the earlier findings of an ozone deficit at 40 km due to: deeper transmission in the Schumann-Runge bands and Herzberg continuum of O₂ than given by the WMO (1986) tables; reductions in the concentration of ClO (due to allowance for production of HCl by the reaction of ClO + OH and the use of observed CH₄ to constrain the models); and the use of O₃ observations that appear to be more accurate than the daytime observations obtained by LIMS.

The remaining uncertainty involving the budget of O₃ in the upper stratosphere concerns the existence of an ozone deficit at altitudes above 45 km. Minschwaner *et al.* (1993) and Osterman *et al.* (1997) (Figure 6-17) have found a sizable ozone deficit above 45 km that appears to possibly carry a signature of production of O₃ by vibrationally excited O₂ (Section 6.3.5). These studies employed the same radiative transfer model. Sandor and Clancy (1998) reached similar conclusions concerning the existence of a deficit and suggested that a 40% reduction in the recommended rate of HO₂ + O would resolve the discrepancy for altitudes between 50 and 70 km. In contrast, Crutzen (1997) and Groß *et al.* (1998) have found close balance between production and loss of O₃ at all altitudes between 35 and 55 km.

The budget of O₃ above 45 km bears further investigation. Significant reductions of O₃ occur at these altitudes over decadal time scales (Figures 6-19 and 6-20; see also Chapter 4). The O₃ loss rate due to ClO for the contemporary atmosphere at 45 km is comparable to the imbalance between production and loss found in some studies. Reductions in O₃ at these altitudes have little direct effect on column ozone and thus on the Earth's surface, but they affect the radiative balance of the stratosphere and also cause increased production of O₃ at lower altitudes owing to the so-called "self-healing" effect. Consequently, a comprehensive understanding

of upper stratospheric O₃ requires better definition of the budget at 45 km and higher altitudes.

Future work in this area would benefit from either measurements of the concentration of atomic oxygen or, as suggested by Eluszkiewicz and Allen (1993), better constraints for the uncertainty of the rate constant of O + O₂ + M → O₃ + M (the dominant sink for atomic oxygen). A reexamination of the rate constant of HO₂ + O in the laboratory may also be useful given the importance of this reaction for the budget of O₃ above 45 km (e.g., Summers *et al.*, 1997a; Sandor and Clancy, 1998) and the many studies (Section 6.3.1) that have found that measured profiles of OH and HO₂ are better simulated using a slower rate than the currently recommended value. There is also considerable uncertainty for the rate of OH + HO₂ → H₂O + O₂ (±50% for temperatures relevant to the upper stratosphere) (DeMore *et al.*, 1997), the primary sink for HO_x that also impacts substantially the budget of upper stratospheric O₃ (e.g., Crutzen *et al.*, 1995; Jucks *et al.*, 1998).

There is no consensus within the atmospheric sciences community concerning the broadband parameterization that should be used to treat transmittance in the Schumann-Runge bands and Herzberg continuum of O₂ (e.g., Section 6.3.5 and discussion in DeMore *et al.*, 1997), and it is likely that future studies of the budget of O₃ will continue to be influenced by which treatment is used. Additional measurements of atmospheric transmittance in this spectral region (e.g., Anderson and Hall, 1983) would provide an important test of radiative transfer models as well as calculated O₃ production rates (Minschwaner *et al.*, 1993). Further laboratory studies are necessary to better define the role of production of O₃ following photolysis of vibrationally excited O₂ (Section 6.3.5). Finally, it must be stressed that scrutiny of the budget of upper stratospheric O₃ is and will continue to be dependent upon highly accurate measurements of O₃.

6.4.2 Seasonal Cycle of Ozone

Owing to the fact that upper stratospheric ozone is mostly in photochemical steady state, its seasonal cycle is determined by the seasonal cycle of the production and loss terms. Outside of the tropics, for altitudes just below the stratopause (Umkehr level 9, 48-42 km), the maximum concentration of ozone occurs in winter and the minimum in early summer. Summer values are about 25% lower than winter values (Figure 6-18). In this

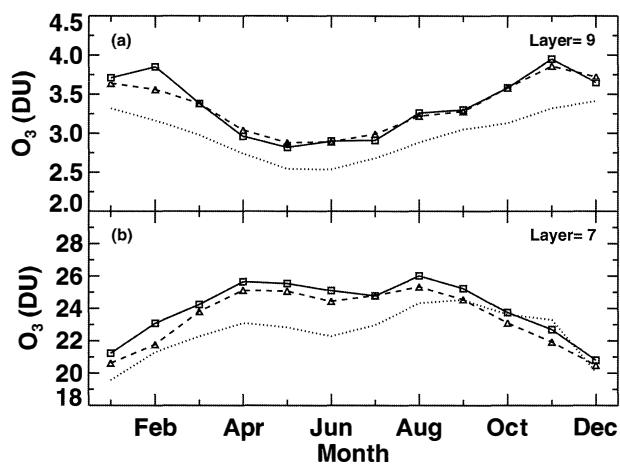


Figure 6-18. Seasonal cycle of the ozone amount in Umkehr layer 9 (1-2 hPa, ~48-42 km, top panel) and 7 (4-8 hPa, ~38-33 km, bottom panel). Each point is a monthly mean value; latitude region is between 35°N and 45°N. The squares and solid lines indicate SAGE II values (Version 5.96); the triangles and dashed lines, SBUV(2). Shown are average monthly mean values using all SAGE and SBUV data between October 1984 and October 1994. (Adapted from Wang *et al.*, 1996). Dotted line shows results from the Max Planck Institute for Chemistry (MPIC) model (see Chapter 12) for 1990, including the reaction $\text{ClO} + \text{OH} \rightarrow \text{HCl} + \text{O}_2$.

altitude range, the seasonal variation of ozone is controlled by the temperature variation of the relevant ozone destruction rates; i.e., ozone destruction rates are most rapid when temperatures are warmest during summer (Perliski *et al.*, 1989). For Umkehr layer 7 (38-33 km) outside the tropics, in contrast, concentrations of ozone during winter are about 20% lower than maximum concentrations that occur during summer (Figure 6-18). For these altitudes, the seasonal variation is strongly influenced by the variation of the odd-oxygen production rates, which peak during summer (Perliski *et al.*, 1989). The seasonal behavior of upper stratospheric ozone is reasonably well reproduced by current 2-D models (e.g., Figure 6-18). Chandra *et al.* (1993) showed that the agreement in the amplitude of the seasonal cycle of upper stratospheric ozone between model simulations and Solar Backscatter Ultraviolet (SBUV) spectrometer observations was improved if models allowed for production of HCl from a minor channel of the reaction $\text{ClO} + \text{OH}$.

6.4.3 Solar Effects on Ozone

Stratospheric O_3 is produced by the photolysis of O_2 at ultraviolet wavelengths (Section 6.3.5). The solar ultraviolet flux has been observed to vary as a consequence of the 27-day period of solar rotation and the 11-year variation in the frequency of solar sunspots and faculae, commonly referred to as the 11-year solar cycle. Spaceborne measurements obtained by instruments aboard UARS have led to accurate definitions of the amplitude of the variation of solar irradiance, as a function of wavelength, for both the 27-day solar rotation (e.g., London *et al.*, 1993) and 11-year solar cycle (e.g., Lean *et al.*, 1997). These measurements have been used in a number of model studies described below.

The effects of the 27-day solar rotation on stratospheric O_3 are small, with an amplitude of 0.2 to 0.3% variation (Hood and Cantrell, 1988). Chen *et al.* (1997) have shown that the observed amplitude and phase of this variation of stratospheric O_3 is simulated well using a model that allows for feedbacks between temperature and O_3 (the temperature response in the middle atmosphere is largely determined by the solar-induced variation of O_3). Neglecting the observed solar-induced temperature variation worsens the agreement between measured and calculated changes in O_3 (Chen *et al.*, 1997). The small variations of O_3 over the 27-day period of solar rotation have no direct consequences for long-term changes in stratospheric O_3 . However, these studies provide increased confidence in our quantitative understanding of the sensitivity of O_3 to changes in solar flux and temperature, which is relevant for understanding decadal reductions in upper stratospheric O_3 (see Sections 6.4.4 and 6.5).

Significant variations in upper stratospheric O_3 occur over the 11-year solar cycle. Chandra and McPeters (1994) reported changes of 5 to 7%, with O_3 peaking during solar maximum due primarily to the 7 to 8% increase in solar irradiance near 200 nm. McCormack and Hood (1996) have conducted a detailed analysis of the latitude, altitude, and seasonal dependence of the variations of upper stratospheric O_3 and temperature over the 11-year solar cycle based on 15 years of satellite data. They found that the largest variations of O_3 occur between 42 and 47 km, with peak values of $5.9 \pm 1.2\%$ near 40°S and $4.6 \pm 1.0\%$ near 40°N.

The amplitude of the solar-induced response of O_3 between 40 and 50 km is larger than found by models,

whereas the observed variation in O_3 between 30 and 40 km is smaller than calculated (McCormack and Hood, 1996). The three models described in that study have various means of accounting for O_3 -temperature feedbacks. Best agreement with the observed change in O_3 near 40 km is found by the model of Fleming *et al.* (1995), the only model constrained by the observed temperature variation. It must be noted, however, that the observed variations in temperature, especially at higher latitudes in the altitude regime between 35 and 40 km, are not simulated particularly well by a radiative model constrained by observed variations in solar irradiance and O_3 (McCormack and Hood, 1996). This has led McCormack and Hood (1996) to suggest that changes in dynamical heating of the stratosphere over the 11-year solar cycle, perhaps related to solar-induced changes in the mean meridional circulation, may contribute to the observed temperature response at higher latitudes. The recent study of Siskind *et al.* (1998) has established the need to consider variations in CH_4 (which may also be affected by the mean circulation and which regulates the partitioning of ClO relative to HCl in the upper stratosphere) as well in studies of the response of upper stratospheric O_3 to the 11-year solar cycle.

It has been clearly established that upper stratospheric O_3 varies with an amplitude of 5 to 7% over the 11-year solar cycle. While models are able to simulate the general response of O_3 , the lack of precise quantitative agreement between theory and observation requires further study. The satellite record for profiles of upper stratospheric O_3 currently covers slightly less than two full solar-cycles, so continued observation will be important for gaining a better understanding of this problem.

Because the amplitude of the response of upper stratospheric O_3 to the 11-year solar cycle is comparable to the magnitude of the expected decrease in O_3 due to the build-up of anthropogenic chlorine during a 10-year time period, it is important that this process be considered when studying long-term trends of O_3 . The signature of the 11-year solar cycle is straightforward to identify in a long time series of O_3 observations (e.g., Chandra and McPeters, 1994; Miller *et al.*, 1997). Typically, the 11-year solar cycle is accounted for when estimating long-term trends of stratospheric O_3 by using statistical analyses based on a proxy for the variation in solar ultraviolet irradiance (e.g., Miller *et al.*, 1997; Stolarski and Randel, 1998), often provided by the long-term space-based measurement of the chromospheric MgII absorption line at 280 nm (e.g., DeLand and Cebula,

1993). The estimates for the long-term trends of stratospheric O_3 described in Section 6.4.4 and Section 6.5 have been found by accounting for this effect. Reconstructions of the variation of solar ultraviolet irradiance over the time period from 1980 to 1996 (e.g., Figure 20 of Lean *et al.*, 1997) show that the maximum and minimum irradiances over the past two solar cycles repeat in a similar fashion, demonstrating that the observed decline in upper stratospheric O_3 over this period was not driven by changes in solar irradiance. Other solar-related processes, such as production of NO_x and HO_x by solar proton events, can have significant effects on polar upper stratospheric O_3 over short time periods but are unimportant when considering long-term trends of O_3 (Jackman *et al.*, 1996).

6.4.4 Ozone Trends

A significant decline of upper stratospheric ozone has been identified between the years 1979 to 1991 (i.e., before the eruption of Mt. Pinatubo) from analysis of satellite, Umkehr, and lidar measurements of ozone profiles for both the Northern and Southern Hemisphere midlatitudes (e.g., WMO, 1995; Claude *et al.*, 1994; Hollandsworth *et al.*, 1995; Wang *et al.*, 1996; Harris *et al.*, 1997; Miller *et al.*, 1997; see also Chapter 4). Comparisons of the trends derived from different instruments for the Northern Hemisphere midlatitudes in the 1980s (Miller *et al.*, 1997) agree relatively well and show a statistically significant decline, increasing from about 2.5% per decade at 30 km to about 7.5% per decade at 40 to 45 km (Figure 6-19). Because most of the stratospheric ozone column resides in the lower stratosphere, total ozone measurements (e.g., from TOMS or Dobson instruments) are not useful for the detection of changes in upper stratospheric ozone.

Consideration of a longer time series of Stratospheric Aerosol and Gas Experiment (SAGE), SBUV, and Umkehr measurements, from 1980 to 1996, yields very similar estimates of the long-term decline in upper stratospheric ozone (Figure 6-19; Chapter 4; see also Stolarski and Randel, 1998). Generally, the confidence intervals are somewhat smaller because of the longer time period. These findings are confirmed by an analysis of a 9-year time series of midlatitude lidar observations (Steinbrecht *et al.*, 1998). The quantitative similarity of the observed trends from several independent measurement systems provides confidence that a true atmospheric phenomenon has been observed.

UPPER STRATOSPHERIC PROCESSES

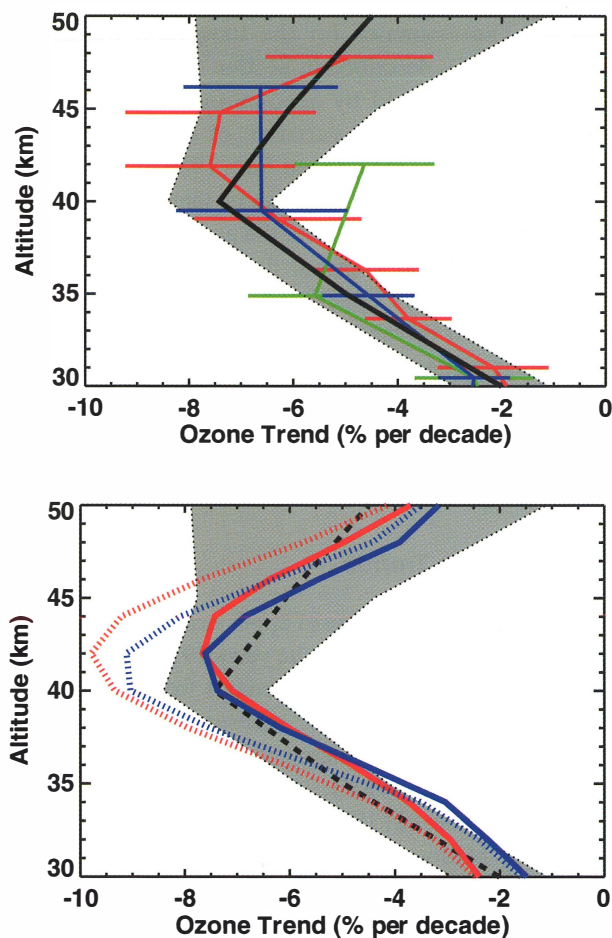


Figure 6-19. Ozone trends for the Northern Hemisphere midlatitudes (30°N-50°N). Top panel: trends derived from SBUV (1979-1991, blue line), from Umkehr (1968-1991, green line), and from SAGE (1979-1990, red line) observations, in %/decade (adapted from Miller *et al.*, 1997). The combined trend (black line) of all three measurement systems for the period 1980-1996 (adapted from Stolarski and Randel, 1998) is also shown with an estimate of the trend uncertainty (gray shaded area). Bottom panel: the combined trend (black dashed line) of all three measurement systems for the period 1980 to 1996 compared to ozone trends (likewise for 30°N-50°N) calculated by the Goddard Space Flight Center (GSFC) (red lines) and the Lawrence Livermore National Laboratory (LLNL) (blue lines) two-dimensional models, for scenario A (see Chapter 12) for the period 1979 to 1995, in %/decade. Both the standard scenario (solid lines) and results neglecting reaction $\text{ClO} + \text{OH} \rightarrow \text{HCl} + \text{O}_2$ (stippled lines) are shown.

Recent calculations of the long-term changes in ozone found using 2-D models are in reasonable agreement with the latitude and altitude characteristics of the observed trends in upper stratospheric ozone (e.g., Jackman *et al.*, 1996; Considine *et al.*, 1998), but the calculated trends are somewhat larger than those derived from observations. However, these models also tend to overestimate ClO (Chandra *et al.*, 1995; Jackman *et al.*, 1996), leading to an overestimate of the ozone loss rate due to the chlorine catalytic cycle (6-2).

As discussed in Section 6.3.3, allowing for production of HCl from a minor (~6%) channel of the reaction $\text{ClO} + \text{OH}$ (Lipson *et al.*, 1997) leads to good agreement between calculated and observed ClO (e.g., Stachnik *et al.*, 1992) and consequently results in a reduction of the calculated long-term trend of O_3 at 40 km. Calculated trends for Northern Hemisphere mid-latitudes from current 2-D models that include the HCl channel are now in *good quantitative agreement* with observations (solid lines in Figure 6-19). If the HCl channel is neglected, the observed trends are overestimated (stippled lines in Figure 6-19).

The meridional pattern of the observed ozone decline (Figure 6-20) shows that trends are significantly different from zero in the upper stratosphere at all latitudes outside the tropics. The largest negative trend remains at about 40 to 45 km in this global view; however, the declines in ozone are larger for higher latitudes than for the lower latitudes (Figure 6-20). A larger trend at high latitudes is consistent with the fact that the “oldest” stratospheric air resides in this region (Section 6.2). An older age of air enhances the efficiency of the ozone-depleting chlorine cycle in two ways. As air ages, a larger fraction of total available chlorine is converted to the inorganic forms that react with O_3 . Second, and more importantly, older air is characterized by smaller abundances of CH_4 (Figure 6-4), leading to a shift in the partitioning of Cl_y species towards Cl and ClO, and away from HCl, thus enhancing the ozone loss rates (Solomon and Garcia, 1984). In the past, interhemispheric differences (i.e., larger trends in the Southern Hemisphere) were reported for upper stratospheric ozone trends (WMO, 1995; Hollandsworth *et al.*, 1995; Harris *et al.*, 1997). However, in the most recent evaluation of upper stratospheric ozone measurements (Stolarski and Randel, 1998; see also Figure 6-20), there is no longer evidence for this difference.

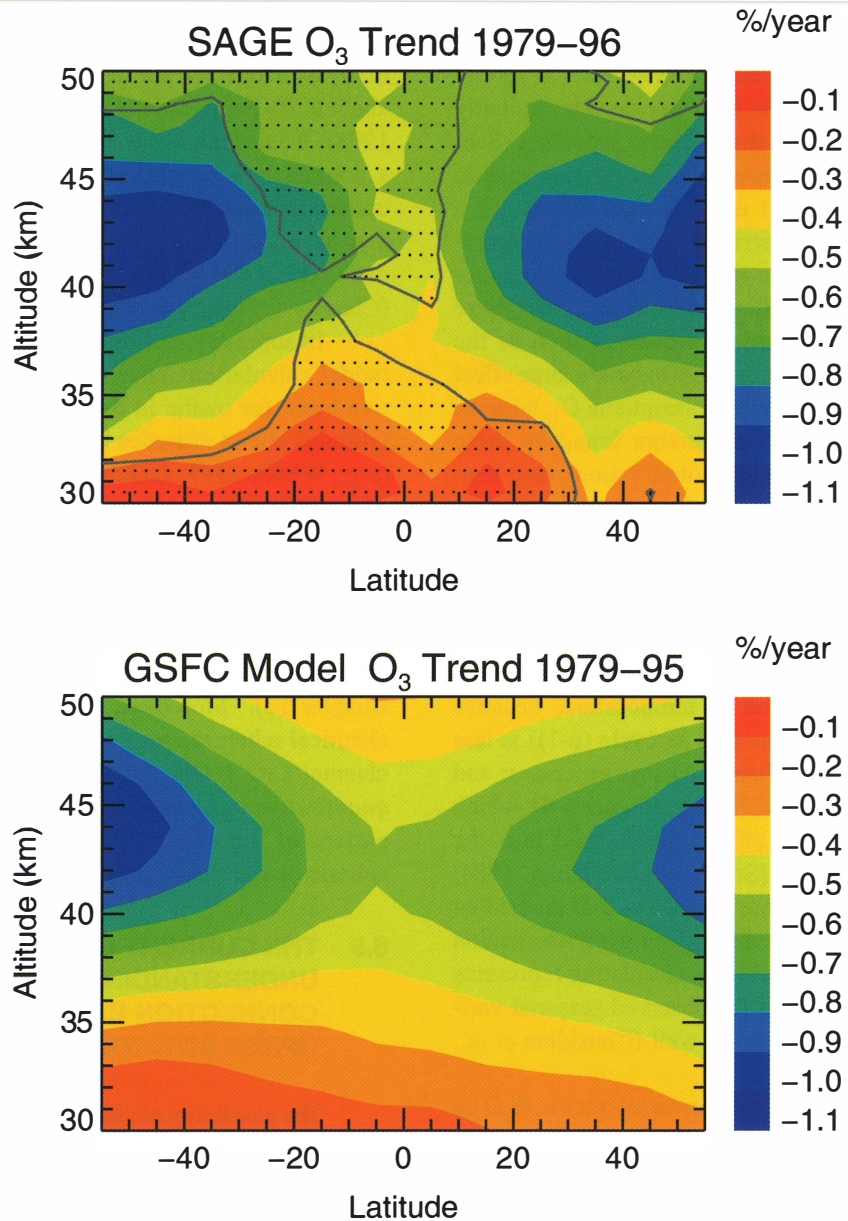


Figure 6-20. The meridional and vertical structure of stratospheric ozone trends. Top panel: Ozone trends derived from SAGE I/II observations from 1979 to 1996 expressed in %/year of the midpoint of the time series (1987). Results are contoured from calculations done in 5° latitude bands and 1-km altitude intervals. The stippled areas inside the gray contour lines indicate regions where the trends do not differ from zero, within 95% confidence limits. The estimate of uncertainty contains terms due to the SAGE I reference height correction and the SAGE II sunrise/sunset trend differences (adapted from Stolarski and Randel, 1998). Bottom panel: Ozone trends calculated by the GSFC two-dimensional model, for the standard scenario including the reaction channel $\text{ClO} + \text{OH} \rightarrow \text{HCl} + \text{O}_2$ (scenario A, see Chapter 12), for the period 1979 to 1995 (in %/year).

UPPER STRATOSPHERIC PROCESSES

Although 2-D assessment models are successful in reproducing the observed ozone decline, it should be noted that these models typically do not explicitly represent several relevant stratospheric processes (Section 6.2). Usually, the observed decline of stratospheric temperatures (Chapter 5) is neglected, which has a small impact on stratospheric O₃ due to the temperature dependence of the rate-limiting steps of the ozone-depleting cycles (see Section 6.5 below). The failure to include detailed dynamical processes such as the SAO in most 2-D models is unlikely to have a large effect on calculated trends for upper stratospheric O₃, because the distribution of radical precursors found by these models agrees fairly well with observations (see Section 6.2).

There are few published studies investigating how well the observed seasonal variation of ozone trends (Chapter 4; Stolarski and Randel, 1998) is reproduced in current 2-D assessment models. Likely causes for the seasonal variation of upper stratospheric ozone trends are: the seasonal variation of temperature, because the chlorine cycle (6-2) (as well as cycle (6-1)) is less sensitive to temperature than other loss processes; and the seasonal variability of CH₄ (e.g., Figure 6-4), which impacts the partitioning of Cl_y species and thus the efficiency of cycle (6-2) (Solomon and Garcia, 1984; Considine *et al.*, 1998). One interactive 2-D model that employs a planetary wave dissipation parameterization for the calculation of the residual circulation represents the general morphology of the observed seasonal variation of the ozone trends fairly well (Considine *et al.*, 1998).

If a long-term trend in upper stratospheric H₂O on the order of 55 to 150 ppbv/year as observed from 1992 to 1996/1997 (see Section 6.3.1) had occurred over the whole period for which trends in O₃ are analyzed here (1980 to 1996), it would have had an appreciable impact on upper stratospheric O₃ (Evans *et al.*, 1998; Siskind *et al.*, 1998). However, this is unlikely, as a much lower H₂O trend is observed in the lower stratosphere for the period 1981 to 1994 (Oltmans and Hofmann, 1995) and because ATMOS measurements obtained at Northern Hemisphere midlatitudes during 1985, 1992, 1993, and 1994 (Abbas *et al.*, 1996a) show no evidence for dramatic increases in upper stratospheric H₂O. Further, the upper stratospheric H₂O trend has substantially weakened after 1996 (Randel *et al.*, 1998b). Even if a trend of ~70 ppbv/year would have persisted over the period 1980-1996 (leading to an increase in upper stratospheric H₂O of ~1

ppmv), this would have only led to an additional decrease in O₃ of about 3% per decade at 50 km (~1 hPa) and about 0.5% per decade at 40 km (~3 hPa) (Evans *et al.*, 1998). Therefore, while changes in H₂O possibly led to a noticeable acceleration of the ozone decline in the uppermost stratosphere at ~50 km, it seems unlikely that they have contributed a substantial fraction to the stronger ozone decline at 40 km observed over the last decades (Chapter 4; Figures 6-19 and 6-20).

In summary, during recent years 2-D assessment model calculations have indicated a maximum negative trend for ozone in the upper stratosphere at high latitudes and at altitudes between about 40 and 45 km (e.g., WMO, 1995; Jackman *et al.*, 1996; Considine *et al.*, 1998), in accordance with the meridional and vertical structure of the observed trends for upper stratospheric ozone (WMO, 1995; Harris *et al.*, 1997; Chapter 4). This finding is confirmed by the results from a variety of current 2-D assessment models, which are in reasonable agreement among each other (see Chapter 12). Moreover, if current reaction rates and chemical schemes are employed, including the reaction channel ClO + OH → HCl + O₂, there is now *good quantitative agreement* in the meridional and vertical pattern of the observed and simulated upper stratospheric ozone trends (Figure 6-20).

6.5 THE CURRENT AND HISTORICAL UNDERSTANDING OF THE CONNECTION BETWEEN CFCS AND UPPER STRATOSPHERIC OZONE

The possibility of chlorine-catalyzed loss of O₃ was first introduced by Stolarski and Cicerone (1974) and in the same year related to the accumulation of anthropogenic chlorofluorocarbons in the atmosphere by Molina and Rowland (1974). Early model studies (e.g., Crutzen, 1974) indicated that the largest loss of O₃ would occur in the upper stratosphere, a view that was confirmed by a variety of models thereafter (WMO, 1986). Indeed, the first policy measures were taken based on these early findings. The United States phased out the use of CFCs as a propellant in spray cans as of 1 January 1979. This action was soon followed by similar bans in Canada, Sweden, and Norway.

It was later discovered that processes involving industrially produced halogens lead to substantial — and in the polar regions even dramatic — chemical depletion of O₃ in the lower stratosphere due to reactions related

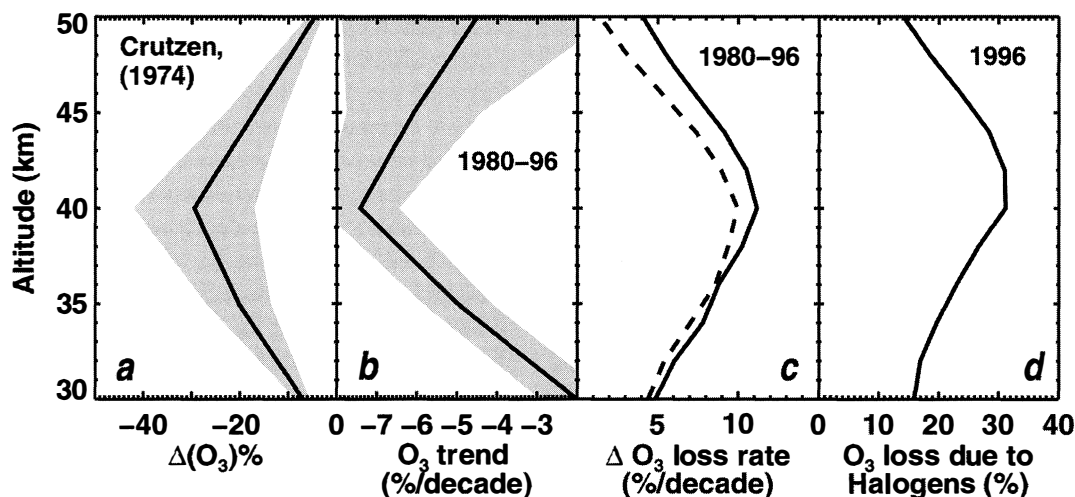


Figure 6-21. Upper stratospheric ozone trend and ozone loss rate due to chlorine-catalyzed reaction cycles for midlatitudes of the Northern Hemisphere. Panel (a) shows the percentage reduction in ozone concentrations predicted to occur by Crutzen (1974) due to the build-up of CFCs. The calculation assumed a growth of Cl_y to a level of 5.3 ppbv in the uppermost stratosphere. Panel (b) shows the observed reduction of upper stratospheric ozone for the latitude range 30° to $50^\circ N$, between 1980 and 1996, derived from SAGE, SBUV, and Umkehr measurements (Stolarski and Randel, 1998; see also Figure 6-19). The shaded areas indicate the range of uncertainty. Panel (c) shows the change in the total odd-oxygen loss rate for $35^\circ N$, September (solid line), calculated using the photochemical model described by Osterman *et al.* (1997), allowing for a change in Cl_y from 2.0 ppbv (appropriate for 1980) to 3.6 ppbv (appropriate for 1996). The model result represented by the dashed line allows for the observed decrease in temperature between 1980 and 1996 (Chapter 5) in addition to the increase in Cl_y . Changes in the total O_3 loss rate are expressed in units of %/decade to be directly comparable to the observed change in O_3 . Panel (d) shows the fraction of the total odd-oxygen loss rate due to the catalytic cycle limited by $ClO + O$ (cycle (6-2); see Section 6.1) for $35^\circ N$, September 1996 ($Cl_y = 3.6$ ppbv in the uppermost stratosphere) based on the model described by Osterman *et al.* (1997).

to the interactions of gaseous species and aerosol particles (e.g., Chapter 7; WMO, 1995). These processes have led to substantial reductions of the column abundance of O_3 over the past several decades (Chapter 4). The depletion of lower stratospheric O_3 has prompted activities that led to the Montreal Protocol and its successive Amendments, limiting and then essentially banning the use of CFCs. It is appropriate now that the halogen loading of the stratosphere is approaching its peak level to ask how well the early predictions of upper stratospheric O_3 depletion have been substantiated.

In retrospect, the predictions of the early studies were remarkably farsighted. It was stated that CFCs (mainly CFC-11 and CFC-12) would accumulate in the lower atmosphere, with photolysis in the middle and upper stratosphere being the major sink. It was understood already in 1974 that this constituted a long-term

problem, on the time scale of many decades. Most importantly, it was predicted that enhanced levels of stratospheric chlorine would lead to a decline of ozone in the upper stratosphere by a catalytic cycle limited by the reaction of $ClO + O$ (cycle (6-2), Section 6.1).

Now, more than 20 years later, ozone decline has been unequivocally detected in the altitude region between 30 and 50 km by a variety of ground-based and spaceborne instruments (WMO, 1995; Stolarski and Randel, 1998; see also Chapter 4 and Section 6.4.4). There is, in general, good quantitative agreement for the long-term decline of stratospheric O_3 derived from many different measurement systems (Stolarski and Randel, 1998). The observed altitude variation of loss of upper stratospheric ozone — peak percentage losses around 40 km — was correctly predicted by the first model studies (e.g., Crutzen, 1974; see also Figure 6-21, panel a).

UPPER STRATOSPHERIC PROCESSES

Through a more precise knowledge of the relevant chemical kinetics, datasets with improved long-term calibration and internal consistency, as well as refined photochemical and dynamical models, there is now good quantitative agreement between observed and calculated long-term reductions of O₃ between 30 and 50 km altitude (Section 6.4.4).

The relation of the observed decline of upper stratospheric ozone and the increase of the stratospheric chlorine loading is depicted schematically in Figure 6-21. A significant reduction in the concentration of ozone was observed during the 1980s and 1990s, with the largest losses reaching $7.4 \pm 1.0\%$ /decade at 40 km altitude (Figure 6-21, panel b). A similar pattern of the decline in upper stratospheric O₃ due to the build-up of industrially derived chlorine was predicted by the earliest modeling efforts (Figure 6-21, panel a). These calculations were based on a projected increase of Cl_y to a level of 5.3 ppbv, a value never reached in the contemporary stratosphere.

Photochemical model calculations using the most recent set of the relevant kinetic parameters (DeMore *et al.*, 1997; Lipson *et al.*, 1997) show that a substantial fraction of the loss of O₃ in today's upper stratosphere occurs by the ClO + O cycle, peaking at a value of ~30% of the overall ozone loss rate at an altitude of 40 km (Figure 6-21, panel d, and Figure 6-2). Current models have been shown to reproduce accurately the observed concentrations of the hydrogen, nitrogen, and chlorine gases that regulate photochemical removal of O₃ (Section 6.3).

Allowing in a photochemical model for the growth of upper stratospheric Cl_y (at 55 km) from a value of 2 ppbv in 1980 to 3.6 ppbv in 1996, and keeping everything else unchanged, leads to a calculated increase in the overall O₃ loss rate very similar in shape and magnitude to the observed decline in O₃ (Figure 6-21, panel c, solid line). Allowing in addition for the decrease in upper stratospheric temperature observed during the past 16 years (Chapter 5) results in a slightly lower estimate for the increase in the overall O₃ loss rate (Figure 6-21, panel c, dashed line) mainly because of the temperature dependencies of the rate-limiting reactions for O₃ removal. Both the observed reduction in O₃ as well as the calculated increase in the O₃ loss rate peak at a value of ~7 to 8% per decade at about 40 km altitude. More sophisticated models, allowing for radiative, dynamical, and chemical feedbacks associated with the increased burden of stratospheric chlorine, lead to calculated

reductions in upper stratospheric O₃ that also agree very closely with the observed depletion (e.g., Figures 6-19 and 6-20; see also Chapter 12).

A decrease in the concentration of stratospheric chlorine is expected because of the Montreal Protocol and its subsequent Amendments. Indeed, the tropospheric burden of ozone-depleting chlorine compounds has reached its maximum between mid-1992 and mid-1994 and is beginning to decline slowly (Montzka *et al.*, 1996; see also Chapter 1). Near 40 km altitude there is a direct and strong correspondence between the concentration of ClO and loss of O₃, less variability and shorter lifetimes of O₃ than in lower regions of the atmosphere, and little direct effect of transport or small changes in temperature on the concentration of O₃. Therefore, it is conceivable that the "recovery" of O₃ due to the decreasing burden of stratospheric chlorine will first become apparent at 40 km (Chapter 12). Future observations of the upper stratosphere will likely be directed toward detecting the expected recovery of upper stratospheric ozone.

REFERENCES

- Abbas, M.M., M.R. Gunson, M.J. Newchurch, H.A. Michelsen, R.J. Salawitch, M. Allen, M.C. Abrams, A.Y. Chang, A. Goldman, F.W. Irion, E.J. Moyer, R. Nagaraju, C.P. Rinsland, G.P. Stiller, and R. Zander, The hydrogen budget of the stratosphere inferred from ATMOS measurements of H₂O and CH₄, *Geophys. Res. Lett.*, 23, 2405-2408, 1996a.
- Abbas, M.M., H.A. Michelsen, M.R. Gunson, M.C. Abrams, M.J. Newchurch, R.J. Salawitch, A.Y. Chang, A. Goldman, F.W. Irion, G.L. Manney, E.J. Moyer, R. Nagaraju, C.P. Rinsland, G.P. Stiller, and R. Zander, Seasonal variations of water vapor in the lower stratosphere inferred from ATMOS/ATLAS-3 measurements of H₂O and CH₄, *Geophys. Res. Lett.*, 23, 2401-2404, 1996b.
- Abrams, M.C., G.L. Manney, M.R. Gunson, M.M. Abbas, A.Y. Chang, A. Goldman, F.W. Irion, H.A. Michelsen, M.J. Newchurch, C.P. Rinsland, R.J. Salawitch, G.P. Stiller, and R. Zander, ATMOS/ATLAS-3 observations of long-lived tracers and descent in the Antarctic vortex in November 1994, *Geophys. Res. Lett.*, 23, 2345-2348, 1996a.

- Abrams, M.C., G.L. Manney, M.R. Gunson, M.M. Abbas, A.Y. Chang, A. Goldman, F.W. Irion, H.A. Michelsen, M.J. Newchurch, C.P. Rinsland, R.J. Salawitch, G.P. Stiller, and R. Zander, Trace gas transport in the Arctic vortex inferred from ATMOS ATLAS-2 observations during April 1993, *Geophys. Res. Lett.*, *23*, 2341-2344, 1996b.
- Aellig, C.P., J. Bacmeister, R.M. Bevilacqua, M. Daehler, D. Kriebel, T. Pauls, D. Siskind, N. Kämpfer, J. Langen, G. Hartmann, A. Berg, J.H. Park, and J.M. Russell III, Space-borne H₂O observations in the Arctic stratosphere and mesosphere in the spring of 1992, *Geophys. Res. Lett.*, *23*, 2325-2328, 1996a.
- Aellig, C.P., N. Kämpfer, C. Rudin, R.M. Bevilacqua, W. Degenhardt, P. Hartogh, C. Jarchow, K. Künzi, J.J. Olivero, C. Croskey, J.W. Waters, and H.A. Michelsen, Latitudinal distribution of upper stratospheric ClO as derived from space borne microwave spectroscopy, *Geophys. Res. Lett.*, *23*, 2321-2324, 1996b.
- Allen, D.R., J.L. Stanford, L.S. Elson, E.F. Fishbein, L. Froidevaux, and J.W. Waters, The 4-day wave as observed from the Upper Atmosphere Research Satellite Microwave Limb Sounder, *J. Atmos. Sci.*, *54*, 420-434, 1997.
- Allen, M., and M.L. Delitsky, Inferring the abundances of ClO and HO₂ from Spacelab 3 Atmospheric Trace Molecule Spectroscopy observations, *J. Geophys. Res.*, *96*, 2913-2919, 1991.
- Allen, M., and J.E. Frederick, Effective photodissociation cross sections for molecular oxygen and nitric oxide in the Schumann-Runge bands, *J. Atmos. Sci.*, *39*, 2066-2075, 1982.
- Amoruso, A., L. Crescentini, M.S. Cola, and G. Fiocco, Oxygen absorption cross-section in the Herzberg continuum, *J. Quant. Spectrosc. Radiat. Transfer*, *56*, 145-152, 1996.
- Anderson, G.P., and L.A. Hall, Attenuation of solar irradiance in the stratosphere: Spectrometer measurements between 191 and 207 nm, *J. Geophys. Res.*, *88*, 6801-6806, 1983.
- Andrews, D.G., J.R. Holton, and C.B. Leovy, *Middle Atmosphere Dynamics*, Academic Press, London, U.K., 1987.
- Appenzeller, C., J.R. Holton, and K.H. Rosenlof, Seasonal variation of mass transport across the tropopause, *J. Geophys. Res.*, *101*, 15071-15078, 1996.
- Bacmeister, J.T., M.R. Schoeberl, M.E. Summers, J.R. Rosenfield, and X. Zhu, Descent of long-lived trace gases in the winter polar vortex, *J. Geophys. Res.*, *100*, 11669-11684, 1995.
- Bacmeister, J.T., D.E. Siskind, M.E. Summers, and S.D. Eckermann, Age of air in a zonally averaged two-dimensional model, *J. Geophys. Res.*, *103*, 11263-11288, 1998.
- Bates, D.R., and M. Nicolet, The photochemistry of atmospheric water vapor, *J. Geophys. Res.*, *55*, 301-327, 1950.
- Bekki, S., M.P. Chipperfield, J.A. Pyle, J.J. Remedios, S.E. Smith, R.G. Grainger, A. Lambert, J.B. Kumer, and J.L. Mergenthaler, Coupled aerosol-chemical modeling of UARS HNO₃ and N₂O₅ measurements in the Arctic upper stratosphere, *J. Geophys. Res.*, *102*, 8977-8994, 1997.
- Blindauer, C., V. Rozanov, and J.P. Burrows, Actinic flux and photolysis frequency comparison computations using the model PHOTOGT, *J. Atmos. Chem.*, *24*, 1-21, 1996.
- Burnett, C.R., and E.B. Burnett, The regime of decreased OH vertical column abundances at Fritz Peak Observatory, CO: 1991-1995, *Geophys. Res. Lett.*, *23*, 1925-1927, 1996.
- Callis, L.B., and J.D. Lambeth, NO_y formed by precipitating electron events in 1991 and 1992: Descent into the stratosphere as observed by ISAMS, *Geophys. Res. Lett.*, *25*, 1875-1878, 1998.
- Callis, L.B., D.N. Baker, M. Natarajan, J.B. Blake, R.A. Mewaldt, R.S. Selesnick, and J.R. Cummings, A 2D model simulation of downward transport of NO_y into the stratosphere: Effects on the 1994 austral spring O₃ and NO_y, *Geophys. Res. Lett.*, *23*, 1905-1908, 1996.
- Carr, E.S., R.S. Harwood, P.W. Mote, G.E. Peckham, R.A. Suttie, W.A. Lahoz, A. O'Neill, L. Froidevaux, R.F. Jarnot, W.G. Read, J.W. Waters, and R. Swinbank, Tropical stratospheric water vapor measured by the Microwave Limb Sounder (MLS), *Geophys. Res. Lett.*, *22*, 691-694, 1995.
- Chance, K., W.A. Traub, D.G. Johnson, K.W. Jucks, P. Ciarpallini, R.A. Stachnik, R.J. Salawitch, and H.A. Michelsen, Simultaneous measurements of stratospheric HO_x, NO_x, and Cl_x: Comparison with a photochemical model, *J. Geophys. Res.*, *101*, 9031-9043, 1996.

UPPER STRATOSPHERIC PROCESSES

- Chandra, S., and R.D. McPeters, The solar cycle variation of ozone in the stratosphere inferred from Nimbus 7 and NOAA 11 satellites, *J. Geophys. Res.*, *99*, 20665-20671, 1994.
- Chandra, S., C.H. Jackman, A.R. Douglass, E.L. Fleming, and D.B. Considine, Chlorine catalyzed destruction of ozone: Implications for ozone variability in the upper stratosphere, *Geophys. Res. Lett.*, *20*, 351-354, 1993.
- Chandra, S., C.H. Jackman, and E.L. Fleming, Recent trends in ozone in the upper stratosphere: Implications for chlorine chemistry, *Geophys. Res. Lett.*, *22*, 843-846, 1995.
- Chen, L., J. London, and G. Brasseur, Middle atmospheric ozone and temperature responses to solar irradiance variations over 27-day periods, *J. Geophys. Res.*, *102*, 29957-29979, 1997.
- Chipperfield, M.P., L.J. Gray, J.S. Kinnersley, and J. Zawodny, A two-dimensional model study of the QBO signal in SAGE II NO₂ and O₃, *Geophys. Res. Lett.*, *21*, 589-592, 1994.
- Clancy, R.T., B.J. Sandor, D.W. Rusch, and D.O. Muhleman, Microwave observations and modeling of O₃, H₂O, and HO₂ in the mesosphere, *J. Geophys. Res.*, *99*, 5465-5473, 1994.
- Claude, H., F. Schöenborn, W. Steinbrecht, and W. Vandersee, New evidence for ozone depletion in the upper stratosphere, *Geophys. Res. Lett.*, *21*, 2409-2412, 1994.
- Coffey, M.T., Observations of the impact of volcanic activity on stratospheric chemistry, *J. Geophys. Res.*, *101*, 6767-6780, 1996.
- Connor, B.J., D.E. Siskind, J.J. Tsou, A. Parrish, and E.E. Remsberg, Ground-based microwave observations of ozone in the upper stratosphere and mesosphere, *J. Geophys. Res.*, *99*, 16757-16770, 1994.
- Considine, D.B., A.E. Dessler, C.H. Jackman, J.E. Rosenfield, P.E. Meade, M.R. Schoeberl, A.E. Roche, and J.W. Waters, Interhemispheric asymmetry in the 1 mbar O₃ trend: An analysis using an interactive zonal mean model and UARS data, *J. Geophys. Res.*, *103*, 1607-1618, 1998.
- Considine, G.D., L. Deaver, E.E. Remsberg, and J.M. Russell III, HALOE observations of a slowdown in the rate of increase of HF in the lower mesosphere, *Geophys. Res. Lett.*, *24*, 3217-3220, 1997.
- Conway, R.R., M.H. Stevens, J.G. Cardon, S.E. Zasadil, C.M. Brown, J.S. Morrill, and G.H. Mount, Satellite measurements of hydroxyl in the mesosphere, *Geophys. Res. Lett.*, *23*, 2093-2096, 1996.
- Coy, L., and R. Swinbank, Characteristics of stratospheric winds and temperatures produced by data assimilation, *J. Geophys. Res.*, *102*, 25763-25781, 1997.
- Crutzen, P.J., The influence of nitrogen oxides on the atmospheric ozone content, *Quart. J. Roy. Meteorol. Soc.*, *96*, 320-325, 1970.
- Crutzen, P.J., Estimates of possible future ozone reductions from continued use of fluorochloro-methanes (CF₂Cl₂, CFCl₃), *Geophys. Res. Lett.*, *1*, 205-208, 1974.
- Crutzen, P.J., Mesospheric mysteries, *Science*, *277*, 1951-1952, 1997.
- Crutzen, P.J., and U. Schmailzl, Chemical budgets of the stratosphere, *Planet. Space Sci.*, *31*, 1009-1032, 1983.
- Crutzen, P.J., J.-U. Groöb, C. Brühl, R. Müller, and J.M. Russell III, A reevaluation of the ozone budget with HALOE UARS data: No evidence for the ozone deficit, *Science*, *268*, 705-708, 1995.
- Dahlback, A., and K. Stamnes, A new spherical model for computing the radiation field available for photolysis and heating at twilight, *Planet. Space Sci.*, *39*, 671-683, 1991.
- DeLand, M.T., and R.P. Cebula, Composite Mg II solar activity index for solar cycles 21 and 22, *J. Geophys. Res.*, *98*, 12809-12823, 1993.
- DeMore, W.B., S.P. Sander, D.M. Golden, R.F. Hampson, M.J. Kurylo, C.J. Howard, A.R. Ravishankara, C.E. Kolb, and M.J. Molina, *Chemical Kinetics and Photochemical Data for Use in Stratospheric Modeling, Evaluation No. 11*, JPL Publ. 94-26, Jet Propulsion Laboratory, Pasadena, Calif., 1994.
- DeMore, W.B., S.P. Sander, D.M. Golden, R.F. Hampson, M.J. Kurylo, C.J. Howard, A.R. Ravishankara, C.E. Kolb, and M.J. Molina, *Chemical Kinetics and Photochemical Data for Use in Stratospheric Modeling, Evaluation No. 12*, JPL Publ. 97-4, Jet Propulsion Laboratory, Pasadena, Calif., 1997.
- Dessler, A.E., E.M. Weinstock, E.J. Hints, J.G. Anderson, C.R. Webster, R.D. May, J.W. Elkins, and G.S. Dutton, An examination of the total hydrogen budget of the lower stratosphere, *Geophys. Res. Lett.*, *21*, 2563-2566, 1994.

- Dessler, A.E., D.B. Considine, G.A. Morris, M.R. Schoeberl, J.M. Russell III, A.E. Roche, J.B. Kumer, J.L. Mergenthaler, J.W. Waters, J.C. Gille, and G.K. Yue, Correlated observations of HCl and ClONO₂ from UARS and implications for stratospheric chlorine partitioning, *Geophys. Res. Lett.*, *22*, 1721-1724, 1995.
- Dessler, A.E., S.R. Kawa, A.R. Douglass, D.B. Considine, J.B. Kumer, A.E. Roche, J.L. Mergenthaler, J.W. Waters, J.M. Russell III, and J.C. Gille, A test of the partitioning between ClO and ClONO₂ using simultaneous UARS measurements of ClO, NO₂, and ClONO₂, *J. Geophys. Res.*, *101*, 12515-12521, 1996.
- Donahue, N.M., M.K. Dubey, R. Mohrschladt, K.L. Demerjian, and J.G. Anderson, High-pressure flow study of the reactions OH + NO_x → HONO_x: Errors in the falloff region, *J. Geophys. Res.*, *102*, 6159-6168, 1997.
- Douglass, A.R., R.B. Rood, S.R. Kawa, and D.J. Allen, A three-dimensional simulation of the evolution of the middle latitude winter ozone in the middle stratosphere, *J. Geophys. Res.*, *102*, 19217-19232, 1997.
- Dunkerton, T.J., The role of gravity waves in the quasi-biennial oscillation, *J. Geophys. Res.*, *102*, 26053-26076, 1997.
- Dunkerton, T.J., and D.P. Delisi, Interaction of the quasi-biennial oscillation and stratopause semiannual oscillation, *J. Geophys. Res.*, *102*, 26107-26116, 1997.
- Eckman, R.S., W.L. Grose, R.E. Turner, W.T. Blackshear, J.M. Russell III, L. Froidevaux, J.W. Waters, J.B. Kumer, and A.E. Roche, Stratospheric trace constituents simulated by a three-dimensional general circulation model: Comparison with UARS data, *J. Geophys. Res.*, *100*, 13951-13966, 1995.
- Eluszkiewicz, J., and M. Allen, A global analysis of the ozone deficit in the upper stratosphere and lower mesosphere, *J. Geophys. Res.*, *98*, 1069-1082, 1993.
- Eluszkiewicz, J., R.A. Plumb, and N. Nakamura, Dynamics of wintertime stratospheric transport in the Geophysical Fluid Dynamics Laboratory SKYHI general circulation model, *J. Geophys. Res.*, *100*, 20883-20900, 1995.
- Eluszkiewicz, J., D. Crisp, R. Zurek, L. Elson, E. Fishbein, L. Froidevaux, J. Waters, R.G. Grainger, A. Lambert, R. Harwood, and G. Peckham, Residual circulation in the stratosphere and lower mesosphere as diagnosed from Microwave Limb Sounder data, *J. Atmos. Sci.*, *53*, 217-240, 1996.
- Engel, A., C. Schiller, U. Schmidt, R. Borchers, H. Ovarlez, and J. Ovarlez, The total hydrogen budget in the Arctic winter stratosphere during the European Arctic Stratospheric Ozone Experiment, *J. Geophys. Res.*, *101*, 14495-14503, 1996.
- Evans, S.J., R. Toumi, J.E. Harries, M.P. Chipperfield, and J.M. Russell III, Trends in stratospheric humidity and the sensitivity of ozone to these trends, *J. Geophys. Res.*, *103*, 8715-8725, 1998.
- Fleming, E.L., S. Chandra, C.H. Jackman, D.B. Considine, and A.R. Douglass, The middle atmospheric response to short and long term solar UV variations: An analysis of observations and 2D model results, *J. Atmos. Terr. Phys.*, *57*, 333-365, 1995.
- Fisher, M., A. O'Neill, and R. Sutton, Rapid descent of mesospheric air into the stratospheric polar vortex, *Geophys. Res. Lett.*, *20*, 1267-1270, 1993.
- Frank, L.A., and J.B. Sigwarth, Atmospheric holes and small comets, *Rev. Geophys.*, *31*, 1-28, 1993.
- Frank, L.A., and J.B. Sigwarth, Transient decreases of Earth's far-ultraviolet dayglow, *Geophys. Res. Lett.*, *24*, 2423-2426, 1997.
- Froidevaux, L., M. Allen, and Y.L. Yung, A critical analysis of ClO and O₃ in the mid-latitude stratosphere, *J. Geophys. Res.*, *90*, 12999-13029, 1985.
- Garcia, R.R., and B.A. Boville, "Downward control" of the mean meridional circulation and temperature distribution of the polar winter stratosphere, *J. Atmos. Sci.*, *51*, 2238-2245, 1994.
- Gordley, L.L., J.M. Russell III, L.J. Mickely, J.E. Frederick, J.H. Park, K.A. Stone, G.M. Beaver, J.M. McInerney, L.E. Deaver, G.C. Toon, F.J. Murcray, R.D. Blatherwick, M.R. Gunson, J.P.D. Abbatt, R.L. Mauldin III, G.H. Mount, B. Sen, and J.-F. Blavier, Validation of nitric oxide and nitrogen dioxide measurements made by the Halogen Occultation Experiment for UARS platform, *J. Geophys. Res.*, *101*, 10241-10266, 1996.
- Gray, L.J., and J.A. Pyle, The semi-annual oscillation and equatorial tracer distributions, *Quart. J. Roy. Meteorol. Soc.*, *112*, 387-407, 1986.

UPPER STRATOSPHERIC PROCESSES

- Groß, J.-U., R. Müller, G. Becker, D.S. McKenna, and P.J. Crutzen, The upper stratospheric ozone budget: An update of calculations based on HALOE data, *J. Atmos. Chem.*, submitted, 1998.
- Gunson, M.R., C.B. Farmer, R.H. Norton, R. Zander, C.P. Rinsland, J.H. Shaw, and B.-C. Gao, Measurements of CH₄, N₂O, CO, H₂O, and O₃ in the middle atmosphere by the Atmospheric Trace Molecule Spectroscopy experiment on Spacelab 3, *J. Geophys. Res.*, *95*, 13867-13882, 1990.
- Gunson, M.R., M.C. Abrams, L.L. Lowes, E. Mahieu, R. Zander, C.P. Rinsland, M.K.W. Ko, N.D. Sze, and D.K. Weisenstein, Increase in levels of stratospheric chlorine and fluorine loading between 1985 and 1992, *Geophys. Res. Lett.*, *21*, 2223-2226, 1994.
- Gunson, M.R., M.M. Abbas, M.C. Abrams, M. Allen, L.R. Brown, T.L. Brown, A.Y. Chang, A. Goldman, F.W. Irion, L.L. Lowes, E. Mahieu, G.L. Manney, H.A. Michelsen, M.J. Newchurch, C.P. Rinsland, R.J. Salawitch, G.P. Stiller, G.C. Toon, Y.L. Yung, and R. Zander, The Atmospheric Trace Molecule Spectroscopy (ATMOS) experiment: Deployment on the ATLAS Space Shuttle missions, *Geophys. Res. Lett.*, *23*, 2333-2336, 1996.
- Hall, T.M., and R.A. Plumb, Age as a diagnostic of stratospheric transport, *J. Geophys. Res.*, *99*, 1059-1070, 1994.
- Hall, T.M., and D.W. Waugh, Timescales for the stratospheric circulation derived from tracers, *J. Geophys. Res.*, *102*, 8991-9001, 1997.
- Hannegan, B., S. Olsen, M. Prather, X. Zhu, D. Rind, and J. Lerner, The dry stratosphere: A limit on cometary water influx, *Geophys. Res. Lett.*, *25*, 1649-1652, 1998.
- Harnisch, J., R. Borchers, P. Fabian, and M. Maiss, Tropospheric trends for CF₄ and C₂F₆ since 1982 derived from SF₆ dated stratospheric air, *Geophys. Res. Lett.*, *23*, 1099-1102, 1996.
- Harries, J.E., J.M. Russell III, A.F. Tuck, L.L. Gordley, P. Purcell, K. Stone, R.M. Bevilacqua, M.R. Gunson, G. Nedoluha, and W.A. Traub, Validation of measurements of water vapor from the Halogen Occultation Experiment (HALOE), *J. Geophys. Res.*, *101*, 10205-10216, 1996.
- Harris, N.R.P., G. Ancellet, L. Bishop, D.J. Hofmann, J.B. Kerr, R.D. McPeters, M. Prendez, W.J. Randel, J. Staehelin, B.H. Subbaraya, A. Volz-Thomas, J. Zawodny, and C.S. Zerefos, Trends in stratospheric and free tropospheric ozone, *J. Geophys. Res.*, *102*, 1571-1590, 1997.
- Hartmann, D.L., and R.R. Garcia, A mechanistic model of ozone transport by planetary waves in the stratosphere, *J. Atmos. Sci.*, *36*, 350-364, 1979.
- Harvey, V.L., and M.H. Hitchman, A climatology of the Aleutian High, *J. Atmos. Sci.*, *53*, 2088-2101, 1996.
- Hernandez, R., R. Toumi, and D.C. Clary, State-selected vibrational-relaxation rates for highly vibrationally excited oxygen molecules, *J. Chem. Phys.*, *102*, 9544-9556, 1995.
- Hilsenrath, E., R.P. Cebula, and C.H. Jackman, Ozone depletion in the upper stratosphere estimated from satellite and Space Shuttle data, *Nature*, *358*, 131-133, 1992.
- Hitchman, M.H., M. McKay, and C.R. Trepte, A climatology of stratospheric aerosol, *J. Geophys. Res.*, *99*, 20689-20700, 1994.
- Hollandsworth, S.M., R.D. McPeters, L.E. Flynn, W. Planet, A.J. Miller, and S. Chandra, Ozone trends deduced from combined Nimbus 7 SBUV and NOAA 11 SBUV/2 data, *Geophys. Res. Lett.*, *22*, 905-908, 1995.
- Holton, J.R., P.H. Haynes, M.E. McIntyre, A.R. Douglass, R.B. Rood, and L. Pfister, Stratosphere-troposphere exchange, *Rev. Geophys.*, *33*, 403-439, 1995.
- Hood, L.L., and S. Cantrell, Stratospheric ozone and temperature responses to short term solar ultraviolet variations: Reproducibility of low-latitude response measurements, *Ann. Geophys.*, *6*, 525-530, 1988.
- Iwagami, N., S. Inomata, I. Murata, and T. Ogawa, Doppler detection of hydroxyl column abundance in the middle atmosphere, *J. Atmos. Chem.*, *20*, 1-15, 1995.
- Iwagami, N., S. Inomata, and T. Ogawa, Doppler detection of hydroxyl column abundance in the middle atmosphere: 2. Measurement for three years and a comparison with a 1D model, *J. Atmos. Chem.*, *29*, 195-216, 1998.
- Jackman, C.H., R.S. Stolarski, and J.A. Kaye, Two-dimensional monthly average ozone balance from Limb Infrared Monitor of the Stratosphere and Stratospheric and Mesospheric Sounder data, *J. Geophys. Res.*, *91*, 1103-1116, 1986.
- Jackman, C.H., E.L. Fleming, S. Chandra, D.B. Considine, and J.E. Rosenfield, Past, present, and future modeled ozone trends with comparisons to observed trends, *J. Geophys. Res.*, *101*, 28753-28767, 1996.

- Johnston, J.C., S.S. Cliff, and M.H. Thieme, Measurement of multioxygen isotopic ($\delta^{18}\text{O}$ and $\delta^{17}\text{O}$) fractionation factors in the stratospheric sink reactions of nitrous oxide, *J. Geophys. Res.*, *100*, 16801-16804, 1995.
- Jones, D.B.A., H.R. Schneider, and M.B. McElroy, Effects of the quasi-biennial oscillation on the zonally averaged transport of tracers, *J. Geophys. Res.*, *103*, 11235-11249, 1998.
- Jucks, K.W., D.G. Johnson, K.V. Chance, W.A. Traub, R.J. Salawitch, and R.A. Stachnik, Ozone production and loss rate measurements in the middle stratosphere, *J. Geophys. Res.*, *101*, 28785-28792, 1996.
- Jucks, K.W., D.G. Johnson, K.V. Chance, W.A. Traub, J.J. Margitan, G.B. Osterman, R.J. Salawitch, and Y. Sasano, Observations of OH, HO₂, H₂O, and O₃ in the upper stratosphere: Implications for HO_x photochemistry, *Geophys. Res. Lett.*, *25*, 3935-3938, 1998.
- Kawa, S.R., J.B. Kumer, A.R. Douglass, A.E. Roche, S.E. Smith, F.W. Taylor, and D.J. Allen, Missing chemistry of reactive nitrogen in the upper stratospheric polar winter, *Geophys. Res. Lett.*, *22*, 2629-2632, 1995.
- Kaye, J.A., S. Penkett, and F.M. Ormond (eds.), *Report on Concentrations, Lifetimes, and Trends of CFCs, Halons, and Related Species*, NASA Reference Publication 1339, NASA Office of Mission to Planet Earth, 247 pp., National Aeronautics and Space Administration, Washington, D.C., 1994.
- Kennaugh, R., S. Ruth, and L.J. Gray, Modeling quasi-biennial variability in the semiannual double peak, *J. Geophys. Res.*, *102*, 16169-16187, 1997.
- Khosravi, R., G.P. Brasseur, A.K. Smith, D.W. Rusch, J.W. Waters, and J.M. Russell III, Significant reduction in the stratospheric ozone deficit using three-dimensional model constrained with UARS data, *J. Geophys. Res.*, *103*, 16203-16219, 1998.
- Kim, K.R., and H. Craig, Nitrogen-15 and oxygen-18 characteristics of nitrous oxide: A global perspective, *Science*, *262*, 1855-1857, 1993.
- Kondo, Y., U. Schmidt, T. Sugita, A. Engel, M. Koike, P. Amedieu, M.R. Gunson, and J. Rodriguez, NO_y correlation with N₂O and CH₄ in the midlatitude stratosphere, *Geophys. Res. Lett.*, *23*, 2369-2372, 1996.
- Kondo, Y., T. Sugita, R.J. Salawitch, M. Koike, and T. Deshler, Effect of Pinatubo aerosols on stratospheric NO, *J. Geophys. Res.*, *102*, 1205-1213, 1997.
- Koppers, G.A.A., and D.P. Murtagh, Model studies of the influence of O₂ photodissociation parameterizations in the Schumann-Runge bands on ozone related photolysis in the upper atmosphere, *Ann. Geophys.*, *14*, 68-79, 1996.
- Lahoz, W.A., A. O'Neill, E.S. Carr, R.S. Harwood, L. Froidevaux, W.G. Read, J.W. Waters, J.B. Kumer, J.L. Mergenthaler, A.E. Roche, G.E. Peckham, and R. Swinbank, Three-dimensional evolution of water vapor distributions in the Northern Hemisphere stratosphere as observed by the MLS, *J. Atmos. Sci.*, *51*, 2914-2930, 1994.
- Lahoz, W.A., A. O'Neill, A. Heaps, V.D. Pope, R. Swinbank, R.S. Harwood, L. Froidevaux, W.G. Read, J.W. Waters, and G.E. Peckham, Vortex dynamics and the evolution of water vapour in the stratosphere of the southern hemisphere, *Quart. J. Roy. Meteorol. Soc.*, *122*, 423-450, 1996.
- Lary, D.J., A.M. Lee, R. Toumi, M.J. Newchurch, M. Pirre, and J.B. Renard, Carbon aerosols and atmospheric photochemistry, *J. Geophys. Res.*, *102*, 3671-3682, 1997.
- Lean, J.L., G.J. Rottman, H.L. Kyle, T.N. Woods, J.R. Hickey, and L.C. Puga, Detection and parameterization of variations in solar mid- and near-ultraviolet radiation (200-400 nm), *J. Geophys. Res.*, *102*, 29939-29956, 1997.
- Lipson, J.B., M.J. Elrod, T.W. Beiderhase, L.T. Molina, and M.J. Molina, Temperature dependence of the rate constant and branching ratio for the OH + ClO reaction, *J. Chem. Soc., Faraday Trans.*, *93*, 2665-2673, 1997.
- London, J., G.J. Rottman, T.N. Woods, and F. Wu, Time variations of solar UV irradiance as measured by the SOLSTICE (UARS) instrument, *Geophys. Res. Lett.*, *20*, 1315-1318, 1993.
- Luo, M., R.J. Cicerone, and J.M. Russell III, Analysis of Halogen Occultation Experiment HF versus CH₄ correlation plots: Chemistry and transport implications, *J. Geophys. Res.*, *100*, 13927-13937, 1995.
- Luo, M., J.H. Park, K.M. Lee, J.M. Russell III, and C. Brühl, An analysis of HALOE observations in summer high latitudes using air mass trajectory and photochemical model calculations, *J. Geophys. Res.*, *102*, 16145-16156, 1997a.

UPPER STRATOSPHERIC PROCESSES

- Luo, M., J.M. Russell III, and T.Y.W. Huang, Halogen Occultation Experiment observations of the quasi-biennial oscillation and the effects of Pinatubo aerosols in the tropical stratosphere, *J. Geophys. Res.*, *102*, 19187-19198, 1997b.
- Manney, G.L., R.W. Zurek, A. O'Neill, and R. Swinbank, On the motion of air through the stratospheric polar vortex, *J. Atmos. Sci.*, *51*, 2973-2994, 1994a.
- Manney, G.L., R.W. Zurek, A. O'Neill, R. Swinbank, J.B. Kumer, J.L. Mergenthaler, and A.E. Roche, Stratospheric warmings during February and March 1993, *Geophys. Res. Lett.*, *21*, 813-816, 1994b.
- Manney, G.L., L. Froidevaux, J.W. Waters, R.W. Zurek, J.C. Gille, J.B. Kumer, J.L. Mergenthaler, A.E. Roche, A. O'Neill, and R. Swinbank, Formation of low-ozone pockets in the middle stratospheric anticyclone during winter. *J. Geophys. Res.*, *100*, 13939-13950, 1995a.
- Manney, G.L., R.W. Zurek, W.A. Lahoz, R.S. Harwood, J.C. Gille, J.B. Kumer, J.L. Mergenthaler, A.E. Roche, A. O'Neill, R. Swinbank, and J.W. Waters, Lagrangian transport calculations using UARS data: Part I, Passive tracers, *J. Atmos. Sci.*, *52*, 3049-3068, 1995b.
- Manney, G.L., J.C. Bird, D.P. Donovan, T.J. Duck, J.A. Whiteway, S.R. Pal, and A.I. Carswell, Modeling ozone laminae in ground-based arctic wintertime observations using trajectory calculations and satellite data, *J. Geophys. Res.*, *103*, 5797-5814, 1998.
- McCormack, J.P., and L.L. Hood, Apparent solar cycle variations of upper stratospheric ozone and temperature: Latitude and seasonal dependences, *J. Geophys. Res.*, *101*, 20933-20944, 1996.
- McElroy, M.B., and D.B.A. Jones, Evidence for an additional source of atmospheric N₂O, *Global Biogeochem. Cycles*, *10*, 651-659, 1996.
- McElroy, M.B., and R.J. Salawitch, Changing composition of the global stratosphere, *Science*, *243*, 763-770, 1989.
- McIntyre, M.E., and T.N. Palmer, The "surf zone" in the stratosphere, *J. Atmos. Terr. Phys.*, *46*, 825-849, 1984.
- Michelsen, H.A., R.J. Salawitch, P.O. Wennberg, and J.G. Anderson, Production of O(¹D) from photolysis of O₃, *Geophys. Res. Lett.*, *21*, 2227-2230, 1994.
- Michelsen, H.A., R.J. Salawitch, M.R. Gunson, C. Aellig, N. Kämpfer, M.M. Abbas, M.C. Abrams, T.L. Brown, A.Y. Chang, A. Goldman, F.W. Irion, M.J. Newchurch, C.P. Rinsland, G.P. Stiller, and R. Zander, Stratospheric chlorine partitioning: Constraints from shuttle-borne measurements of [HCl], [ClNO₂], and [ClO], *Geophys. Res. Lett.*, *23*, 2361-2364, 1996.
- Michelsen, H.A., G.L. Manney, M.R. Gunson, C.P. Rinsland, and R. Zander, Correlations of stratospheric abundances of CH₄ and N₂O derived from ATMOS measurements, *Geophys. Res. Lett.*, *25*, 2777-2780, 1998.
- Miller, A.J., L.E. Flynn, S.M. Hollandsworth, J.J. DeLuisi, I.V. Petropavlovskikh, G.C. Tiao, G.C. Reinsel, D.J. Wuebbles, J. Kerr, R.M. Nagatani, L. Bishop, and C.H. Jackman, Information content of Umkehr and solar backscattered ultraviolet (SBUV) 2 satellite data for ozone trends and solar responses in the stratosphere, *J. Geophys. Res.*, *102*, 19257-19263, 1997.
- Miller, R.L., A.G. Suits, P.L. Houston, R. Toumi, J.A. Mack, and A.M. Wodtke, The ozone deficit problem: O₂(X,v ≥ 26) + O(³P) from 226-nm ozone photodissociation, *Science*, *265*, 1831-1838, 1994.
- Minschwaner, K., and D.E. Siskind, A new calculation of nitric oxide photolysis in the stratosphere, mesosphere, and lower thermosphere, *J. Geophys. Res.*, *98*, 20401-20412, 1993.
- Minschwaner, K., G.P. Anderson, L.A. Hall, and K. Yoshino, Polynomial coefficients for calculating O₂ Schumann-Runge cross sections at 0.5 cm⁻¹ resolution, *J. Geophys. Res.*, *97*, 10103-10108, 1992.
- Minschwaner, K., R.J. Salawitch, and M.B. McElroy, Absorption of solar radiation by O₂: Implications for O₃ and lifetimes of N₂O, CFCl₃, and CF₂Cl₂, *J. Geophys. Res.*, *98*, 10543-10561, 1993.
- Molina, M.J., and F.S. Rowland, Stratospheric sink for chlorofluoromethanes: Chlorine atom catalysed destruction of ozone, *Nature*, *249*, 810-812, 1974.
- Montzka, S.A., J.H. Butler, R.C. Meyers, T.M. Thompson, T.H. Swanson, A.D. Clarke, L.T. Lock, and J.W. Elkins, Decline in the tropospheric abundance of halogen from halocarbons: Implications for stratospheric ozone depletion, *Science*, *272*, 1318-1322, 1996.

- Morrey, M.W., and R.S. Harwood, Interhemispheric differences in stratospheric water vapour during late winter, in version 4 MLS measurements, *Geophys. Res. Lett.*, *25*, 147-150, 1998.
- Morris, G.A., D.B. Considine, A.E. Dessler, S.R. Kawa, J. Kumer, J. Mergenthaler, A. Roche, and J.M. Russell III, Nitrogen partitioning in the middle stratosphere as observed by the Upper Atmosphere Research Satellite, *J. Geophys. Res.*, *102*, 8955-8965, 1997.
- Morris, G.A., S.R. Kawa, A.R. Douglass, M.R. Schoeberl, L. Froidevaux, and J.W. Waters, Low-ozone pockets explained, *J. Geophys. Res.*, *103*, 3599-3610, 1998.
- Mosier, A., C. Kroeze, C. Nevison, O. Oenema, S. Seitzinger, and O. van Cleemput, Closing the global atmospheric N₂O budget: Nitrous oxide emissions through the agricultural nitrogen cycle, *Nutr. Cyc. Agroecosyst.*, *52*, 225-248, 1998.
- Mote, P.W., The annual cycle of stratospheric water vapor in a general circulation model, *J. Geophys. Res.*, *100*, 7363-7379, 1995.
- Mote, P.W., K.H. Rosenlof, M.E. McIntyre, E.S. Carr, J.C. Gille, J.R. Holton, J.S. Kinnnersley, H.C. Pumphrey, J.M. Russell III, and J.W. Waters, An atmospheric tape recorder: The imprint of tropical tropopause temperatures on stratospheric water vapor, *J. Geophys. Res.*, *101*, 3989-4006, 1996.
- Nair, H., M. Allen, L. Froidevaux, and R.W. Zurek, Localized rapid ozone loss in the northern winter stratosphere: An analysis of UARS observations, *J. Geophys. Res.*, *103*, 1555-1571, 1998.
- Natarajan, M., and L.B. Callis, Stratospheric photochemical studies with Atmospheric Trace Molecule Spectroscopy (ATMOS) measurements, *J. Geophys. Res.*, *96*, 9361-9370, 1991.
- Nedoluha, G.E., D.E. Siskind, J.T. Bacmeister, R.M. Bevilacqua, and J.M. Russell III, Changes in upper stratospheric CH₄ and NO₂ as measured by HALOE and implications for changes in transport, *Geophys. Res. Lett.*, *25*, 987-990, 1998a.
- Nedoluha, G.E., R.M. Bevilacqua, R.M. Gomez, D.E. Siskind, B.C. Hicks, J.M. Russell III, and B.J. Connor, Increases in middle atmospheric water vapor as observed by the Halogen Occultation Experiment and the ground-based Water Vapor Millimeter-wave Spectrometer from 1991 to 1997, *J. Geophys. Res.*, *103*, 3531-3543, 1998b.
- Nevison, C.D., and E.A. Holland, A reexamination of the impact of anthropogenically fixed nitrogen on atmospheric N₂O and the stratospheric O₃ layer, *J. Geophys. Res.*, *102*, 25519-25536, 1997.
- Nevison, C.D., S. Solomon, and J.M. Russell III, Night-time formation of N₂O₅ inferred from the Halogen Occultation Experiment sunset/sunrise NO_x ratios, *J. Geophys. Res.*, *101*, 6741-6748, 1996.
- Nevison, C.D., S. Solomon, and R.R. Garcia, Model overestimates of NO_y in the upper stratosphere, *Geophys. Res. Lett.*, *24*, 803-806, 1997.
- Nightingale, R.W., A.E. Roche, J.B. Kumer, J.L. Mergenthaler, J.C. Gille, S.T. Massie, P.L. Bailey, D.P. Edwards, M.R. Gunson, G.C. Toon, B. Sen, J.-F. Blavier, and P.S. Connell, Global CF₂Cl₂ measurements by UARS cryogenic limb array etalon spectrometer: Validation by correlative data and a model, *J. Geophys. Res.*, *101*, 9711-9736, 1996.
- Oelhaf, H., G. Wetzel, T. von Clarmann, M. Schmidt, J.B. Renard, M. Pirre, E. Lateltin, P. Amedieu, C. Phillips, F. Goutail, J.-P. Pommereau, Y. Kondo, T. Sugita, H. Nakajima, M. Koike, W.J. Williams, F.J. Murcray, P. Sullivan, A. Engel, U. Schmidt, and A.M. Lee, Correlative balloon measurements of the vertical distribution of N₂O, NO, NO₂, NO₃, HNO₃, N₂O₅, ClONO₂ and total reactive NO_y inside the polar vortex during SESAME, in *Polar Stratospheric Ozone, Proceedings of the Third European Workshop*, 18 to 22 September 1995, edited by J.A. Pyle, N.R.P. Harris, and G.T. Amanatidis, pp. 187-192, European Commission, Luxembourg, 1996.
- Oltmans, S.J., and D.J. Hofmann, Increase in lower-stratospheric water vapour at a mid-latitude Northern Hemisphere site from 1981 to 1994, *Nature*, *374*, 146-149, 1995.
- Osterman, G.B., R.J. Salawitch, B. Sen, G.C. Toon, R.A. Stachnik, H.M. Pickett, J.J. Margitan, and D.B. Peterson, Balloon-borne measurements of stratospheric radicals and their precursors: Implications for the production and loss of ozone, *Geophys. Res. Lett.*, *24*, 1107-1110, 1997.
- Park, J.H., J.M. Russell III, L.L. Gordley, S.R. Drayson, D.C. Benner, J.M. McInerney, M.R. Gunson, G.C. Toon, B. Sen, J.-F. Blavier, C.R. Webster, E.C. Zipf, P. Erdman, U. Schmidt, and C. Schiller, Validation of Halogen Occultation Experiment CH₄ measurements from the UARS, *J. Geophys. Res.*, *101*, 10183-10203, 1996.

UPPER STRATOSPHERIC PROCESSES

- Park, J., M.K.W. Ko, R.A. Plumb, and C. Jackman (eds.), *Report of the 1998 Models and Measurements Workshop II*, NASA Reference Publication, National Aeronautics and Space Administration, Washington, D.C., in press, 1998.
- Parks, G., Brittnacher, M., L.J. Chen, R. Elsen, M. McCarthy, G. Germany, and J. Spann, Does the UVI on Polar detect cosmic snowballs? *Geophys. Res. Lett.*, *24*, 3109-3112, 1997.
- Perliski, L.M., S. Solomon, and J. London, On the interpretation of seasonal variations of stratospheric ozone, *Planet. Space Sci.*, *37*, 1527-1538, 1989.
- Peter, R., Stratospheric and mesospheric latitudinal water vapor distributions obtained by an airborne millimeter-wave spectrometer, *J. Geophys. Res.*, *103*, 16275-16290, 1998.
- Pickett, H.M., and D.B. Peterson, Comparison of measured stratospheric OH with prediction, *J. Geophys. Res.*, *101*, 16789-16796, 1996.
- Plumb, R.A., A "tropical pipe" model of stratospheric transport, *J. Geophys. Res.*, *101*, 3957-3972, 1996.
- Plumb, R.A., and M.K.W. Ko, Interrelationships between mixing ratios of long-lived stratospheric constituents, *J. Geophys. Res.*, *97*, 10145-10156, 1992.
- Prasad, S.S., Natural atmospheric sources and sinks of nitrous oxide: 1, An evaluation based on 10 laboratory experiments, *J. Geophys. Res.*, *99*, 5285-5294, 1994.
- Prasad, S.S., Potential atmospheric sources and sinks of nitrous oxide: 2, Possibilities from excited O₂, "embryonic" O₃, and optically pumped excited O₃, *J. Geophys. Res.*, *102*, 21527-21536, 1997.
- Prather, M.J., and E.E. Remsberg (eds.), *The Atmospheric Effects of Stratospheric Aircraft: Report of the 1992 Models and Measurements Workshop*, NASA Reference Publication 1292, Vol. I-III, National Aeronautics and Space Administration, Washington, D.C., 1993.
- Prather, M., R. Derwent, D. Ehhalt, P. Fraser, E. Sanhueza, and X. Zhou, Other trace gases and atmospheric chemistry, Chapter 2 in *Climate Change 1994: Radiative Forcing of Climate Change and an Evaluation of the IPCC IS92 Emission Scenarios*, edited by J.T. Houghton, L.G. Meira Filho, J. Bruce, H. Lee, B.A. Callander, E. Haites, N. Harris, and K. Maskell, Intergovernmental Panel on Climate Change, Cambridge University Press, Cambridge, U.K., 1995.
- Rahn, T., and M. Whalen, Stable isotope enrichment in stratospheric nitrous oxide, *Science*, *278*, 1776-1778, 1997.
- Randel, W.J., J.C. Gille, A.E. Roche, J.B. Kumer, J.L. Mergenthaler, J.W. Waters, E.F. Fishbein, and W.A. Lahoz, Stratospheric transport from the tropics to middle latitudes by planetary-wave mixing, *Nature*, *365*, 533-535, 1993.
- Randel, W.J., B.A. Boville, J.C. Gille, P.L. Bailey, S.T. Massie, J.B. Kumer, J.L. Mergenthaler, and A.E. Roche, Simulation of stratospheric N₂O in the NCAR CCM2: Comparison with CLAES data and global budget analyses, *J. Atmos. Sci.*, *51*, 2834-2845, 1994.
- Randel, W.J., F. Wu, J.M. Russell III, A. Roche, and J.W. Waters, Seasonal cycles and QBO variations in stratospheric CH₄ and H₂O observed in UARS HALOE data, *J. Atmos. Sci.*, *55*, 163-185, 1998a.
- Randel, W.J., F. Wu, J.M. Russell III, J.W. Waters, and M.L. Santee, Space-time patterns of trends in stratospheric constituents derived from UARS measurements, *J. Geophys. Res.*, in press, 1998b.
- Randeniya, L.K., P.F. Vohralik, I.C. Plumb, and K.R. Ryan, Heterogeneous BrONO₂ hydrolysis: Effect on NO₂ columns and ozone at high latitudes in summer, *J. Geophys. Res.*, *102*, 23543-23557, 1997.
- Ravishankara, A.R., G. Hancock, M. Kawasaki, and Y. Matsumi, Photochemistry of ozone: Surprises and recent lessons, *Science*, *280*, 60-61, 1998.
- Ray, E.A., J.R. Holton, E.F. Fishbein, L. Froidevaux, and J.W. Waters, The tropical semiannual oscillation in temperature and ozone as observed by the MLS, *J. Atmos. Sci.*, *51*, 3045-3052, 1994.
- Rinsland, C.P., M.R. Gunson, R.J. Salawitch, H.A. Michelsen, R. Zander, M.J. Newchurch, M.M. Abbas, M.C. Abrams, G.L. Manney, A.Y. Chang, F.W. Irion, A. Goldman, and E. Mahieu, ATMOS/ATLAS-3 measurements of stratospheric chlorine and reactive nitrogen partitioning inside and outside the November 1994 Antarctic vortex, *Geophys. Res. Lett.*, *23*, 2365-2368, 1996.
- Rizk, B., and A.J. Dessler, Small comets: Naked-eye visibility, *Geophys. Res. Lett.*, *24*, 3121-3124, 1997.
- Rogaski, C.A., J.M. Price, J.A. Mack, and A.M. Wodtke, Laboratory evidence for a possible non-LTE mechanism of stratospheric ozone formation, *Geophys. Res. Lett.*, *20*, 2885-2888, 1993.

- Rogaski, C.A., J.A. Mack, and A.M. Wodtke, State-to-state rate constants for relaxation of highly vibrationally excited O₂ and implications for its atmospheric fate, *Faraday Discuss. Chem. Soc.*, *100*, 229-251, 1995.
- Rosenfield, J.E., D.B. Considine, P.E. Meade, J.T. Bacmeister, C.H. Jackman, and M.R. Schoeberl, Stratospheric effects of Mount Pinatubo aerosol studied with a coupled two-dimensional model, *J. Geophys. Res.*, *102*, 3649-3670, 1997.
- Rosenlof, K.H., Seasonal cycle of the residual mean meridional circulation in the stratosphere, *J. Geophys. Res.*, *100*, 5173-5191, 1995.
- Rosenlof, K.H., A.F. Tuck, K.K. Kelly, J.M. Russell III, and M.P. McCormick, Hemispheric asymmetries in water vapor and inferences about transport in the lower stratosphere, *J. Geophys. Res.*, *102*, 13213-13234, 1997.
- Russell, J.M. III, M. Luo, R.J. Cicerone, and L.E. Deaver, Satellite confirmation of the dominance of chlorofluorocarbons in the global stratospheric chlorine budget, *Nature*, *379*, 526-529, 1996.
- Ruth, S.L., J.J. Remedios, B.N. Lawrence, and F.W. Taylor, Measurements of N₂O by the UARS Improved Stratospheric and Mesospheric Sounder during the early northern winter 1991/92, *J. Atmos. Sci.*, *51*, 2818-2833, 1994.
- Ruth, S.L., R. Kennaugh, L.J. Gray, and J.M. Russell III, Seasonal, semiannual, and interannual variability seen in measurements of methane made by the UARS Halogen Occultation Experiment, *J. Geophys. Res.*, *102*, 16189-16199, 1997.
- Sandor, B.J., and R.T. Clancy, Mesospheric HO_x chemistry from diurnal microwave observations of HO₂, O₃, and H₂O, *J. Geophys. Res.*, *103*, 13337-13351, 1998.
- Sassi, F., and R.R. Garcia, The role of equatorial waves forced by convection in the tropical semiannual oscillation, *J. Atmos. Sci.*, *54*, 1925-1942, 1997.
- Schoeberl, M.R., and P.A. Newman, A multiple-level trajectory analysis of vortex filaments, *J. Geophys. Res.*, *100*, 25801-25815, 1995.
- Sen, B., G.C. Toon, J.-F. Blavier, E.L. Fleming, and C.H. Jackman, Balloon-borne observations of mid-latitude fluorine abundance, *J. Geophys. Res.*, *101*, 9045-9054, 1996.
- Sen, B., G.C. Toon, G.B. Osterman, J.-F. Blavier, J.J. Margitan, R.J. Salawitch, and G.K. Yue, Measurements of reactive nitrogen in the stratosphere, *J. Geophys. Res.*, *103*, 3571-3585, 1998.
- Siskind, D.E., and J.M. Russell III, Coupling between middle and upper atmospheric NO: Constraints from HALOE observations, *Geophys. Res. Lett.*, *23*, 137-140, 1996.
- Siskind, D.E., and M.E. Summers, Implications of enhanced mesospheric water vapor observed by HALOE, *Geophys. Res. Lett.*, *25*, 2133-2136, 1998.
- Siskind, D.E., K. Minschwaner, and R.S. Eckman, Photodissociation of O₂ and H₂O in the middle atmosphere: Comparison of numerical methods and impact on model O₃ and OH, *Geophys. Res. Lett.*, *21*, 863-866, 1994.
- Siskind, D.E., B.J. Connor, R.S. Eckman, E.E. Remsberg, J.J. Tsou, and A. Parrish, An intercomparison of model ozone deficits in the upper stratosphere and mesosphere from two data sets, *J. Geophys. Res.*, *100*, 11191-11202, 1995.
- Siskind, D.E., J.T. Bacmeister, M.E. Summers, and J.M. Russell III, Two-dimensional model calculations of nitric oxide transport in the middle atmosphere and comparison with Halogen Occultation Experiment data, *J. Geophys. Res.*, *102*, 3527-3545, 1997.
- Siskind, D.E., L. Froidevaux, J.M. Russell III, and J. Lean, Implications of upper stratospheric trace constituent changes observed by HALOE for O₃ and ClO from 1992 to 1995, *Geophys. Res. Lett.*, *25*, 3513-3516, 1998.
- Solomon, S., and R.R. Garcia, On the distributions of long-lived tracers and chlorine species in the middle atmosphere, *J. Geophys. Res.*, *89*, 11633-11644, 1984.
- Solomon, S., R.W. Portmann, R.R. Garcia, W. Randel, F. Wu, R. Nagatani, J. Gleason, L. Thomason, L.R. Poole, and M.P. McCormick, Ozone depletion at mid-latitudes: Coupling of volcanic aerosols and temperature variability to anthropogenic chlorine, *Geophys. Res. Lett.*, *25*, 1871-1874, 1998.
- Stachnik, R.A., J.C. Hardy, J.A. Tarsala, J.W. Waters, and N.R. Erickson, Submillimeter heterodyne measurements of stratospheric ClO, HCl, and HO₂: First results, *Geophys. Res. Lett.*, *19*, 1931-1934, 1992.
- Steinbrecht, W., H. Claude, and F. Schöenborn, Nine years of lidar measurements at Hohenpeissenberg: Validation and results, in *Atmospheric Ozone: Proceedings of the XVIII Quadrennial Ozone Symposium*, L'Aquila, Italy, 12-21 September 1996, edited by R.D. Bojkov and G. Visconti, pp. 171-174, Parco Scientifico e Tecnologico d'Abruzzo, L'Aquila, Italy, 1998.

UPPER STRATOSPHERIC PROCESSES

- Stolarski, R.S. (ed.), *1995 Scientific Assessment of the Atmospheric Effects of Stratospheric Aircraft*, NASA Reference Publication 1381, National Aeronautics and Space Administration, Washington, D.C., 1995.
- Stolarski, R.S., and R.J. Cicerone, Stratospheric chlorine: A possible sink for ozone, *Can. J. Chem.*, *52*, 1610-1615, 1974.
- Stolarski, R.S., and W. Randel, Ozone change as a function of altitude, Chapter 3 in *Assessment of Trends in the Vertical Distribution of Ozone*, edited by N. Harris, R. Hudson, and C. Phillips, Stratospheric Processes and their Role in Climate (SPARC) Report No. 1, World Meteorological Organization Ozone Research and Monitoring Project—Report No. 43, Verrières le Buisson, France, 1998.
- Summers, M.E., R.R. Conway, D.E. Siskind, M.H. Stevens, D. Offermann, M. Riese, P. Preusse, D.F. Strobel, and J.M. Russell III, Implications of satellite OH observations for middle atmospheric H₂O and ozone, *Science*, *277*, 1967-1970, 1997a.
- Summers, M.E., D.E. Siskind, J.T. Bacmeister, R.R. Conway, S.E. Zasadil, and D.F. Strobel, Seasonal variation of middle atmospheric CH₄ and H₂O with a new chemical-dynamical model, *J. Geophys. Res.*, *102*, 3503-3526, 1997b.
- Sutton, R.T., H. MacLean, R. Swinbank, A. O'Neill, and F.W. Taylor, High-resolution stratospheric tracer fields estimated from satellite observations using Lagrangian trajectory calculations, *J. Atmos. Sci.*, *51*, 2995-3005, 1994.
- Tabazadeh, A., and R.P. Turco, Stratospheric chlorine injection by volcanic eruptions: HCl scavenging and implications for ozone, *Science*, *260*, 1082-1086, 1993.
- Toumi, R., and S. Bekki, The importance of the reactions between OH and ClO for stratospheric ozone, *Geophys. Res. Lett.*, *20*, 2447-2450, 1993.
- Toumi, R., P.L. Houston, and A.M. Wodtke, Reactive O₂(X, v ≥ 26) as a source of stratospheric O₃, *J. Chem. Phys.*, *104*, 775-776, 1996.
- Wang, H.J., D.M. Cunnold, and X. Bao, A critical analysis of Stratospheric Aerosol and Gas Experiment ozone trends, *J. Geophys. Res.*, *101*, 12495-12514, 1996.
- Watson, R.T., H. Rodhe, H. Oeschger, and U. Siegenthaler, Greenhouse gases and aerosols, Chapter 1 in *Climate Change: The IPCC Scientific Assessment*, edited by J.T. Houghton, G.J. Jenkins, and J.J. Ephraums, Intergovernmental Panel on Climate Change, Cambridge University Press, Cambridge, U.K., 1990.
- Waugh, D.W., T.M. Hall, W.J. Randel, P.J. Rasch, B.A. Boville, K.A. Boering, S.C. Wofsy, B.C. Daube, J.W. Elkins, D.W. Fahey, G.S. Dutton, C.M. Volk, and P.F. Vohralik, Three-dimensional simulations of long-lived tracers using winds from MACCM2, *J. Geophys. Res.*, *102*, 21493-21513, 1997.
- WMO (World Meteorological Organization), *Atmospheric Ozone 1985: Assessment of Our Understanding of the Processes Controlling Its Present Distribution and Change*, World Meteorological Organization Global Ozone Research and Monitoring Project—Report No. 16, Geneva, 1986.
- WMO (World Meteorological Organization), *Scientific Assessment of Ozone Depletion: 1994*, World Meteorological Organization Global Ozone Research and Monitoring Project—Report No. 37, Geneva, 1995.
- Wood, S.W., D.J. Keep, C.R. Burnett, and E.B. Burnett, Column abundance measurements of atmospheric hydroxyl at 45°S, *Geophys. Res. Lett.*, *21*, 1607-1610, 1994.
- Woods, D.C., R.L. Chuan, and W.I. Rose, Halite particles injected into the stratosphere by the 1982 El Chichón eruption, *Science*, *230*, 170-172, 1985.
- Yung, Y.L., and C.E. Miller, Isotopic fractionation of stratospheric nitrous oxide, *Science*, *278*, 1778-1780, 1997.
- Zander, R., E. Mahieu, M.R. Gunson, M.C. Abrams, A.Y. Chang, M.M. Abbas, C. Aellig, A. Engel, A. Goldman, F.W. Irion, N. Kämpfer, H.A. Michelsen, M.J. Newchurch, C.P. Rinsland, R.J. Salawitch, G.P. Stiller, and G.C. Toon, The 1994 northern midlatitude budget of stratospheric chlorine derived from ATMOS/ATLAS-3 observations, *Geophys. Res. Lett.*, *23*, 2357-2360, 1996.
- Zawodny, J.M., and M.P. McCormick, Stratospheric Aerosol and Gas Experiment II measurements of the quasi-biennial oscillation of ozone and nitrogen dioxide, *J. Geophys. Res.*, *96*, 9371-9377, 1991.